Antibody Responses Against HIV-1 Vaccine Candidates

Antibody responses against HIV-1 vaccine candidates

A dissertation presented

by

Zi Han Kang

to

The Division of Medical Sciences

in partial fulfillment of the requirements

for the degree of

Doctor of Philosophy

in the subject of

Virology

Harvard University

Cambridge, Massachusetts

August 2018

Dissertation Advisor: Dr. Dan H. Barouch Zi Han Kang

Antibody responses against HIV-1 vaccine candidates

Abstract

The elicitation of protective antibody responses is likely to be important in developing a successful human immunodeficiency virus type 1 (HIV-1) vaccine. As HIV-1 infection in humans is predominantly transmitted via the mucosal route, it is thus likely that a prophylactic vaccine will need to elicit protective antibody responses at mucosal sites of infection. While studies have shown that vaccine-elicited immunoglobulin G (IgG) responses are important in preventing simian/human immunodeficiency virus (SHIV) transmission in rhesus monkeys, IgA's role and function in protection, and whether it is in fact beneficial or detrimental, remain poorly defined. In this thesis, we investigated the relationship between mucosal and systemic vaccine-elicited IgG and IgA antibody responses in rhesus monkeys that were intramuscularly immunized with candidate HIV-1 vaccine vectors. Systemic and mucosal antibody responses exhibited similar kinetics, and the isotype, functionality, and epitope specificity of mucosal IgG responses were further shown to be similar to those of systemic IgG responses. This suggests that mucosal and systemic responses are likely to be immunologically coordinated. IgG and IgA responses, in terms of magnitude of antibody responses and antibody specificities against linear HIV-1 epitopes, were also shown to be correlated and immunologically related. Mucosal and systemic antibody responses were similarly observed to be correlated in mice immunized with microspheres encapsulating the HIV-1 envelope protein (Env). Non-traditional vaccine delivery modalities have long been investigated as a way to improve vaccination coverage and immunogenicity. We developed multiple biodegradable poly(lactic-co-glycolic acid) (PLGA) microsphere formulations containing HIV-1 Env and different adjuvants, and evaluated their effects on the antibody response in a mouse model. Microspheres containing HIV-1 Env elicited comparable or

higher antibody responses in both the systemic and mucosal compartments, and also generated a more diverse antibody response that targeted more linear Env epitopes, when compared to similar amounts of soluble Env. These data help to improve our understanding of mucosal and systemic antibody responses following immunization, and could help improve future vaccine design.

TABLE OF CONTENTS

LIST OF FIGURES AND TABLES

Chapter 1: Introduction

Chapter 2: Common Features of Mucosal and Peripheral Antibody Responses Elicited by Candidate HIV-1 Vaccines in Rhesus Monkeys

Chapter 3: Serum IgG and IgA antibodies elicited following Ad26 vector-Env protein immunization are directed against similar epitope sequences

Chapter 4: Evaluating novel delivery methods of vaccination that may improve induction of antigen-specific mucosal antibodies

Chapter 5: Conclusion

Appendix: Supplemental Figures

Dedication

I would first like to dedicate my dissertation to my parents for their support, teaching me the importance of education and perseverance, and for being understanding when I have not visited in years. I would also like to dedicate this dissertation to my advisor Dan Barouch for his mentorship, patience, and for imparting his wisdom and advice. I would finally like to dedicate this dissertation to my friends, colleagues, and family, for their help, support and friendship through the long graduate school years.

CHAPTER 1:

Introduction

STATE OF THE HIV-1 PANDEMIC

AIDS history and scale of HIV-1 epidemic

The human immunodeficiency virus type 1 (HIV-1) was first identified as the causative agent for acquired immunodeficiency virus syndrome (AIDS) in 1983-1984 (1-5). Previously healthy patients, usually young male homosexuals and intravenous drug users, were presenting with symptoms of immune dysfunction, characterised by opportunistic infections (usually Pneumocystis jirovecii pneumonia) and viral-associated cancers (such as Kaposi's sarcoma and non-Hodgkin's lymphoma) from the late 1970s and 1980s. Since then, it has expanded to affect more than 70 million people worldwide.

In 2016, there were 36.7 million HIV-1 positive individuals. 25.5 million live in the sub-Saharan region of Africa (6), of which women and girls account for more than half of the total number of people living with HIV. In the USA, there are about 1.1 million people living in HIV, and men who have sex with men (MSM) account for the majority (68%) of all new diagnoses (7).

AIDS pathogenesis

The most common cause of HIV-1 transmission worldwide is due to sexual transmission, with the greatest risk happening in the men who have sex with men population. Parenteral transmission, either during blood transfusions or through needle sharing/needle sticks, as well as mother to infant transmissions are also other modes of HIV-1 transmission.

HIV-1 infects and kills cells that are important for effective immune responses, leading to immune suppression. In the early stages of acute infection, high numbers of CD4+ T cells are infected, and are subsequently lost. Many of these cells are found in the gut-associated lymphatic tissue (GALT), and are important for maintaining the integrity of the mucosal barrier. The subsequent loss of epithelial integrity allows gut-associated microbial products to

be translocated into the systemic circulation, resulting in systemic and chronic immune activation. Chronic antigenic stimulation eventually results in T cell exhaustion – T cells important for adaptive immune responses become dysfunctional and lose effector functions (such as being able to secrete multiple cytokines or kill infected target cells). With the decline in CD4 T cell counts and exhaustion of the CD8 T cells, the resulting immune dysfunction results in the multiple opportunistic infections and malignancies seen in HIV-1 patients with advanced disease. HIV-1 is also suggested to accelerate the ageing process, and has been associated with increased risk of cardiovascular disease, neurological dysfunction, nephropathy and loss of bone mineral density (reviewed in (8)).

Consequences of the AIDS epidemic

Beyond shortening life expectancy and increasing morbidity in infected populations, HIV/AIDS has additional consequences. It negatively impacts economic growth in developing countries, severely reducing the growth of the gross domestic product, and prolongs poverty by generating substantial medical, funeral and legal costs. The number of children orphaned by AIDS totaled 13.4 million in 2015 (9) and many more have their education curtailed by the lack of funds available for school fees or having lost their teachers to HIV/AIDS. These forces result in regional instability and deplete national infrastructures and human resources in the worst-affected countries (10).

Antiretroviral therapy (ART) involves antiviral drugs that have been developed to treat HIV-1 infection. These are usually taken in combination, and include reverse transcription inhibitors, protease inhibitors, integrase inhibitors, and entry inhibitors. They block different stages of the HIV-1 viral replication cycle, lower viral loads, maintain CD4 T cell counts, and reduce the risk of transmission. However, they have toxic side effects and are expensive – especially for patients in developing nations where HIV-1 is the most prevalent. The

complexity of pill regimens and poor tolerability also result in poor adherence, all of which could foster the development of drug-resistant HIV-1 strains.

Current state of the AIDS epidemic

While the annual number of new HIV-1 infections and AIDS-related deaths are declining with a global effort to strengthen HIV-1 prevention and treatment programmes and a scale up of ART, there were still 1.8 million new HIV-1 infections and 1 million AIDS-related deaths in 2016 (6). This rate of decline is still far too slow to reach the target set by the United Nations General Assembly of having fewer than 500,000 new infections by 2020.

HIV-1 GENOME AND REPLICATION

HIV-1 Genome

HIV-1 is a lentivirus in the Retroviridae family, with a single-stranded, positive-sense RNA genome. The HIV-1 genome contains 3 primary genes encoding structural proteins or enzymes (gag, pol, and env), as well as several other open reading frames (ORFs) (Figure 1.1A). These 3 primary genes are initially translated into polyprotein precursors, which are subsequently processed, post-translation, by either host or viral proteases, into mature proteins. The Gag precursor is cleaved into the matrix (MA – p17), capsid (CA – p24), nucleocapsid (NC – p7), p6, as well as 2 spacer proteins (SP1 and SP2). The Gag-Pol polyprotein is cleaved to form the protease (PR), reverse transcriptase (RT) and integrase (IN) proteins, and the envelope (Env) precursor (Env gp160) is cleaved to form the gp120 surface subunit and gp41 transmembrane subunit (TM). Vif, Vpr, Tat, Rev, Vpu, and Nef, are translated from spliced messenger RNAs (mRNAs). Tat and Rev are regulatory proteins essential for viral replication, while accessory proteins Vif, Vpr, Vpu and Nef are necessary for viral replication *in vivo* (11). The functions of the different viral proteins are summarised in Table 1.1.

Molecular biology of HIV-1 replication

HIV-1 replication begins with viral entry, with the binding of Env gp120 (via the C3 and C4 domains) on the viral particles to host CD4 molecules on susceptible cells (including activated CD4+ T lymphocytes). Interaction of Env (via the V3 loop, along with other highly conserved domains) with a co-receptor, usually CXCR4 or CCR5, is also important and necessary for viral entry (12-14). Binding to both receptor and co-receptor results in conformational changes in gp41 that subsequently lead to fusion of the viral and cellular membranes. Upon entry, the virion is partially uncoated, and the viral nucleoprotein complex

(consisting of viral RNA, RT, CA, NC, IN, and Vpr) enters the cytosol, where reverse transcription is initiated.

Reverse transcription is initiated from the 3'-OH end of a primer tRNA that is annealed near the 5' end of the viral genome, and minus-strand DNA synthesis proceeds to the 5' end of the genome. RNaseH digests the RNA portion of the RNA-DNA hybrid, exposing the short single stranded DNA fragment, allowing it to bind to the 3' end of the viral RNA genome. Minus-strand synthesis then proceeds again to the 5' end of the viral genome, accompanied by RNaseH-mediated degradation of the viral RNA. Fragments of RNA that were not degraded by RNaseH serve as primers for plus-strand synthesis, terminating at the end of the minus strand. RNaseH also degrades the tRNA annealed to the viral genome. Reverse transcription ultimately results in a double stranded DNA molecule that is subsequently integrated into the host cell chromosome in the nucleus.

Integration of viral DNA is catalyzed by integrase, which assembles with the viral DNA, and cleaves it at the 3' end of both strands of the viral DNA. Integrase also cleaves the cellular target DNA, and subsequently catalyzes DNA strand transfer, where the 3' recessed ends of the viral DNA is joined to the 5' overhanging ends of cellular DNA. The cellular repair machinery then repairs the gap, resulting in the ligation of viral DNA into the host genome. The host RNA polymerase subsequently catalyzes the transcription of viral RNA, which is upregulated several hundredfold by Tat (15). The cellular transcriptional factors: NF-κB, nuclear factor of activated T cells (NFAT), and AP-1, are also important for virus replication and viral RNA synthesis. During the early post-integration phase of the viral replication cycle, most of the viral RNAs exported to the cytoplasm consist of multiply spliced viral mRNAs that lack introns. As the transcription of viral proteins progresses, the viral protein Rev is transported through the nuclear pore via importins into the nucleoplasm,

where it binds to the high affinity RRE sites on HIV-1 pre-mRNA, thereby promoting the nuclear export of intron-containing viral RNA (16, 17).

Following viral RNA replication and production of viral proteins, viral assembly occurs, with the incorporation of the viral RNA genome, Env glycoproteins, and Gag-Pol polyprotein precursor into immature virus-like particles (VLPs). NC binding to viral RNA is important for promoting Gag multimerisation. MA regulates membrane binding, and is essential in directing Gag to the viral membrane, via a myristic acid moiety (18-20). Host cellular membrane and protein trafficking proteins are involved with HIV-1 assembly, including AP-1, -2, and -3 complexes, and SNAREs (soluble NSF attachment protein receptors). After viral budding from the infected cell, PR cleaves the Gag and Gag-Pol polyproteins to form MA, CA, NC and p6, along with SP1 and SP2. This processing catalyzes a major structural and morphological rearrangement, resulting in the formation of mature HIV-1 virions. The accessory proteins Vif, Vpr, Vpu and Nef, interact with host restriction factors, assisting in viral replication (Table 1.1).

Env

The viral protein Env is the only HIV-1 protein that is expressed on the surface of the virus and is required for binding and entry into host cells, as well as for determining host cell tropism. Env is found as a trimer on the viral membrane (21, 22) (Figure 1.1C), and the gp160 precursor is cleaved by the protease furin to form two cleavage products gp120 and gp41 that are non-covalently linked to form a single subunit. For Env to be functional and to be able to facilitate viral fusion and entry, the gp160 precursor has to be cleaved.

gp120 is found on the outside of the viral membrane, and is organised into five conserved regions (C1-C5) and five variable loops (V1-V5) (Figure 1.1B). Most of the sequence diversity of Env is found in the V loops of gp120, with the sequence changing 1-2%

per year, and this is mostly driven by immune escape (reviewed in (23)). The V1, V2, V4, and V5 loops are the main targets for host antibodies.

The primary receptor for HIV-1, CD4, binds to conserved regions of gp120 on either side of V4, resulting in a series of conformational changes in gp120. CD4 is found on many different cells types, including T cells, monocytes, and macrophages. Binding of gp120 to a co-receptor is also required for viral entry, and different co-receptors can be utilised by HIV-1, with CCR5 and CXCR4 being the most important. The co-receptor bound determines viral tropism. Viruses using CCR5 as a co-receptor are commonly found in recently infected patients during the asymptomatic phase and infect memory CD4 T cells (CCR5 is exclusively expressed in memory CD4 T cells *in vivo*), while CXCR4-using viruses emerge during the symptomatic phase and predominantly infect naïve and memory CD4 T cells.

The surface of Env is also heavily glycosylated, shielding the surface of the protein from exposure to antibodies (24, 25). These glycans are also essential for the correct folding of Env and viral assembly, and as they originate from the host, they act as decoys to the immune system, eliciting autoreactive antibodies. They also stearically block antibodies from binding to more conserved sites on Env.

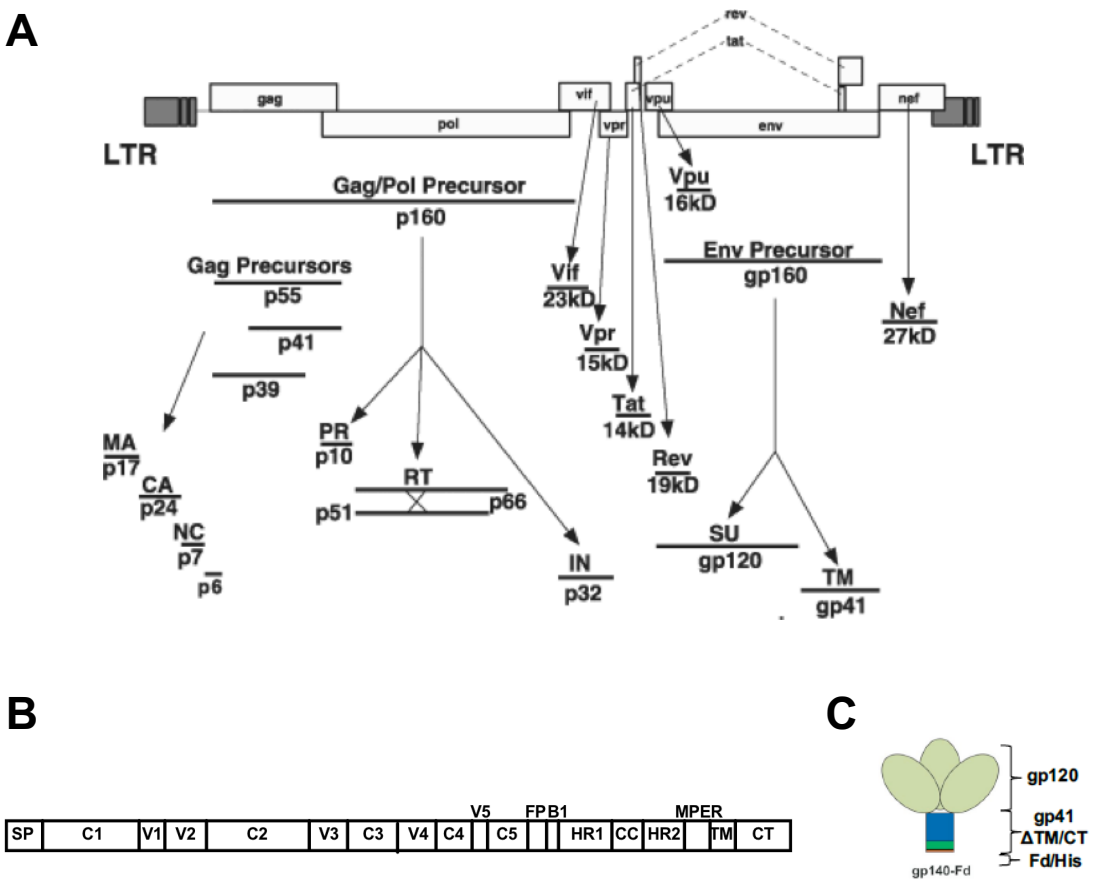

Figure 1.1 – Genomic organization of HIV-1 and the HIV-1 Env gp160 protein

(A) The HIV-1 genome contains 3 primary genes encoding structural proteins or enzymes (gag, pol, and env), as well as several other open reading frames (ORFs). These 3 primary genes are initially translated into polyprotein precursors, which are subsequently processed, post-translation, by either host or viral proteases, into mature proteins.

(B) The full length Env gp160 contains a surface subunit (gp120) and transmembrane spanning region (gp41) after cleavage by furin. The gp120 subunit contains five constant regions (C1-C5), five variable loops (V1-V5). The gp41 region contains a fusion peptide (FP), heptad repeats 1 and 2 (HR1 and HR2), the C-C loop, the membrane proximal external region (MPER), and the transmembrane docking regions including the transmembrane domain (TM) and cytoplasmic tail (CT).

(C) In the viral membrane, Env exists as a trimer.

Figure modified from: (11) and (28)

Table 1.1 – HIV-1 viral proteins and their functions

Env	Cleaved to form gp120 and gp41. **gp120**: binds to CD4 and other co-receptor **gp41**: exposed upon gp120 conformation change, and helps mediates fusion Contains the RNA response element
Pol	Pol polyprotein encodes the following components: **Reverse transcriptase (Rev):** transcribes viral RNA into viral DNA **Integrase (IN):** integrates viral DNA into host's genome **Protease (PR):** cleaves polyproteins **RNaseH**: mediates degradation of the viral RNA during reverse transcription
Gag	Gag polyprotein is cleaved by PR to form the following components: **Matrix (MA):** Myristoylation of MA helps target Gag polyprotein to lipid rafts Implicated in the nuclear import of the HIV pre-integration complex (PIC) **Capsid (CA)**: forms the viral capsid **Nucleocapsid (NC):** forms the viral nucleocapsid **p6**: recruits TSG101 to initiate viral budding
Rev	Regulates viral gene expression via binding to the Rev response element Inhibits viral RNA splicing and promotes nuclear export of incompletely spliced viral RNAs
Tat	Binds the trans-activation response element and increases transcription of HIV double stranded DNA together with host cyclin T1 and CDK9 Antagonises the CXCR4 receptor, promoting macrophage-tropic HIV strains
Vif	Inactivates the APOBEC family of cytidine deaminases, which are involved in antiviral activity
Vpr	Promotes G2 cell cycle arrest Nuclear import of HIV PIC Transcriptional transactivation of viral and cellular promoters Apoptosis
Vpu	Enhancement of particle release Counteracts tetherin Promotes CD4 degradation
Nef	Down-regulates surface CD4, MHC-1, CD3, CD28 Enhances virus infectivity Alters cellular activation pathways

HIV-1 global distribution

HIV-1 is extremely genetically diverse, with heterogeneity observed in isolates from different geographical regions (26), and even within a single HIV-1 infected individual (27). Most of this variability occurs within the Env protein. Reverse transcription is highly error-prone (resulting in mutation rates of 5 X 10^{-5} mutations/nucleotide/replication cycle), and also result in high recombination frequencies, when an individual is infected with 2 different viral strains (superinfection), or after sequence diversification has occurred. Viral replication in infected individuals is high, which also contributes to this high mutation rate. All these factors result in a pool of heterogenic and constantly changing virus populations in an infected individual.

HIV-1 is divided into four distinct groups: M (main), O (outlier), N, and P. Group M is further divided into 9 clades (A, B, C, D, F, G, H, J, and K), which are phylogenetically equidistant from each other. Env sequences between different clades differ by 20-30%, while Env sequences within a clade differ by 5-12%. All 9 clades are present in Africa. Clade C was found to be the most prevalent subtype globally, accounting for about half of all infections, while Clade B is most prevalent in Europe, North America, and Australia. There are additionally 49 circulating inter-clade recombinant forms (CRFs), due to the intermixing and recombination of genetically different strains within a single infected cell, which resemble a patchwork of juxtaposed HIV-1 subtype segments. These CRFs account for about 20% of global HIV-1 strains, and are the most common in regions where multiple HIV-1 subtypes coexist – Africa, South America, and South-East Asia. HIV-1 group O is rare, and is found in Cameroon, Gabon and Equatorial Guinea, while HIV-1 group N and group P strains are rare groups found mainly in Cameroon (Figure 1.2).

This large genetic diversity of HIV-1 presents a huge challenge, both in terms of treatment, as well as in the development of a single vaccine. Rapid mutation leads to the

selection of drug resistant variants, and aids viral escape from the immune system. Sequence diversity also complicates the choice of immunogens for a vaccine, as a successful vaccine would have to be able to elicit highly cross-reactive broadly neutralizing antibody responses that would be protective against multiple HIV-1 clades.

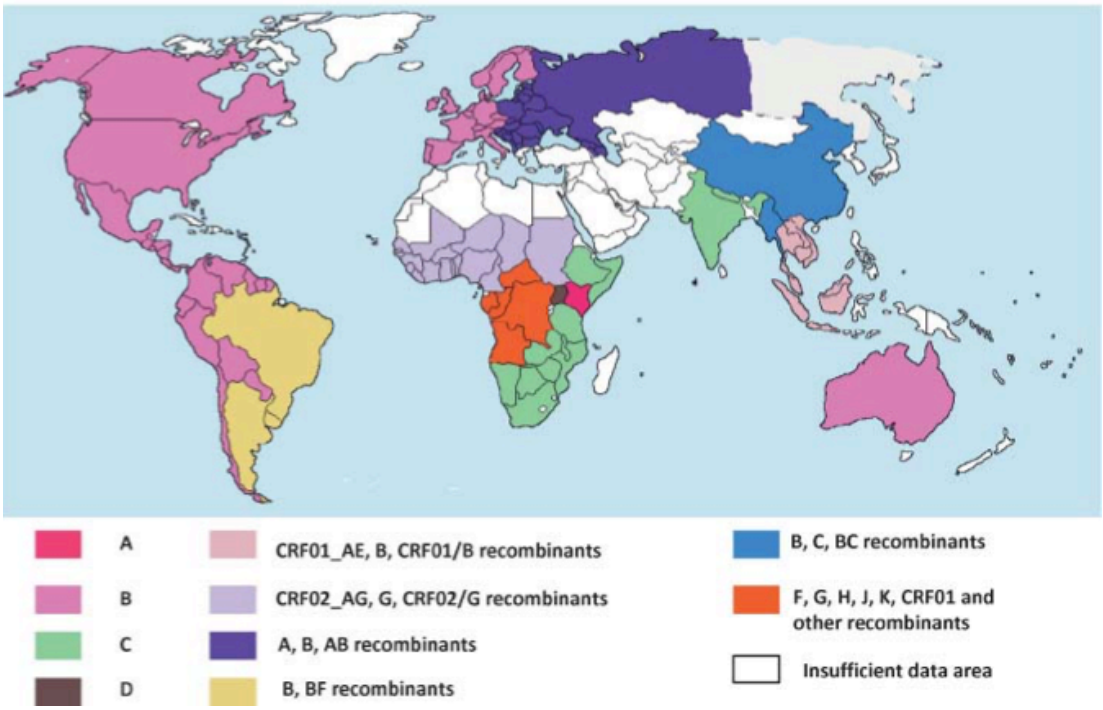

Figure 1.2 – global distribution of HIV-1 clades and circulating recombinant forms

Each colour represents a distinct clade or circulating recombinant form. There are 9 clades in group M (A, B, C, D, F, G, H, J, and K), which are phylogenetically equidistant from each other. Clade C is the most prevalent global subtype, while Clade B is most prevalent in Europe, North America, and Australia. There are 49 circulating inter-clade recombinant forms (CRFs), and these are the most common in regions where multiple HIV-1 subtypes coexist (Africa, South America, and South-East Asia).

Figure adapted from (11).

HIV-1 VACCINATION STRATEGIES

Completed HIV-1 vaccine trials

There are many methods and programmes being implemented to prevent and slow the spread of HIV-1 infections. These include programmes encouraging condom use, and circumcision to minimise the risk of transmission, the use of ART in infected individuals, and the use of oral pre-exposure prophylaxis (PrEP). An effective HIV-1 vaccine would help reduce the rate of HIV-1 transmissions and AIDS-related deaths.

To date, there have only been 6 phase IIb/III HIV-1 vaccine efficacy trials, using 4 different vaccine modalities (summarised in Table 1.2). Only one of these 6 trials – the RV144 Thai trial – demonstrated vaccine-mediated protection, with a 31.2% efficacy rate (29). RV144 was a double-blinded, placebo-controlled, vaccine efficacy trial that was conducted in Thailand, in 16,402 healthy participants who were mainly at risk of heterosexual transmission. Participants were vaccinated 4 times (at weeks 0, 4, 12, 24) with a recombinant canarypox vector vaccine (ALVAC-HIV vCP1521 expressing gag, pol, gp41 transmembrane domain and gp120 env), and then boosted twice (at weeks 12, 24) with a recombinant gp120 subunit vaccine (AIDSVAX B/E) (29).

Correlations of protection

32 different antibody, T-cell, and innate immunity assays were performed and evaluated in a correlates analysis, and 6 primary variables were chosen for assessment as correlates of infection risk. They were: (i) IgG binding to V1V2 in Env, (ii) avidity of IgG binding to Env, (iii) ADCC activity, (iv) IgA binding to Env, (v) neutralizing antibody titers, (vi) Env-specific CD4+ T cells. Of these, IgG binding to V1V2 region of Env was inversely correlated with infection, while composite IgA binding to a set of 14 different Env was directly associated with infection risk (30). Subsequent analysis showed that the breadth of

the IgG response against the V1V2 Env region was significantly correlated with decreased infection risk (31). Env-specific IgG3 responses were also found to correlate with decreased HIV-1 risk (32), and these were highly coordinated with Fc effector functions (33). The IgG3 subclass is associated with highly functional antibody responses, including increased neutralization activity, complement binding, ADCC (34), and antibody dependent cellular phagocytosis (ADCP) (35). Plasma IgA binding to the C1 region of Env was found to correlate with increased risk (36), and this was thought to be due to IgA competing with and blocking functional IgG responses that mediate ADCC (37) and also bind to the C1-C2 region of Env (36, 38, 39). IgG antibodies against different Env epitopes were also observed to synergise with each other for neutralization, virion capture, and ADCC (40). Finally 2 polyfunctional CD4+ T cell subsets were also observed to correlate with decreased risk (41).

These primary and secondary analyses of correlates of protection in RV144 suggest that their nature is complex, and that there could potentially be multiple factors that act together to protect against HIV-1 acquisition and transmission in vaccinated individuals (42, 43). Furthermore, while the above-mentioned factors have been observed to be statistically correlated, there is no evidence that they have any direct mechanistic effect on protection. Indeed it has been suggested in a study that analysed the humoral responses elicited in RV144 via system serology that it was unlikely that IgA directly contributed to impaired humoral immune responses, and was likely just a marker for a less functional response (44). Finally, all 6 of the vaccine efficacy trials have tested preventative vaccination strategies by the administration of a combination of viral vectors and protein subunits. Other approaches that are currently undergoing early clinical trials involve the prophylactic delivery of broadly neutralizing antibodies (bnAbs), either passively, or by vectored immunoprophylaxis (immune gene transfer via viral vectors) (45).

Table 1.2 – Completed Phase IIb/III HIV-1 vaccine efficacy trials

Trial	Vaccine description	Outcome
VAX003	Protein: AIDSVAX B/E gp120 (subtype B MN and CRF01_AE CM244)	No efficacy
VAX004	Protein: AIDSVAX B/B gp120 (MN and GNE8 subtype B)	No efficacy
HVTN 502 (STEP Trial)	DNA-Ad5: Adenovirus type 5 Clade B gag/pol/nef	No efficacy, increased infection risk
HVTN 503 (Phambili Trial)	DNA-Ad5: Adenovirus type 5 Clade B gag/pol/nef	No efficacy, increased infection risk
RV144	Pox-Protein: ALVAC-HIV (recombinant canarypox vector)/ vCP1521 AIDSVAX B/E rgp120	31.2% efficacy after 42 months
HVTN 505	DNA-Ad-5: DNA Gag, Pol, and Nef from HIV-1 subtype B Env from subtypes A, B, and C rAd5 subtype B Gag-Pol and Env A, B, and C	No efficacy

THE HUMORAL IMMUNE RESPONSE

Antibody structure

Immunoglobulins are made up of two heavy (H) chains and two light (L) chains, where the L chain consists of either a κ or λ chain. Each chain contains one NH2-terminal variable (V) domain, and one or more COOH-terminal constant (C) domains. Each V or C domain is made up of about 110-130 amino acids (12,000-13,000 kDa). While the Ig L chains contain only 1 C domain, the Ig H chains contain three to four C domains. H chains with 3 C domains usually include a spacer hinge region between the first (C_H1) and second (C_H2) domains.

Antigen recognition and binding occur within the paired V domains of the immunoglobulin, while the C domains of the H chain determines the effector function of the immunoglobulin. Each C_H region folds into a consistent structure consisting of a three strand-four strand beta sheet covalently linked by a disulphide bond. There are 5 different antibody heavy chain isotypes – IgD, IgM, IgA, IgG, IgE, which confer different properties to the antibody. IgD, IgA and IgG consist of 3 H chain constant domains, while IgM and IgE have an additional domain. The Fc region (consisting of CH2-CH3 or CH2-CH4) defines the antibody isotype and subclass, and mediates effector function by binding to Fc receptors (FcR) on cells or activating other immune mediators, such as complement, and can also affect the affinity or kinetics of antigen binding.

Glycosylation of immunoglobulins, especially to the Fc region, are also known to affect antibody function. Glycosylation varies by isotype, with IgA being the most heavily glycosylated. Glycosylation can affect binding to Fc receptors on effector cells, as well as immune mediators, and elimination of glycosylation of IgG was shown to reduce or ameliorate entirely its binding to its Fc receptor (46).

IgG subclass structure and distribution

IgG is one of the most abundant proteins in human serum, making up 10-20% of plasma proteins. Humans and non-human primates encode for four different IgG subclasses (IgG1, IgG2, IgG3, and IgG4), which are more than 90% identical in their primary protein structure, but differ in antigen binding and effector functions (47). Most of the variation between the different IgG isotypes is found in the hinge region and the N-terminal CH2 region. Different IgG isotypes vary widely in the length and flexibility of their hinge region – while IgG1 has a very flexible 15 amino acid long hinge region, the hinge region of IgG2 is only 12 amino acids long, and is very inflexible due to a poly-proline helix that is stabilised by disulphide bridges. IgG3 has the longest hinge region of up to 62 amino acids, while IgG4 has a hinge region of 14 amino acids (48, 49). IgG1 is the most abundant subclass, and is typically induced in response to soluble protein antigens (47). IgG2 is typically induced against bacterial capsular polysaccharide antigens (50, 51). Viral infections result in the induction of IgG3 (as well as IgG1), which is a short-lived antibody that is very effective in inducing effector responses (51). IgG4 is typically induced following exposure to allergens, or following continual antigen exposure in a non-infectious setting (52). There are additional modifications on IgG, via glycosylation sites, which can subsequently affect effector function (49).

IgG function in viral infections

IgG is an important component of the systemic immune response against microorganisms, including viruses, and IgG from serum may contribute to the antibody responses on mucosal surfaces. Different IgG subclasses have different effector mechanisms – IgG1 and IgG3 are strong triggers of effector mechanisms, while IgG2 and IgG4 induce more subtle responses.

One of the main functions of IgG is virus neutralization by preventing the binding of microorganisms to cellular receptors of entry, as well as prevent fusion and entry of the virus to the host cell (53, 54). Binding of IgG to antigen/microorganisms (opsonisation) also enhances endocytosis of the antigen by phagocytic cells, including macrophages, neutrophils, cDCs and pDCs (55), with the binding of IgG in the IgG-antigen complex to FcγR on phagocytic cells. This leads to subsequent degradation of the virus by specific lysosomes. Antigen-bound IgG also mediates antibody-dependent cell-mediated cytotoxicity (ADCC), by binding to FcγRIIc or FcγRIIIa receptors on NK cells (56). Activated immune cells, including NK cells, monocytes, and macrophages, mediate ADCC lysis of virus-infected cells by degranulation of effector cells (57).

IgA subclass structure and distribution

Humans, chimpanzees, gorillas, and gibbons have 2 α heavy-chain constant region Cα genes that encode 2 different IgA subclasses (IgA1 and IgA2), while most other mammals possess a single Cα gene (58-60). The main difference between IgA1 and IgA2 lies in the hinge region. The hinge region in IgA1 consists of 19 amino acids and O-linked oligosaccharides (61, 62), while the hinge region in IgA2 is only 6 amino acids long and lacks glycosylation (63). This results in a more open 'T-shaped' structure between the Fab regions in IgA1, with the distance between Fab regions measuring about 16nm (64, 65), and a more 'Y-shaped' structure for IgA2, with a distance of about 10nm (64-66) (Figure 1.3A). The differences between structure and glycosylation could result in different biological activities between IgA1 and IgA2, although it is not currently known if this is the case. However, there is a different susceptibility of IgA1 and IgA2 to bacterial IgA1 proteases.

Further heterogeneity occurs with dimeric (dIgA) and polymeric IgA. (pIgA) A 15kDa joining chain (J chain) links monomers together at the Fc region via disulphide linkages

between the carboxy-terminal extension of one of the heavy chains of each monomer (Figure 1.3B).

Secretory IgA (SIgA) is the major form of IgA in mucosal fluids. The secretory component (SC) is added to dIgA during its passage through the epithelial layer into the mucosal compartment (Figure 1.3C). dIgA is secreted by mucosal plasma cells in the lamina propria below the epithelium, and then binds to the polymeric immunoglobulin receptor (pIgR), via the J chain (67, 68). The dIgA-pIgR complex is then endocytosed and transported across the epithelial cell in a vesicle. The dIgA-pIgR complex is then released into the lumen of the mucosal compartment, where proteases cleave off part of the pIgR, resulting in free dIgA molecules containing part of the pIgR – the SC region.

Serum IgA in humans consists of about 90% IgA1 and 10% IgA2, and is mainly monomeric (80%-99%). The ratio of IgA1 and IgA2 is more variable in different mucosal compartments: vaginal and rectal secretions contain approximately 60% IgA2, nasal fluids and male genital secretions contain about 80-90% IgA1, saliva contains about 60% IgA1 (69).

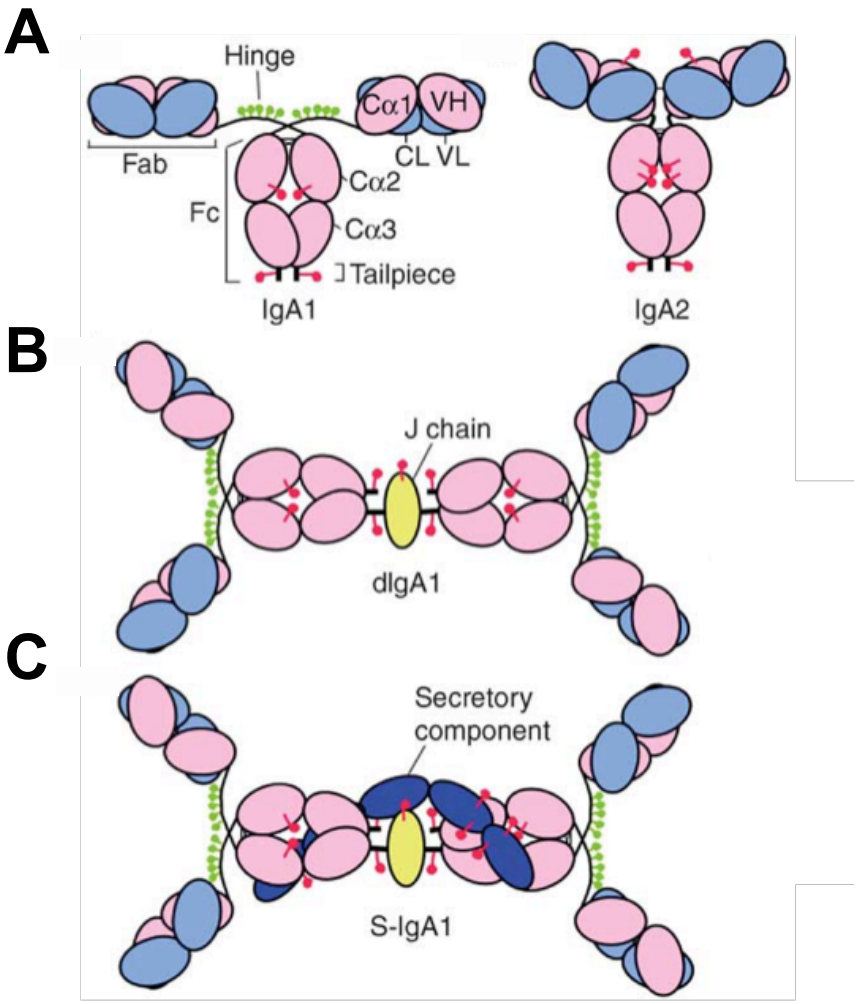

Figure 1.3 – structure of the different IgA subclasses

(A) There are 2 different IgA subclasses, IgA1 and IgA2. The hinge region in IgA1 consists of 19 amino acids, while the hinge region in IgA2 is only 6 amino acids long. This results in a more open 'T-shaped' structure (about 16nm between the Fab regions) in IgA1, and a more 'Y-shaped' structure (about 10nm between the Fab regions) for IgA2.

(B) IgA monomers are joined together by a 15kDa joining chain (J chain) at the Fc region via disulphide linkages between the carboxy-terminal extension of one of the heavy chains of each monomer, forming dimers or polymers.

(C) The secretory component is added to dIgA during its passage through the epithelial layer into the mucosal compartment, and subsequently secreted by mucosal plasma cells in the lamina propria below the epithelium. It binds to the polymeric immunoglobulin receptor via the J chain

Figure adapted from (65).

Protective Mechanisms of IgA

SIgA is an important component of mucosal protection (70, 71). SIgA inhibits adherence of microorganisms to mucosal surfaces, including the pharyngeal, intestinal and genitourinary tract epithelial. This is due to (i) the hydrophilic and negatively charged nature of the SC region in SIgA, (ii) pIgA and SIgA agglutinating microorganisms via the Fc region and via their carbohydrate chains (glycans) on SIgA. SIgA also inhibit enzymes and toxins, including IgA proteases and superantigens from group A streptococcus.

SIgA can directly also neutralize antigens and microorganisms. They are important in immune exclusion (72) – a phenomenon where virions and other microbial pathogens are retained in the lumen of the mucosal compartment, via agglutination, entrapment in mucus, and/or clearance by peristalsis (73, 74). SIgA is thought to associate with mucins in the mucus layer overlying mucosal epithelium (75), and this entraps IgA-bound antigens and microorganisms in the mucus layer. The mucus trapping ability is considerably greater when IgA is complexed with the SC region, probably due to the association of the oligosaccharide side chains of SC with mucus (76). However, when neutralizing monoclonal antibodies (mAb) in the form of dIgAs were given directly into the rectal lumen, in a passive immunization study, they protected monkeys from SHIV acquisition, even though they did not contain the SC region, although they may have associated with free SC in mucosal secretions (77).

Intracellular neutralization is another method by which non-neutralizing IgA mAbs is thought to bind to viral antigens in endocytic vesicles during transepithelial transport, preventing viral assembly (78-80). It has also been hypothesized that antigen-bound dIgA complexes are transported via pIgR binding from the apical to the luminal side. Immunized mice with strong mucosal antigen-specific IgA responses were subsequently administered the administered antigen intravenously. The antigen was detected within epithelial cells of the

small intestinal crypts and villi, but not in control animals immunized with a irrelevant antigen, suggesting that antigen was transported by epithelial cells from the basolateral side only in the presence of IgA-antigen complexes (81). In an *in vitro* system, mAb-HIV immune complexes were placed in the bottom chamber in transwell plates that were overlaid with a tight epithelial layer expressing pIgR on the basolateral surface. Transport of HIV particles was detected in the upper chamber culture fluid that overlayed the apical side, and was correlated with the virion binding ability of IgA, as well as to pIgR expression (82).

Anti-HIV IgA responses have been linked to protection in both humans and in the non-human primate (NHP) model. In HIV-exposed, persistently seronegative people (HEPS), IgA purified from sera were shown to bind HIV-1, to conserved epitopes in the MPER of HIV-1 gp41 (83), while IgA purified from sera, vaginal secretions and saliva, were shown to mediate cross-clade neutralization of HIV-1 (84). Contrary to the observations of these studies, HIV-1 specific mucosal responses were absent or detectable in low amounts in a small proportion of (HEPS) in other cohorts (85-88), although this could be due to the use of different methods of IgA isolation, assay sensitivity and other differences in IgA purification and mucosal fluid collection (89).

In mice that were intravenously injected with pIgA, mIgA, or IgG1 mAb against the H1 hemaglutinin of influenza, and subsequently challenged, only pIgA was protective (90). In NHPs that were immunized with a truncated gp41-derived peptide, and which developed systemic and mucosal antibody responses, they were protected against a SHIV challenge, and blocked transcytosis of HIV *in vitro*. Depletion of IgA ameliorated this inhibition of transcytosis of HIV (91). In NHPs that were passively immunized with dIgA1, dIgA2 and IgG1 versions of a mAb HGN194, only dIgA1 provided the best protection (83% protection) against a intrarectal SHIV challenge, even though all 3 isotypes had a similar neutralizing activity *in vitro* (77).

Anti-HIV IgA responses may be harmful

In vitro studies have implied that HIV-1 infection could be enhanced by serum derived IgA, possibly mediated by the FcαR (92, 93). Enhancement of HIV-1 infection was blocked by either pre-incubating cells with an anti-FcαR (92), or by pre-treating cells with IgA isolated from HIV-seronegative individuals. However, it is unknown how physiologically relevant these observations are to mucosal HIV-1 transmission.

In the RV144 clinical trail, plasma anti-HIV Env IgA was linked to an increased risk of HIV-1 infection (30). Vaccine-induced plasma IgA, specific for the C1 region of Env, was reported to compete with and block the binding of ADCC-mediating IgG1 (36). One of the factors associated with beneficial outcomes was plasma IgG-mediated ADCC activity (30). Env-specific monomeric IgA mAb isolated from the plasma of a RV144 participant was also shown to inhibit the IgG-mediated ADCC activity of NK cells to kill HIV-1 infected CD4+ T cells (36). However, it has also been suggested that these Env-spcific HIV-1 IgA responses may not have a direct mechanistic effect on protective humoral responses, but is rather a marker of correlates of risk of infection (44).

Class switching

Mature naïve B cells co-express both IgM and IgD on their surface. During an immune response or vaccination, in the presence of antigen, mature B cells undergo class switch recombination, substituting the heavy chain constant regions of IgM and IgD (Cμ and Cδ respectively) with the heavy chain constant regions of IgG, IgA, and IgE (Cγ, Cα, and Cε respectively). This takes place in the germinal centre of secondary lymphoid follicles, and is an irreversible DNA recombination event that diversifies antibody isotypes (and subsequently effector functions) with similar antigen specificities. Repetitive DNA sequences consisting of

G-rich non-template strands, known as switch regions (S regions), are found upstream of each of the immunoglobulin C-region genes, and switching is initiated at these regions with transcription at upstream promoter regions, resulting in extended regions of single-stranded DNA. These serve as substrates of activation-induced deaminase (AID), which deaminates cytosine residues on both strands of the S regions, generating clustered lesions which are ultimately processed into double stranded DNA breaks by uracil DNA glycosylase (UNG) and apurinic/apyrimidinic endonuclease (APE). DNA-PK and other repair proteins initiate double-strand break repair and fuse the 2 switch regions, and excise the intervening sequences to form an extra-chromosomal switch circle. Class switch recombination is an irreversible and one-way process – class switching to an antibody isotype renders it unable to switch to any isotype upstream of it. As such, the order of heavy chain exons is at follows: IgM > IgD > IgG3 > IgG1 > IgA1 > IgG2 > IgG4 > IgE > IgA2 (Figure 1.4).

Cytokines and other molecules regulate class switching and the selection of the antibody isotype. For example, in mice, IL-4 induces class switching to IgG1 and IgE, IFN-γ induces class switching to IgG3 and IgG2a, while TGF-β induces class switching to IgG2b and IgA. CD40L cooperates with TGF-β to induce IgA class switching, but can only do so in combination with other cytokines (e.g. IL-2, IL-4, IL-5, IL-6, and IL-10) (94). These cytokines are produced by T cell-dependent responses to antigens. T cell-independent antigens can also initiate class switching – for example, lipopolysaccharide (LPS – a component of gram negative bacteria that induces a strong immune response) activates B cells through toll-like receptor (TLR) signalling pathways, while polysaccharides signal through the B-cell receptor (BCR) (94). T cell-independent IgA class switching can also be regulated through BAFF and APRIL, in the presence of TGF-β.

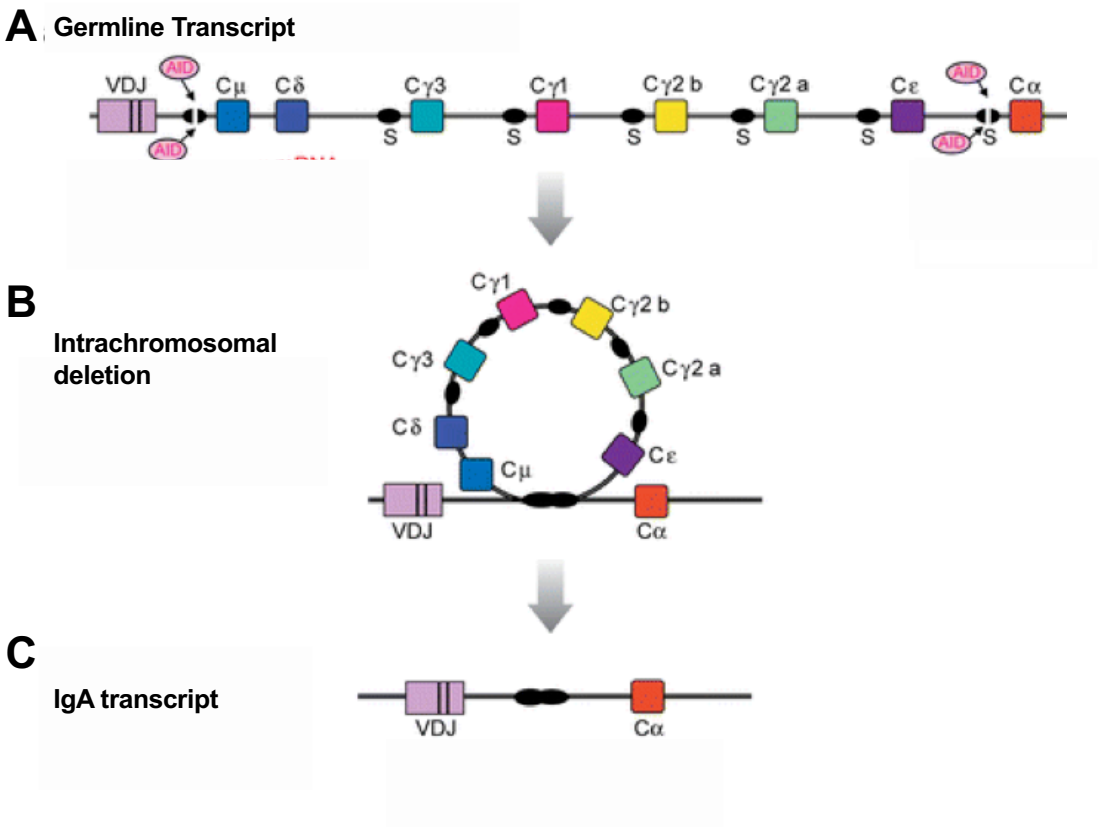

Figure 1.4 – Diagram of mechanism of class switch recombination

The IgH locus undergoes class switch recombination (CSR) from IgM to IgA.

(A) Activation-induced cytidine deaminase (AID) deaminates dC residues in both strands of the transcriptionally active switch regions (S regions), generating clustered lesions. This is eventually processed by intrachromosomal deletion into double-strand DNA breaks (DSBs).

(B) Repair proteins initiate double-strand break repair and fuse the 2 switch regions

(C) The intervening sequence is excised to form an extra-chromosomal switch circle, and the IgH locus is class switched to IgA

Figure adapted from (159).

Affinity maturation in the germinal centre

Upon exposure to an antigen, antigen specific antibodies undergo affinity maturation – a phenomenon where the affinity of the antibodies to the antigen increases over time (95, 96). This process occurs in the germinal centre (GC), and is a result of iterative rounds of selection of high affinity mutants generated by somatic hypermutation (SHM) that is driven by AID (97-99). Multiple rounds of selection and subsequent proliferation result in an antibody population that binds with high affinity to the antigen (95, 96).

The formation of GCs begin with resting B cells encountering and capturing antigen (100, 101). The mature GC has 2 different compartments – the dark zone, consisting of proliferating B cells, and the light zone, consisting of GC B cells, follicular dendritic cells (FDCs), infiltrating naïve B cells (102), and T follicular helper (Tfh) cells (103, 104). Proliferation and hypermutation occur in the dark zone, while antigen-driven selection of high affinity B cells occur in the light zone, and cells migrate between both zones in iterative cycles known as cyclic re-entry during affinity maturation (105, 106). AID is expressed in B cells in the dark zone, where it inserts point mutations in the V regions of the heavy and light chains of immunoglobulins (97, 98). The chemokine receptor CXCR4 is important for ensuring that GC B cells remain in the dark zone. After many cycles of proliferation, CXCR5 is upregulated, allowing B cells to migrate to the light zone (107-109). B cells in the light zone of GCs capture and internalise antigen, held on FDCs, and subsequently present captured antigen to Tfh cells (100, 101). Different amounts of peptide-MHCII complexes are present on the surface densities of different B cells, depending on the affinity to the ligand, and the strength of its interaction with Tfh cells drives selection of higher affinity B cells (99, 107, 109). This is mediated by pro-survival cytokine BAFF, B cell cytokines IL-4 and IL-21, as well as through the upregulation of feed-forward loops (such as ICOSL on B cells and CD40L on T cells), that promote survival of B cells with high affinity mutations (110). B

cells with low affinity mutations do not survive in the light zone. T cell help also triggers cyclic re-entry into the dark zone.

The GC reaction can take 1-2 weeks (soluble protein) to multiple months (infections) (111), and the life span of the GC varies depending on the immune stimulus. After affinity maturation, high affinity B cells interrupt cyclic re-entry and differentiate into either plasma cells or memory B cells. Studies have suggested that higher affinity B cells differentiate into plasma cells (112-114), while lower affinity B cells preferentially differentiate into memory B cells (115). B cell fate choice is also dependent on the course of the antibody response – memory B cells are generated earlier, during the pre-GC and early GC periods, while plasma cells are generated later on in the antibody response (116).

Recent studies in HIV-1 infected individuals who develop broadly neutralizing antibodies (bnAbs) show that these bnAbs are developed through extreme amounts of SHM, with as many as 30% of nucleotides in the V region of the bnAbs differing from their original germline sequence (117), and have additional gene modifications such as nucleotide insertions and deletions (118). It is thus unsurprising that these bnAbs are rare, and only occur in 1-2% of HIV-1 infected individuals. A challenge in the development of a HIV-1 vaccine would thus be how to increase SHM by vaccination, in order to accumulate the high numbers of mutations necessary for broad neutralization, as most GCs induced by vaccination are short-lived and disappear after 3-4 weeks (119).

Antibody receptors

Fc receptors (FcRs) bind to immunoglobulins, and are expressed on hematopoietic cells. Binding of antibody immune complexes to FcRs activates effector cells, leading to antibody-mediated immune responses that link humoral and cellular responses. Fc receptors

are present for all immunoglobulin classes (Table 1.3). In humans, IgG associate with the FcγR family, while IgA associate with FcαRI.

Three classes of Fcγ receptors have been described – FcγRI, FcγRII (FcγRIa, FcγRIIb, FcγRIIc), and FcγRIII (FcγRIIIa, FcγRIIIb). FcγRI, FcγRIIa, FcγRIIc, and FcγRIIIa are activating receptors. FcγRIIa and FcγRIIc contain the activatory signal transduction ITAM motif, while FcγRI and FcγRIIIa interacts with the ITAM-containing FcRγ or T-cell receptor ζ (for FcγRIIIa only) for signaling. Binding of IgG immune complexes to activating Fcγ receptors result in the binding of src family kinases to the tyrosines in the ITAM motif and their subsequent phosphorylation. Different kinases bind depending on the particular cell type activated by the Fcγ receptor - FcγRIIIA activates lck in NK cells, and lyn and hck in monocytic and mast cells (120, 121). This triggers downstream signaling pathways, including the activation of PI3 kinase and the recruitment of PH domain-containing molecules, including Tec kinases (e.g. Btk, Itk, and Emt) (122). The binding of monomeric IgG to FcγRIIa may also result in the suboptimal phosphorylation of the ITAM motif, resulting in the generation of inhibitory signals (123).

FcγRIIb is an inhibitory receptor, and contains an immunoreceptor tyrosine-based inhibitory motif (ITIM). ITIM recruits SHIP1 (SH2 domain-containing inositol 5′ - phosphatase 1) and SHP-2, which are phosphatases, and subsequently leads to the dissociation of PH domain containing proteins, and the inhibition of ITAM-triggered calcium release (124, 125). FcγRIIb also influences B-cell selection and subsequently antibody affinity maturation. Engagement of FcγRIIb exclusively on B cells induces pro-apoptotic signals, while co-ligation of FcγRIIb with the B-cell receptor attenuates these signals. The remaining FcγRIIIb receptor contains no signaling component, and is thought to act synergistically with other receptors like FcγRIIa, or integrins, and uses their signaling apparatus for signal transduction and cell activation. FcγRIIIb has been reported to activate

complement receptor dependent inflammatory pathways. Different Fcγ receptors have different affinities towards different IgG subclasses (Table 1.3).

The ITAM or ITIM-mediated signaling eventually influences the cytotoxicity of effector cells, including phagocytosis, induction of ADCC, induction of respiratory burst, and the degranulation of cells such as eosinophils, which are dependent on calcium release. (126) They also modulate immune responses directly by affecting different leukocyte populations, such as modulating the differentiation and activation of APCs, modulating the release of cytokines and chemokines, enhancing the uptake of antigen and its presentation on APCs, regulating T cell activation by APCs, modulating affinity maturation, and plasma cell survival and regulation of antibody production (127). IgG and Fc receptors also interact with the complement system, helping to remove opsonized inflammatory and infectious agents and enhancing immune responses (reviewed in (128))

FcαRI is expressed on cells of the myeloid lineage, including neutrophils, monocytes, macrophages and eosinophils (129-133). Unlike the FcγR family, FcαRI does not contain any known signaling motifs in its cytoplasmic tail, and has to associate with the 2 FcγR subunits for signal transduction (134). Binding of FcαRI by polymeric IgA result in activating signal transduction pathways. IgA immune complexes bind FcαRI, resulting in cross-linking, and the association of FcαRI with the FcRγ subunit, which contains an immunoreceptor tyrosine-based activation motif (ITAM). The Src protein tyrosine kinase Lyn phosphorylates the tyrosines within the ITAM, which serve as docking sites for Syk, another tyrosine kinase (135-137). This triggers the activation of multiple downstream targets, including Phosphoinositide 3-kinase (PI3K), Raf-1-MEK-MAP kinases, and eventually calcium and cytokine release (135, 138, 139). FcαRI also relocates to sphingolipid-cholesterol membrane rafts following cross-linking (135). The activatory properties of FcαRI include the induction of phagocytosis in polymorphonuclear leukocytes, the induction of respiratory burst activity,

ADCC, and the release of inflammatory mediators and cytokines. FcαRI also facilitates antigen presentation (129, 140).

Monomeric IgA interacts only transiently with FcαRI, FcαRI predominantly associates with polymeric IgA (141); complement receptor 3 (Mac-1) is crucial for dimeric or polymeric SIgA binding of FcαRI (142). FcαRI is a bi-functional receptor, and the low valency of monomeric IgA binding instead results in inhibitory ITAM signaling through the FcαRI-FcγR chain complex (143). The inhibitory molecule SHP-1 (Src homology region 2 domain-containing phosphatase-1), a tyrosine phosphatase, is recruited by Syk, and dephosphorylates and downregulates activating receptors (143, 144). FcαRI also binds IgA in the absence of the FcRγ chain, protecting them from degradation, and recycling internalized serum IgA (145, 146).

Both IgG and IgA also bind to other receptors. IgA binds to asialoglycoprotein receptor that may be involved in clearing IgA from the blood, in particular IgA2 (147, 148). Transferrin receptor selectively binds IgA1 (149). The secretory component receptor binds the secretory component and SIgA (150), but not serum IgA, triggering the degranulation of eonsinophils and basophils (150-152).

TRIM21 binds to the Fc domain of IgG, and acts as an immunological sensor, targeting IgG-opsonized microorgansims for antibody-dependent intracellular neutralization by the ubiquitin-dependent proteasome (153-156). DC-SIGN binds to the CH2–CH3 interface of the Fc domain of IgG due to charged sialic acid (47), and is thought to upregulate expression of the inhibitory FcγRIIb (157). Fc receptor-like proteins, FCRL4 and FCRL5, was found to bind some IgG subclasses and IgA, and is thought to be involved in negative feedback inhibition through antigen-specific IgG and IgA (158). CD23 binds to sialylated IgG Fc, and regulates IgG affinity maturation and responses, by inducing FcγRIIb on B cells.

Table 1.3 – Human Antibody/Fc receptor binding

The number of (+) symbols represent the affinity of respective antibody-Fc receptor binding. The greater the number of (+) symbols, the higher the binding affinity.

	IgM	**IgD**	**IgG1**	**IgG2**	**IgG3**	**IgG4**	**IgA1**	**IgA2**	**IgE**
Serum concentration (mg/mL)	1.5	0.03	9	3	1	0.5	3	0.5	10^{-4}
Half life (days)	5	3	23	23	8	23	6	6	2.5
Antibody/FcR binding affinity									
FcγRI (CD64)	-	-	++++	-	++++	+++	-	-	-
FcγRII (CD32)									
FcγRIIa (R131)	-	-	++	+	++	+/-	-	-	-
FcγRIIa (H131)	-	-	++	++	++	-	-	-	-
FcγRIIb	-	-	++	+	++	++	-	-	-
FcγRIII (CD16)									
FcγRIIIa	-	-	++	(+/-)	(+/-)	(+/-)	-	-	-
FcγRIIIb	-	-	++	?	++	?	-	-	-
FcεRI	-	-	-	-	-	-	-	-	++++
FcεRII (CD23)	-	-	-	-	-	-	-	-	++
FcδR	-	+	-	-	-	-	-	-	-
FcαR (CD89)	-	-	-	-	-	-	+	+	-
PolyIg	+	-	-	-	-	-	++	++	-
FcRn (placental transfer)	-	-	+	+	+	+	-	-	-

COMPARISON OF THE HUMORAL IMMUNE SYSTEM BETWEEN MICE, RHESUS MACAQUES, AND HUMANS

The following section is a comparison of the differences in the antibody responses between these different species, to be able to put the humoral response following vaccination in different animal models in perspective.

Comparison of mouse and humans IgG and IgA antibody responses

The murine subclasses include IgG1, IgG2b, IgG2a or IgG2c, and IgG3. The C57BL/6, NOD, and SJL strains of mice contain the gene for IgG2c, but not IgG2a, while BALB/c mice and mice of many other strains contain the gene for IgG2a, but not IgG2c (160). The binding of mouse IgG subclasses to mouse Fcγ receptors are different from humans as well, and will be discussed further in the section below. Furthermore, class switching from IgM to the IgG subclasses in mice is different to humans, in that in mice, IgM class switches directly to each of the four IgG subclasses early on in the antibody response, before SHM, and there is generally little class switching between the different IgG subclasses (160).

Mouse IgA is mostly polymeric in serum, while it is predominantly monomeric in human serum (129), and it does not bind to SSL7 (Staphylococcal Superantigen-like 7) (161), unlike human and macaque IgA (162, 163).

Comparison of rhesus macaque and humans IgG and IgA antibody responses

While there are also four different IgG macaque subclasses, IgG1, IgG2, IgG3, and IgG4, not much is known about their properties, and how they compare to the human IgG subclasses. Different studies have shown contradictory results into the functions of primate IgG subclasses – an early study observed similar subclass activities between cynomolgus/rhesus macaque and human IgG (164, 165), while a more recent study showed

divergent activity profiles between macaque and human IgG subclasses (166). Sequence alignment of the four Indian rhesus macaque (*macaca mulatta*) subclasses suggest that the IgG subclasses were more similar to each other than to any human subclass, and most macaque IgG subclasses were the most similar to human IgG – for both the CH2 region (responsible for FcγR recognition), and also for the Fc region (167). Compared to human IgG subclasses, the rhesus macaque subclasses possessed a more uniform binding and functional profile, with IgG1 exhibiting the highest activity, followed by IgG2, then IgG3/IgG4 (167). This corresponded to observations that cynomolgus macaque IgG subclasses are more uniformly active than human IgG subclasses (166, 168). The IgG-FcγR binding activity of humans IgG is not well matched to that of macaques. The less functional human IgG2 and IgG4 are not extremely similar to macaque subclass variants, while human IgG3, which has superior activity in cell-based functional assays, is not structurally similar to any macaque IgG subclass. The four macaque IgG subclasses generally exhibit uniform FcγRI and FcγRII binding and phagocytosis activity profiles in assays using human cells, different from their nominal human IgG counterparts. In serum of rhesus macaques, IgG1 (both in terms of transcript expression and antibody) was the predominant subclass, followed by IgG2 and IgG3, while IgG4 was of the lowest prevalence (165, 167, 169).

One of the main differences between human and macaque IgA is that human IgA consists of two IgA subclasses, IgA1 and IgA2 (as described earlier), while macaque IgA only consists of one subclass. Furthermore, there is a high level of intraspecies heterogeneity in the Cα chain (58, 60, 170), with hinge regions containing different numbers of proline residues, suggesting that rhesus macaque IgA be of variable structure and sequence (171). This variability could contribute to the contradictory information available on the susceptibility of rhesus macaque IgA molecules to bacterial proteases (171-173). It is thus possible that macaque IgA may have different effector functions, and may have additional

protective IgA mechanisms. Purified IgA from vaccinated and SIV-infected rhesus macaques have been shown to have multifunctional effector activities, including phagocytic, neutralizing, and transcytosis-inhibiting activities (162).

Comparison of mouse and humans IgG and IgA Fc receptors

Four classes of Fcγ receptors have been described for mice: the activating FcγRI, FcγRIII, FcγRIV, and the inhibitory FcγRIIb. The three activating mouse FcγRs need to associate with an ITAM-bearing FcRγ for signal transduction, while FcγRIIb contains an ITIM in the cytoplasmic tail (Table 1.4). Amino acid sequence comparisons between mice and human FcγRs show that there are orthologous proteins between the two species. The orthologous mouse and human Fcγ receptors, as well as the main differences between the two, are detailed in Table 1.4. No homologous mouse receptors exist for human FcγRIIc and FcγRIIIb. Mouse Fcγ receptors also bind human IgG subclasses, while human Fcγ receptors do not bind to mouse IgG subclasses – allowing human antibodies with potential therapeutic applications to be evaluated using mouse models (174, 175).

There are no orthologous mouse receptors for human FcαRI, however, mouse Fcα/μR binds to both IgA and IgM, and is expressed on B lymphocytes and macrophages (176, 177).

Comparison of rhesus macaque and humans IgG and IgA Fc receptors

Three classes of Fcγ receptors have been found for macaques: FcγRI, FcγRII (FcγRIIa and FcγRIIb), and FcγRIII. The Fcγ receptors for both species are very similar in amino acid sequences, although macaque Fcγ receptors are very polymorphic in terms of genetic heterogeneity, as well as in potential N-linked glycosylation sites (175). The orthologous macaque and human Fcγ receptors, as well as the main differences between the two, are

detailed in Table 1.4. The orthologous macaque receptor for human FcαRI is macaque FcαRI (178-180).

While macaque FcαRI remains poorly identified, it is highly homologous to its human orthologous form, but share similar cellular expression patterns on different cell types. Despite the heterogeneity in IgA hinge sequences in macaques, macaque IgA still appears to bind to the recombinant form of macaque FcαRI (178).

Table 1.4 – Comparison between human, mouse, and macaque Fcγ receptors

Reviewed in (175). Human receptors are in gray columns, mouse receptors are in blue columns, and macaque receptors are in red columns. Orthologous receptors are grouped together.

(continued on next page)

	FcγRI			FcγRII		
	FcγRI	**FcγRI**	**FcγRI**	**FcγRIIA**	**FcγRIII**	**FcγRIIA**
Protein size (a.a.)	374	404	342	316	267	288
Type of protein	3 Ig-like domains, TM domain, CY tail	3 Ig-like domains, TM domain, CY tail	3 Ig-like domains, TM domain, CY tail	2 Ig-like domains, TM domain, CY tail	2 Ig-like domains, TM domain, CY tail	2 Ig-like domains, TM domain, CY tail
Polymorphism			3 allelic polymorphic residues (V6G, Q18R, V60A)	2 allelic forms (H131, R131) which influences binding to IgG2	Several polymorphic variants, but no effect on binding to ligand	9 allelic polymorphic residues (M55R, V791, T93P, A119T, K1251, S126A, N128K, N113D, Q142R) Unkown effect on ligand affinities
Cellular activation type	Activating	Activating	Activating	Activating	Activating	Activating
Signalling	γ2	γ2	γ2	ITAM		ITAM
Ligands & affinity	IgG1: 6.5 X 10^7 M^{-1} IgG3: 6.1 X 10^7 M^{-1} IgG4: 3.4 X 10^7 M^{-1}	IgG2a: 2.6 X 10^7 M^{-1} IgG2b, IgG3: low affinity	Cyno: IgG1: 7.1 X 10^9 M^{-1} IgG2: 2.5 X 10^9 M^{-1} IgG3: 3.2 X 10^9 M^{-1} IgG4: 3.3 X 10^7 M^{-1}	IgG1: 5.2/3.5 X 10^6 M^{-1} IgG2: 4.5/1.0 X 10^5 M^{-1} IgG3: 8.9/9.1 X 10^5 M^{-1} IgG4: 1.7/2.1 X 10^5 M^{-1}	IgG1: 3.2 X 10^5 M^{-1} IgG2a: 6.9 X 10^5 M^{-1} IgG2b: 6.5 X 10^5 M^{-1} IgE: 2 X 10^4 M^{-1}	Cyno: IgG1: 9.4 X 10^5 M^{-1} IgG2: 4.7 X 10^5 M^{-1} IgG3: 5.2 X 10^5 M^{-1} IgG4: 3.7 X 10^5 M^{-1}
Cellular expression	Monocytes / macrophages, neutrophils, DCs, mast cells	Monocyte-derived DCs	Unknown, but probably similar to humans	Monocytes/ macrophages, neutrophils, DCs, basophils, mast cells, eosinophils, platelets	NK cells, monocytes / macrophages, neutrophils, DCs, basophils, mast cells, eosinophils	NK cells, monocytes/ macrophages, granulocytes for cynomolgus
Sequence homology to human	NA	75% (EC and TM domain)	94-95%	NA	-	88-90%
Similarities		High affinity receptor No ITAM in cytoplasmic domain	High affinity receptor No ITAM in cytoplasmic domain Binds IgG1, IgG3, & IgG4		Low affinity receptor Cellular expression	Low affinity receptor Contains an ITAM in cytoplasmic domain
Differences		Only binds IgG2a (binds IgG2b and IgG3 with low affinity) Cellular expression	Binds IgG2 Higher affinity for IgG4		Does not contain an ITAM Binds IgE Cellular expression hFcγRIIA contains 2 allelic forms that affect binding affinities	hFcγRIIA contains 2 allelic forms that affect binding affinities Expression higher on granulocytes

Table 1.4 – Comparison between human, mouse, and macaque Fcγ receptors (continued)

Reviewed in (175). Human receptors are in gray columns, mouse receptors are in blue columns, and macaque receptors are in red columns. Orthologous receptors are grouped together.

	FcγRII				FcγRIII			
	FcγRIIB	**FcγRIIB**	**FcγRIIB**	**FcγRIIC**	**FcγRIIIA**	**FcγRIV**	**FcγRIII**	**FcγRIIIB**
Protein size (a.a.)	310	329	294	323	254	240		233
Type of protein	2 Ig-like domains, TM domain, CY tail	2 Ig-like domains, TM domain, CY tail	2 Ig-like domains, TM domain, CY tail	2 Ig-like domains, TM domain, CY tail	2 Ig-like domains, TM domain, CY tail	2 Ig-like domains, TM domain, CY tail	2 Ig-like domains, TM domain, CY tail	2 Ig-like domains, TM domain
Polymorphism		Several polymorphic variants, but no effect on binding to ligand	9 allelic polymorphic residues (M55R, V791, T93P, A119T, K1251, S126A, N128K, N113D, Q142R) Unkown effect on ligand affinities		2 allelic forms (F158, V158) V158 shows increased affinity for IgG1		Several polymorphic variants Unknown effect on binding to ligand	3 allelic forms (multiple amino acid subsitutions in the extracellular domain, NA1, NA2, SH)
Cellular activation type	Inhibitory	Inhibitory	Inhibitory	Activating	Activating	Activating	Activating	Unknown
Signalling	ITIM	ITIM	ITIM	ITAM	γ2	γ2	γ2	a-GPI
Ligands & affinity	IgG1: 1.2 X 10^5 M^{-1} IgG2: 2 X 10^4 M^{-1} IgG3: 1.7 X 10^5 M^{-1} IgG4: 2.0 X 10^5 M^{-1}	IgG1: 3.3 X 10^5 M^{-1} IgG2a: 4.2 X 10^5 M^{-1} IgG2b: 2.3 X 10^6 M^{-1} IgE: 2 X 10^4 M^{-1}	Cyno: IgG1: 8.6 X 10^5 M^{-1} IgG2: 5.2 X 10^5 M^{-1} IgG3: 2.8 X 10^5 M^{-1} IgG4: 2.0 X 10^5 M^{-1}	IgG1: 1.2 X 10^5 M^{-1} IgG2: 2 X 10^4 M^{-1} IgG3: 1.7 X 10^5 M^{-1} IgG4: 2 X 10^5 M^{-1}	IgG1: 2.0/1.17 X 10^6 M^{-1} IgG2: 7/3 X 10^4 M^{-1} IgG3: 8/77 X 10^5 M^{-1} IgG4: 2.5/2.0 X 10^5 M^{-1}	IgG2a: 2.9 X 10^7 M^{-1} IgG2b: 1.7 X 10^7 M^{-1} IgE: 2.4 X 10^5 M^{-1}	Cyno: IgG1: 2.1 X 10^6 M^{-1} IgG2: 4.2 X 10^5 M^{-1} IgG3: 1.6 X 10^6 M^{-1} IgG4: 3.5 X 10^5 M^{-1}	IgG1: 2.0 X 10^5 M^{-1} IgG3: 1 X 10^5 M^{-1}
Cellular expression	B cells, monocytes / macrophages, neutrophils, DCs, basophils	B cells, monocytes / macrophages, neutrophils, DCs, basophils, mast cells, eosinophils	NK cells, monocytes / macrophages, granulocytes for cynomolgus	NK cells, monocytes / macrophages, neutrophils	NK cells, monocytes / macrophages	Monocytes / macrophages, neutrophils	NK cells, monocytes / macrophages	Neutrophils / basophils
Sequence homology to human	NA	63%	88-90%		NA	65%	91.7%	
Similarities		Low affinity receptor ITIM in cytoplasmic domain Cellular expression	Low affinity receptor ITIM in cytoplasmic domain			Cellular expression No ITAM in cytoplasmic domain Binds defucosylated IgG with higher affinity	Low affinity receptor Binds defucosylated IgG with higher affinity No ITAM in cytoplasmic domain	
Differences		Binds IgE Cellular expression Mouse FcγRIIIB has similar ligand affinity as activating receptor, while human FcγRIIB has lower ligand affinity than human activating receptors	mac FcγRIIB has higher affinity for ligands Binds IgG2 Expression higher on granulocytes			Binds IgE Is a high affinity receptor Cellular expression human FcγRIIIA has 2 allelic forms that influence binding affinities	Higher affinity for IgG2 and IgG4 human FcγRIIIA has 2 allelic forms that influence binding affinities	

PARENTERAL IMMUNIZATION INDUCES MUCOSAL IMMUNE RESPONSES

The generation of a strong immune response at mucosal sites following vaccination is important for protection against infection against microorgansims invading the body via mucosal surfaces. It has been reported that immunization via the mucosal route elicits the greatest mucosal immune responses at both local and distal immune mucosal sites in other mucosal tissues, and this has been frequently referred to as the 'common mucosal system' (181), where the lymphatic system and blood serve as a conduit for precursor cells to migrate from inductive sites to distal mucosal tissues and glands (182, 183). To that end, much research has been focused on developing vaccines for administration via the mucosal route, rather than conventional parenteral injections (reviewed in (184-187). Successful mucosal vaccines that are currently licensed for human use are usually administered via the oral or nasal route, and include the live-attenuated poliovirus vaccine administered via the oral (188-190), live attenuated influenza vaccine (FluMist) administered via the nasal route (191), oral vaccines against typhoid fever (192), cholera (193-195) and rotavirus gastroenteritis (196, 197). However, in general, mucosal vaccination has its limitations. Immunization via the oral route runs the risk of the vaccine antigen degrading in the gastrointestinal tract (e.g. by gastric acid, mucins and digestive enzymes), or being cleared by peristalsis and mucus secretion, before they even reach the mucosal immune system. Additionally, tolerance against the vaccine antigen may likely be induced by mucosal immunizations, especially since a homeostatic condition is needed at mucosal sites, where they encounter many beneficial antigens (e.g. via ingestion of food or commensal microbiota) (198).

While parenteral immunization has long been thought to by unable to induce protective immune responses at mucosal surfaces, there have been increasing number of studies that suggest that some systemically administered vaccines are in fact capable of eliciting mucosal immune responses, and there are multiple licensed vaccines administered via a parenteral

route that do induce mucosal immunity and are protective against infection by viruses that enter the body through various mucosal sites (199, 200) (Table 1.5). Additionally, there have been multiple *in vivo* studies in animal models which demonstrate that immunizations via a systemic route are able to induce a mucosal immune response (reviewed in (199)).

While most parenteral immunizations predominantly induce IgG responses, IgA antibody secreting cells (ASCs) in systemic circulation have been reported to be induced by parenteral immunization. Polymeric IgA have been observed in serum following vaccination (201), and antigen-specific IgA detected in saliva as well (202, 203). It is thought that systemic antibodies induced by vaccination find their way to the mucosal compartment, either by constitutive transcellular/paracellular transport of IgG from the systemic compartment and other specific transport mechanisms, or by transudation from the systemic compartment to the mucosal compartment.

A well-known example of a licensed vaccine administered via the parenteral route that protects against virus replication in the mucosa is the inactivated polio vaccine. It has been hypothesized that the high levels of IgG induced post vaccination were transudated to the nasopharyngeal surface, and antigen-specific IgA has also been detected in milk, saliva and nasopharyngeal surfaces (reviewed in (204)). The pertussis vaccine protects against infection of the respiratory mucosal surface by Bordetella pertussis (205). The conventional influenza vaccine is also administered systemically, with studies showing that it produces antibody responses in mucosal secretions (90, 206-208), although it is debatable as to whether the antibody response is serum-derived or induced by local cellular responses (209, 210). There are many other instances where parenteral immunization does induce protection against infection and disease in the mucosal compartments, such as the gastroenteric and nasopharyngeal tracts (Table 1.5). Mucosal surfaces represent the main portals of entry for

HIV-1, and as such, it is likely that any prophylactic HIV-1 vaccines administered systemically will need to induce a substantial mucosal antibody response.

While it has been argued that a mucosal vaccine is required to elicit strong mucosal responses, many studies, both in animal models and in humans have shown that a systemic immunization is capable of eliciting a strong mucosal immune response, and indeed, there have been multiple licensed systemic vaccines that are targeted against viruses that are transmitted via the mucosal route, and are able to elicit strong mucosal responses (211).

Table 1.5 – licensed vaccines administered via a systemic route that induce mucosal antibody responses against viruses transmitted via a mucosal route

Reviewed in (200)

Vaccine	Efficacy	Transmission route	Disease Site	Inhibition of mucosal replication?
Inactivated polio vaccine	~ 95%	Faecal-oral and oral-oral	Systemic (central nervous system - CNS)	Yes (respiratory tract (RT) and gastrointestinal tract)
Haemophilus influenzae	~ 95%	Respiratory	Systemic (CNS)	65% (RT)
Pertussis	85-95%	Respiratory	Respiratory mucosae	Unknown
Meningococcal polysaccharide	~ 85%	Nasopharyngeal	Systemic (CNS)	50% (RT)
Influenza subunit	~ 65%	Respiratory	Mucosae/Systemic	90% (RT)
Cholera	~ 50%	Faecal-oral	Mucosae	Unknown
Typhoid	50-75%	Faecal-oral	Mucosae/Systemic	Unknown

MICROPARTICLES AS A VACCINATION AND DRUG DELIVERY STRATEGY

Advantages of using controlled release as a vaccination strategy

The use of controlled release as a vaccination strategy/modality could potentially reduce the need for multiple administrations of the vaccine. This is especially advantageous in the developing world, where patients may have limited access to healthcare, and may not return for a full vaccination regimen with multiple immunizations. This has an additional economic benefit, where the costs related to vaccination programmes – including costs related to personnel and management required to administer the vaccine – would be significantly lowered (212).

The antigen is dispersed throughout a matrix of biodegradable polymer, and upon polymer degradation, it is released into the local microenvironment. Modifications of the polymer composition and formulation method would change the release kinetics of the encapsulated antigen, enabling control of when antigen can be delivered.

PLGA as a polymer and adjuvant

There are several biodegradable polymers that have traditionally been tested for controlled release formulations, these include natural materials like starch and alginate, which degrade via enzymes found in the body, as well as synthetic materials like hydrogels, polyanhydrides and polyesters, which degrade by chemical or enzymatic hydrolysis. Synthetic materials have better reproducibility and are available in multiple different compositions, allowing alterations during polymer processing to achieve the desired release kinetics, while natural materials have more inherent variability, and are more difficult to alter (213) (Sterilization, toxicity, biocompatibility and clinical applications of polylactic acid/polyglycolic acid copolymers.).

The most common biodegradable polymer used in these formulations is poly(lactic-co-glycolic acid) (PLGA). It is well characterised, is Food and Drugs Administration (FDA) approved, has been used as an absorbable suture material since 1974 (214, 215), and has been widely used in many different drug delivery studies, including for vaccines, antibiotics, analgesics, anti-inflammatory drugs and chemotherapeutics (216) .

PLGA degradation *in vivo* occurs by the hydrolysis of ester linkages within the PLGA polymer, resulting in lactic and glycolic acid. As the polymer degrades down to a certain size (about 15 monomer units in length), it becomes soluble and diffuses out of the matrix, resulting in the release of the encapsulated antigen, and a resulting loss of structure. Changing the molecular weight of PLGA used, the composition of lactic:glycolic acid, and adding an end cap (e.g. a carboxylic acid end group) will change the release kinetics and how fast the polymer degrades. Microparticles can be formulated to continuously deliver antigen after an initial burst, or to exhibit pulsatile release to mimic more traditional bolus injections in a vaccination regimen. Antigen can be released over a period days, weeks, or months, depending on the formulation method and polymer used (212).

Encapsulation of antigen in PLGA microparticles have been found to enhance both the T cell and antibody responses (217, 218), as well as subsequent memory antibody responses (219), when compared to bolus immunizations. Recent studies have suggested that microspheres activate the NACHT, LRR and PYD domains-containing protein 3 (NALP3) inflammasome in dendritic cells (220).

While there are many papers in the field studying the immunogenicity of microspheres, most use Bovine Serum Albumin (BSA), or the tetanus toxoid as a model antigen. Few studies have investigated the immunogenicity of encapsulating the HIV-1 Env protein (221).

OVERVIEW

The correlates of protection of RV144 suggest that vaccine-elicited antibody responses are likely to be important for a successful HIV-1 vaccine. Furthermore, as HIV-1 transmission typically occurs at mucosal sites, vaccine-elicited mucosal antibodies are probably important as well. It is thus important to evaluate IgG and IgA responses to HIV-1 vaccine candidates, as well as to develop alternatives to existing HIV-1 vaccination strategies, such as by microparticle-based vaccine delivery strategy.

In this dissertation, I evaluated systemic and mucosal antibody responses against different HIV-1 vaccine candidates. I hypothesize that HIV-1 vaccine candidates administered via the parenteral route can induce coordinated mucosal and systemic immune responses, and that we can improve the induction of these antibody responses via novel delivery methods. In chapter 2, I investigated the common features of mucosal and peripheral antibody responses following parenteral immunization of rhesus monkeys with Adenovirus ad Env HIV-1 vaccine candidates, focusing on the IgG response. Chapter 3 of this dissertation further investigates the relationship between mucosal and peripheral antibody responses, as well as the relationship between vaccine elicited systemic IgG and IgA in rhesus monkeys that were parenterally immunized with an Adenovirus/Env vaccine regimen. Finally, in Chapter 4, I evaluated the immunogenicity of a controlled antigen release vaccination regimen in a mouse model, using biodegradable poly (D, L-lactic-co-glycolic acid) (PLGA) microparticles encapsulating HIV-1 Env as a vaccine delivery modality, where antigen was continuously released over a period of weeks. We evaluated vaccine-induced IgG and IgA responses in the peripheral and mucosal compartments.

REFERENCES:

1. **Allan JS**, **Coligan JE**, **Lee TH**, **McLane MF**, **Kanki PJ**, **Groopman JE**, **Essex M**. 1985. A new HTLV-III/LAV encoded antigen detected by antibodies from AIDS patients. Science **230**:810–813.

2. **Allan JS**, **Coligan JE**, **Barin F**, **McLane MF**, **Sodroski JG**, **Rosen CA**, **Haseltine WA**, **Lee TH**, **Essex M**. 1985. Major glycoprotein antigens that induce antibodies in AIDS patients are encoded by HTLV-III. Science **228**:1091–1094.

3. **Barin F**, **McLane MF**, **Allan JS**, **Lee TH**, **Groopman JE**, **Essex M**. 1985. Virus envelope protein of HTLV-III represents major target antigen for antibodies in AIDS patients. Science **228**:1094–1096.

4. **Barré-Sinoussi F**, **Chermann JC**, **Rey F**, **Nugeyre MT**, **Chamaret S**, **Gruest J**, **Dauguet C**, **Axler-Blin C**, **Vézinet-Brun F**, **Rouzioux C**, **Rozenbaum W**, **Montagnier L**. 1983. Isolation of a T-lymphotropic retrovirus from a patient at risk for acquired immune deficiency syndrome (AIDS). Science **220**:868–871.

5. **Ho DD**, **Rota TR**, **Schooley RT**, **Kaplan JC**, **Allan JD**, **Groopman JE**, **Resnick L**, **Felsenstein D**, **Andrews CA**, **Hirsch MS**. 1985. Isolation of HTLV-III from cerebrospinal fluid and neural tissues of patients with neurologic syndromes related to the acquired immunodeficiency syndrome. N Engl J Med **313**:1493–1497.

6. **UNAIDS**. 2017. UNAIDS data 2017.

7. Basic Statistics | HIV Basics | HIV/AIDS | CDC. https://wwwcdcgov/hiv/basics/statisticshtml.

8. **Kuritzkes DR**, **Koup RA**. 2013. Chapter 50: HIV-1: Pathogenesis, Clinical Manifestations, and Treatment, pp. 1561–1583. *In* Knipe, DM, Howley, PM (eds.), Fields Virology, 6 ed. Two Commerce Square, 2001 Market Street, Philadelphia, PA 19103 USA.

9. **UNICEF**. 2016. United Nations Children's Fund, For Every Child, End AIDS – Seventh Stocktaking Report.

10. **Piot P**, **Bartos M**, **Ghys PD**, **Walker N**, **Schwartländer B**. 2001. The global impact of HIV/AIDS. Nature **410**:968–973.

11. **Freed EO**, **Martin MA**. 2013. Chapter 49: Human Immunodeficiency Viruses: Replication, pp. 1502–1560. *In* Knipe, DM, Howley, PM (eds.), Fields Virology, 6 ed. Fields Virology, Two Commerce Square, 2001 Market Street, Philadelphia, PA 19103 USA.

12. **Alkhatib G**, **Combadiere C**, **Broder CC**, **Feng Y**, **Kennedy PE**, **Murphy PM**, **Berger EA**. 1996. CC CKR5: a RANTES, MIP-1alpha, MIP-1beta receptor as a fusion cofactor for macrophage-tropic HIV-1. Science **272**:1955–1958.

13. **Choe H**, **Farzan M**, **Sun Y**, **Sullivan N**, **Rollins B**, **Ponath PD**, **Wu L**, **Mackay CR**, **LaRosa G**, **Newman W**, **Gerard N**, **Gerard C**, **Sodroski J**. 1996. The beta-chemokine receptors CCR3 and CCR5 facilitate infection by primary HIV-1 isolates.

Cell **85**:1135–1148.

14. **Deng H**, **Liu R**, **Ellmeier W**, **Choe S**, **Unutmaz D**, **Burkhart M**, **Di Marzio P**, **Marmon S**, **Sutton RE**, **Hill CM**, **Davis CB**, **Peiper SC**, **Schall TJ**, **Littman DR**, **Landau NR**. 1996. Identification of a major co-receptor for primary isolates of HIV-1. Nature **381**:661–666.

15. **Kao SY**, **Calman AF**, **Luciw PA**, **Peterlin BM**. 1987. Anti-termination of transcription within the long terminal repeat of HIV-1 by tat gene product. Nature **330**:489–493.

16. **Fischer U**, **Huber J**, **Boelens WC**, **Mattaj IW**, **Lührmann R**. 1995. The HIV-1 Rev activation domain is a nuclear export signal that accesses an export pathway used by specific cellular RNAs. Cell **82**:475–483.

17. **Wen W**, **Meinkoth JL**, **Tsien RY**, **Taylor SS**. 1995. Identification of a signal for rapid export of proteins from the nucleus. Cell **82**:463–473.

18. **Zhou W**, **Resh MD**. 1996. Differential membrane binding of the human immunodeficiency virus type 1 matrix protein. J Virol **70**:8540–8548.

19. **Hermida-Matsumoto L**, **Resh MD**. 1999. Human immunodeficiency virus type 1 protease triggers a myristoyl switch that modulates membrane binding of Pr55(gag) and p17MA. J Virol **73**:1902–1908.

20. **Fäcke M**, **Janetzko A**, **Shoeman RL**, **Kräusslich HG**. 1993. A large deletion in the matrix domain of the human immunodeficiency virus gag gene redirects virus particle assembly from the plasma membrane to the endoplasmic reticulum. J Virol **67**:4972–4980.

21. **Center RJ**, **Leapman RD**, **Lebowitz J**, **Arthur LO**, **Earl PL**, **Moss B**. 2002. Oligomeric Structure of the Human Immunodeficiency Virus Type 1 Envelope Protein on the Virion Surface. J Virol **76**:7863–7867.

22. **Weiss CD**, **Levy JA**, **White JM**. 1990. Oligomeric organization of gp120 on infectious human immunodeficiency virus type 1 particles. J Virol **64**:5674–5677.

23. **Arrildt KT**, **Joseph SB**, **Swanstrom R**. 2012. The HIV-1 env protein: a coat of many colors. Curr HIV/AIDS Rep **9**:52–63.

24. **Wei X**, **Decker JM**, **Wang S**, **Hui H**, **Kappes JC**, **Wu X**, **Salazar-Gonzalez JF**, **Salazar MG**, **Kilby JM**, **Saag MS**, **Komarova NL**, **Nowak MA**, **Hahn BH**, **Kwong PD**, **Shaw GM**. 2003. Antibody neutralization and escape by HIV-1. Nature **422**:307–312.

25. **Binley JM**, **Ban Y-EA**, **Crooks ET**, **Eggink D**, **Osawa K**, **Schief WR**, **Sanders RW**. 2010. Role of complex carbohydrates in human immunodeficiency virus type 1 infection and resistance to antibody neutralization. J Virol **84**:5637–5655.

26. **Benn S**, **Rutledge R**, **Folks T**, **Gold J**, **Baker L**, **McCormick J**, **Feorino P**, **Piot P**, **Quinn T**, **Martin M**. 1985. Genomic heterogeneity of AIDS retroviral isolates from North America and Zaire. Science **230**:949–951.

27. **Meyerhans A**, **Cheynier R**, **Albert J**, **Seth M**, **Kwok S**, **Sninsky J**, **Morfeldt-Månson L**, **Asjö B**, **Wain-Hobson S**. 1989. Temporal fluctuations in HIV quasispecies in vivo are not reflected by sequential HIV isolations. Cell **58**:901–910.

28. **Frey G**, **Peng H**, **Rits-Volloch S**, **Morelli M**, **Cheng Y**, **Chen B**. 2008. A fusion-intermediate state of HIV-1 gp41 targeted by broadly neutralizing antibodies. Proc Natl Acad Sci USA **105**:3739–3744.

29. **Rerks-Ngarm S**, **Pitisuttithum P**, **Nitayaphan S**, **Kaewkungwal J**, **Chiu J**, **Paris R**, **Premsri N**, **Namwat C**, **de Souza M**, **Adams E**, **Benenson M**, **Gurunathan S**, **Tartaglia J**, **McNeil JG**, **Francis DP**, **Stablein D**, **Birx DL**, **Chunsuttiwat S**, **Khamboonruang C**, **Thongcharoen P**, **Robb ML**, **Michael NL**, **Kunasol P**, **Kim JH**, **MOPH-TAVEG Investigators**. 2009. Vaccination with ALVAC and AIDSVAX to prevent HIV-1 infection in Thailand. N Engl J Med **361**:2209–2220.

30. **Haynes BF**, **Gilbert PB**, **McElrath MJ**, **Zolla-Pazner S**, **Tomaras GD**, **Alam SM**, **Evans DT**, **Montefiori DC**, **Karnasuta C**, **Sutthent R**, **Liao HX**, **DeVico AL**, **Lewis GK**, **Williams C**, **Pinter A**, **Fong Y**, **Janes H**, **DeCamp A**, **Huang Y**, **Rao M**, **Billings E**, **Karasavvas N**, **Robb ML**, **Ngauy V**, **de Souza MS**, **Paris R**, **Ferrari G**, **Bailer RT**, **Soderberg KA**, **Andrews C**, **Berman PW**, **Frahm N**, **De Rosa SC**, **Alpert MD**, **Yates NL**, **Shen X**, **Koup RA**, **Pitisuttithum P**, **Kaewkungwal J**, **Nitayaphan S**, **Rerks-Ngarm S**, **Michael NL**, **Kim JH**. 2012. Immune-correlates analysis of an HIV-1 vaccine efficacy trial. N Engl J Med **366**:1275–1286.

31. **Zolla-Pazner S**, **DeCamp A**, **Gilbert PB**, **Williams C**, **Yates NL**, **Williams WT**, **Howington R**, **Fong Y**, **Morris DE**, **Soderberg KA**, **Irene C**, **Reichman C**, **Pinter A**, **Parks R**, **Pitisuttithum P**, **Kaewkungwal J**, **Rerks-Ngarm S**, **Nitayaphan S**, **Andrews C**, **O'Connell RJ**, **Yang Z-Y**, **Nabel GJ**, **Kim JH**, **Michael NL**, **Montefiori DC**, **Liao HX**, **Haynes BF**, **Tomaras GD**. 2014. Vaccine-induced IgG antibodies to V1V2 regions of multiple HIV-1 subtypes correlate with decreased risk of HIV-1 infection. PLoS ONE **9**:e87572.

32. **Yates NL**, **Liao HX**, **Fong Y**, **DeCamp A**, **Vandergrift NA**, **Williams WT**, **Alam SM**, **Ferrari G**, **Yang Z-Y**, **Seaton KE**, **Berman PW**, **Alpert MD**, **Evans DT**, **O'Connell RJ**, **Francis D**, **Sinangil F**, **Lee C**, **Nitayaphan S**, **Rerks-Ngarm S**, **Kaewkungwal J**, **Pitisuttithum P**, **Tartaglia J**, **Pinter A**, **Zolla-Pazner S**, **Gilbert PB**, **Nabel GJ**, **Michael NL**, **Kim JH**, **Montefiori DC**, **Haynes BF**, **Tomaras GD**. 2014. Vaccine-induced Env V1-V2 IgG3 correlates with lower HIV-1 infection risk and declines soon after vaccination. Sci Transl Med **6**:228ra39–228ra39.

33. **Chung AW**, **Ghebremichael M**, **Robinson H**, **Brown E**, **Choi I**, **Lane S**, **Dugast A-S**, **Schoen MK**, **Rolland M**, **Suscovich TJ**, **Mahan AE**, **Liao L**, **Streeck H**, **Andrews C**, **Rerks-Ngarm S**, **Nitayaphan S**, **de Souza MS**, **Kaewkungwal J**, **Pitisuttithum P**, **Francis D**, **Michael NL**, **Kim JH**, **Bailey-Kellogg C**, **Ackerman ME**, **Alter G**. 2014. Polyfunctional Fc-effector profiles mediated by IgG subclass selection distinguish RV144 and VAX003 vaccines. Sci Transl Med **6**:228ra38–228ra38.

34. **Scharf O**, **Golding H**, **King LR**, **Eller N**, **Frazier D**, **Golding B**, **Scott DE**. 2001. Immunoglobulin G3 from polyclonal human immunodeficiency virus (HIV) immune

globulin is more potent than other subclasses in neutralizing HIV type 1. J Virol **75**:6558–6565.

35. **Tay MZ**, **Liu P**, **Williams LD**, **McRaven MD**, **Sawant S**, **Gurley TC**, **Xu TT**, **Dennison SM**, **Liao HX**, **Chenine A-L**, **Alam SM**, **Moody MA**, **Hope TJ**, **Haynes BF**, **Tomaras GD**. 2016. Antibody-Mediated Internalization of Infectious HIV-1 Virions Differs among Antibody Isotypes and Subclasses. PLoS Pathog **12**:e1005817.

36. **Tomaras GD**, **Ferrari G**, **Shen X**, **Alam SM**, **Liao HX**, **Pollara J**, **Bonsignori M**, **Moody MA**, **Fong Y**, **Chen X**, **Poling B**, **Nicholson CO**, **Zhang R**, **Lu X**, **Parks R**, **Kaewkungwal J**, **Nitayaphan S**, **Pitisuttithum P**, **Rerks-Ngarm S**, **Gilbert PB**, **Kim JH**, **Michael NL**, **Montefiori DC**, **Haynes BF**. 2013. Vaccine-induced plasma IgA specific for the C1 region of the HIV-1 envelope blocks binding and effector function of IgG. Proc Natl Acad Sci USA **110**:9019–9024.

37. **Ruiz MJ**, **Ghiglione Y**, **Falivene J**, **Laufer N**, **Holgado MP**, **Socías ME**, **Cahn P**, **Sued O**, **Giavedoni L**, **Salomón H**, **Gherardi MM**, **Rodríguez AM**, **Turk G**. 2016. Env-Specific IgA from Viremic HIV-Infected Subjects Compromises Antibody-Dependent Cellular Cytotoxicity. J Virol **90**:670–681.

38. **Bonsignori M**, **Pollara J**, **Moody MA**, **Alpert MD**, **Chen X**, **Hwang K-K**, **Gilbert PB**, **Huang Y**, **Gurley TC**, **Kozink DM**, **Marshall DJ**, **Whitesides JF**, **Tsao C-Y**, **Kaewkungwal J**, **Nitayaphan S**, **Pitisuttithum P**, **Rerks-Ngarm S**, **Kim JH**, **Michael NL**, **Tomaras GD**, **Montefiori DC**, **Lewis GK**, **DeVico A**, **Evans DT**, **Ferrari G**, **Liao HX**, **Haynes BF**. 2012. Antibody-dependent cellular cytotoxicity-mediating antibodies from an HIV-1 vaccine efficacy trial target multiple epitopes and preferentially use the VH1 gene family. J Virol **86**:11521–11532.

39. **Ferrari G**, **Pollara J**, **Kozink D**, **Harms T**, **Drinker M**, **Freel S**, **Moody MA**, **Alam SM**, **Tomaras GD**, **Ochsenbauer C**, **Kappes JC**, **Shaw GM**, **Hoxie JA**, **Robinson JE**, **Haynes BF**. 2011. An HIV-1 gp120 envelope human monoclonal antibody that recognizes a C1 conformational epitope mediates potent antibody-dependent cellular cytotoxicity (ADCC) activity and defines a common ADCC epitope in human HIV-1 serum. J Virol **85**:7029–7036.

40. **Pollara J**, **Bonsignori M**, **Moody MA**, **Liu P**, **Alam SM**, **Hwang K-K**, **Gurley TC**, **Kozink DM**, **Armand LC**, **Marshall DJ**, **Whitesides JF**, **Kaewkungwal J**, **Nitayaphan S**, **Pitisuttithum P**, **Rerks-Ngarm S**, **Robb ML**, **O'Connell RJ**, **Kim JH**, **Michael NL**, **Montefiori DC**, **Tomaras GD**, **Liao HX**, **Haynes BF**, **Ferrari G**. 2014. HIV-1 vaccine-induced C1 and V2 Env-specific antibodies synergize for increased antiviral activities. J Virol **88**:7715–7726.

41. **Lin L**, **Finak G**, **Ushey K**, **Seshadri C**, **Hawn TR**, **Frahm N**, **Scriba TJ**, **Mahomed H**, **Hanekom W**, **Bart P-A**, **Pantaleo G**, **Tomaras GD**, **Rerks-Ngarm S**, **Kaewkungwal J**, **Nitayaphan S**, **Pitisuttithum P**, **Michael NL**, **Kim JH**, **Robb ML**, **O'Connell RJ**, **Karasavvas N**, **Gilbert P**, **C De Rosa S**, **McElrath MJ**, **Gottardo R**. 2015. COMPASS identifies T-cell subsets correlated with clinical outcomes. Nat Biotechnol **33**:610–616.

42. **Plotkin SA**. 2013. Complex correlates of protection after vaccination. Clin Infect Dis

56:1458–1465.

43. **Tomaras GD**, **Plotkin SA**. 2017. Complex immune correlates of protection in HIV-1 vaccine efficacy trials. Immunol Rev **275**:245–261.

44. **Chung AW**, **Kumar MP**, **Arnold KB**, **Yu WH**, **Schoen MK**, **Dunphy LJ**, **Suscovich TJ**, **Frahm N**, **Linde C**, **Mahan AE**, **Hoffner M**, **Streeck H**, **Ackerman ME**, **McElrath MJ**, **Schuitemaker H**, **Pau MG**, **Baden LR**, **Kim JH**, **Michael NL**, **Barouch DH**, **Lauffenburger DA**, **Alter G**. 2015. Dissecting Polyclonal Vaccine-Induced Humoral Immunity against HIV Using Systems Serology. Cell **163**:988–998.

45. **Stephenson KE**, **D'Couto HT**, **Barouch DH**. 2016. New concepts in HIV-1 vaccine development. Current Opinion in Immunology **41**:39–46.

46. **Schroeder HW**, **Cavacini L**. 2010. Structure and function of immunoglobulins. J Allergy Clin Immunol **125**:S41–52.

47. **Vidarsson G**, **Dekkers G**, **Rispens T**. 2014. IgG subclasses and allotypes: from structure to effector functions. Front Immunol **5**:520.

48. **Roux KH**, **Strelets L**, **Michaelsen TE**. 1997. Flexibility of human IgG subclasses. J Immunol **159**:3372–3382.

49. **Hamilton RG**. 1987. Human IgG subclass measurements in the clinical laboratory. Clin Chem **33**:1707–1725.

50. **Barrett DJ**, **Ayoub EM**. 1986. IgG2 subclass restriction of antibody to pneumococcal polysaccharides. Clinical & Experimental Immunology **63**:127–134.

51. **Ferrante A**, **Beard LJ**, **Feldman RG**. 1990. IgG subclass distribution of antibodies to bacterial and viral antigens. Pediatr Infect Dis J **9**:S16–24.

52. **Larché M**, **Akdis CA**, **Valenta R**. 2006. Immunological mechanisms of allergen-specific immunotherapy. Nat Rev Immunol **6**:761–771.

53. **Su B**, **Moog C**. 2014. Which Antibody Functions are Important for an HIV Vaccine? Front Immunol **5**:289.

54. **Holl V**, **Peressin M**, **Decoville T**, **Schmidt S**, **Zolla-Pazner S**, **Aubertin A-M**, **Moog C**. 2006. Nonneutralizing antibodies are able to inhibit human immunodeficiency virus type 1 replication in macrophages and immature dendritic cells. J Virol **80**:6177–6181.

55. **Guilliams M**, **Bruhns P**, **Saeys Y**, **Hammad H**, **Lambrecht BN**. 2014. The function of Fcγ receptors in dendritic cells and macrophages. Nat Rev Immunol **14**:94–108.

56. **Ackerman ME**, **Dugast AS**, **McAndrew EG**, **Tsoukas S**, **Licht AF**, **Irvine DJ**, **Alter G**. 2013. Enhanced Phagocytic Activity of HIV-Specific Antibodies Correlates with Natural Production of Immunoglobulins with Skewed Affinity for Fc R2a and Fc R2b. J Virol **87**:5468–5476.

57. **Smalls-Mantey A**, **Connors M**, **Sattentau QJ**. 2013. Comparative efficiency of HIV-1-infected T cell killing by NK cells, monocytes and neutrophils. PLoS ONE **8**:e74858.

58. **Kawamura S**, **Saitou N**, **Ueda S**. 1992. Concerted evolution of the primate immunoglobulin alpha-gene through gene conversion. J Biol Chem **267**:7359–7367.

59. **Vaerman JP**, **Heremans JF**, **Van Kerckhoven G**. 1969. Communications. Identification of IgA in several mammalian species. J Immunol **103**:1421–1423.

60. **Kawamura S**, **Omoto K**, **Ueda S**. 1990. Evolutionary hypervariability in the hinge region of the immunoglobulin alpha gene. J Mol Biol **215**:201–206.

61. **Mattu TS**, **Pleass RJ**, **Willis AC**, **Kilian M**, **Wormald MR**, **Lellouch AC**, **Rudd PM**, **Woof JM**, **Dwek RA**. 1998. The glycosylation and structure of human serum IgA1, Fab, and Fc regions and the role of N-glycosylation on Fcα receptor interactions. J Biol Chem **273**:2260–2272.

62. **Royle L**, **Roos A**, **Harvey DJ**, **Wormald MR**, **Van Gijlswijk-Janssen D**, **Redwan E-RM**, **Wilson IA**, **Daha MR**, **Dwek RA**, **Rudd PM**. 2003. Secretory IgA N- and O-Glycans Provide a Link between the Innate and Adaptive Immune Systems. J Biol Chem **278**:20140–20153.

63. **Tomana M**, **Niedermeier W**, **Mestecky J**, **Skvaril F**. 1976. The differences in carbohydrate composition between the subclasses of IgA immunoglobulins. Immunochemistry **13**:325–328.

64. **Furtado PB**, **Whitty PW**, **Robertson A**, **Eaton JT**, **Almogren A**, **Kerr MA**, **Woof JM**, **Perkins SJ**. 2004. Solution Structure Determination of Monomeric Human IgA2 by X-ray and Neutron Scattering, Analytical Ultracentrifugation and Constrained Modelling: A Comparison with Monomeric Human IgA1. J Mol Biol **338**:921–941.

65. **Woof JM**, **Russell MW**. 2011. Structure and function relationships in IgA. Mucosal Immunol **4**:590–597.

66. **Bonner A**, **Almogren A**, **Furtado PB**, **Kerr MA**, **Perkins SJ**. 2009. The nonplanar secretory IgA2 and near planar secretory IgA1 solution structures rationalize their different mucosal immune responses. J Biol Chem **284**:5077–5087.

67. **Kaetzel CS**, **Robinson JK**, **Chintalacharuvu KR**, **Vaerman JP**, **Lamm ME**. 1991. The polymeric immunoglobulin receptor (secretory component) mediates transport of immune complexes across epithelial cells: a local defense function for IgA. PNAS **88**:8796–8800.

68. **Braathen R**, **Hohman VS**, **Brandtzaeg P**, **Johansen FE**. 2007. Secretory Antibody Formation: Conserved Binding Interactions between J Chain and Polymeric Ig Receptor from Humans and Amphibians. J Immunol **178**:1589–1597.

69. **Crago SS**, **Kutteh WH**, **Moro I**, **Allansmith MR**, **Radl J**, **Haaijman JJ**, **Mestecky J**. 1984. Distribution of IgA1-, IgA2-, and J chain-containing cells in human tissues. J Immunol **132**:16–18.

70. **Mantis NJ**, **Rol N**, **Corthésy B**. 2011. Secretory IgA's complex roles in immunity and mucosal homeostasis in the gut. Mucosal Immunol **4**:603–611.

71. **Russell MW**, **Kilian M**. 2005. Chapter 14 - Biological Activities of IgA, pp. 267–289. *In* Mestecky, J, Lamm, ME, McGhee, JR, Bienenstock, J, Mayer, L, Strober, W (eds.), Mucosal Immunology (Third Edition). Academic Press, Burlington.

72. **Stokes CR**, **Soothill JF**, **Turner MW**. 1975. Immune exclusion is a function of IgA. Nature **255**:745–746.

73. **Liévin-Le Moal V**, **Servin AL**. 2006. The front line of enteric host defense against unwelcome intrusion of harmful microorganisms: mucins, antimicrobial peptides, and microbiota. Clin Microbiol Rev **19**:315–337.

74. **Deplancke B**, **Gaskins HR**. 2001. Microbial modulation of innate defense: goblet cells and the intestinal mucus layer. Am J Clin Nutr **73**:1131S–1141S.

75. **Biesbrock AR**, **Reddy MS**, **Levine MJ**. 1991. Interaction of a salivary mucin-secretory immunoglobulin A complex with mucosal pathogens. Infect Immun **59**:3492–3497.

76. **Phalipon A**, **Cardona A**, **Kraehenbuhl JP**, **Edelman L**, **Sansonetti PJ**, **Corthésy B**. 2002. Secretory component: a new role in secretory IgA-mediated immune exclusion in vivo. Immunity **17**:107–115.

77. **Watkins JD**, **Sholukh AM**, **Mukhtar MM**, **Siddappa NB**, **Lakhashe SK**, **Kim M**, **Reinherz EL**, **Gupta S**, **Forthal DN**, **Sattentau QJ**, **Villinger F**, **Corti D**, **Ruprecht RM**, **CAVD Project Group**. 2013. Anti-HIV IgA isotypes: differential virion capture and inhibition of transcytosis are linked to prevention of mucosal R5 SHIV transmission. AIDS **27**:F13–20.

78. **Mazanec MB**, **Coudret CL**, **Fletcher DR**. 1995. Intracellular neutralization of influenza virus by immunoglobulin A anti-hemagglutinin monoclonal antibodies. J Virol **69**:1339–1343.

79. **Mazanec MB**, **Kaetzel CS**, **Lamm ME**, **Fletcher D**, **Nedrud JG**. 1992. Intracellular neutralization of virus by immunoglobulin A antibodies. PNAS **89**:6901–6905.

80. **Burns JW**, **Siadat-Pajouh M**, **Krishnaney AA**, **Greenberg HB**. 1996. Protective effect of rotavirus VP6-specific IgA monoclonal antibodies that lack neutralizing activity. Science **272**:104–107.

81. **Robinson JK**, **Blanchard TG**, **Levine AD**, **Emancipator SN**, **Lamm ME**. 2001. A Mucosal IgA-Mediated Excretory Immune System In Vivo. J Immunol **166**:3688–3692.

82. **Wright A**, **Lamm ME**, **Huang YT**. 2008. Excretion of human immunodeficiency virus type 1 through polarized epithelium by immunoglobulin A. J Virol **82**:11526–11535.

83. **Pastori C**, **Barassi C**, **Piconi S**, **Longhi R**, **Villa ML**, **Siccardi AG**, **Clerici M**,

Lopalco L. 2000. HIV neutralizing IgA in exposed seronegative subjects recognise an epitope within the gp41 coiled-coil pocket. J Biol Regul Homeost Agents **14**:15–21.

84. **Devito C**, **Hinkula J**, **Kaul R**, **Kimani J**, **Kiama P**, **Lopalco L**, **Barass C**, **Piconi S**, **Trabattoni D**, **Bwayo JJ**, **Plummer F**, **Clerici M**, **Broliden K**. 2002. Cross-clade HIV-1-specific neutralizing IgA in mucosal and systemic compartments of HIV-1-exposed, persistently seronegative subjects. J Acquir Immune Defic Syndr **30**:413–420.

85. **Buchacz K**, **Parekh BS**, **Padian NS**, **van der Straten A**, **Phillips S**, **Jonte J**, **Holmberg SD**. 2001. HIV-specific IgG in cervicovaginal secretions of exposed HIV-uninfected female sexual partners of HIV-infected men. AIDS Res Hum Retroviruses **17**:1689–1693.

86. **Dorrell L**, **Hessell AJ**, **Wang M**, **Whittle H**, **Sabally S**, **Rowland-Jones S**, **Burton DR**, **Parren PW**. 2000. Absence of specific mucosal antibody responses in HIV-exposed uninfected sex workers from the Gambia. AIDS **14**:1117–1122.

87. **Skurnick JH**, **Palumbo P**, **DeVico A**, **Shacklett BL**, **Valentine FT**, **Merges M**, **Kamin-Lewis R**, **Mestecky J**, **Denny T**, **Lewis GK**, **Lloyd J**, **Praschunus R**, **Baker A**, **Nixon DF**, **Stranford S**, **Gallo R**, **Vermund SH**, **Louria DB**. 2002. Correlates of nontransmission in US women at high risk of human immunodeficiency virus type 1 infection through sexual exposure. J Infect Dis **185**:428–438.

88. **Ghys PD**, **Bélec L**, **Diallo MO**, **Ettiègne-Traoré V**, **Becquart P**, **Maurice C**, **Nkengasong JN**, **Coulibaly IM**, **Greenberg AE**, **Laga M**, **Wiktor SZ**. 2000. Cervicovaginal anti-HIV antibodies in HIV-seronegative female sex workers in Abidjan, Côte d'Ivoire. AIDS **14**:2603–2608.

89. **Zhou M**, **Ruprecht RM**. 2014. Are anti-HIV IgAs good guys or bad guys? Retrovirology, 3rd ed. **11**:64–11.

90. **Renegar KB**, **Small PA**. 1991. Passive transfer of local immunity to influenza virus infection by IgA antibody. J Immunol **146**:1972–1978.

91. **Bomsel M**, **Tudor D**, **Drillet A-S**, **Alfsen A**, **Ganor Y**, **Roger M-G**, **Mouz N**, **Amacker M**, **Chalifour A**, **Diomede L**, **Devillier G**, **Cong Z**, **Wei Q**, **Gao H**, **Qin C**, **Yang G-B**, **Zurbriggen R**, **Lopalco L**, **Fleury S**. 2011. Immunization with HIV-1 gp41 Subunit Virosomes Induces Mucosal Antibodies Protecting Nonhuman Primates against Vaginal SHIV Challenges. Immunity **34**:269–280.

92. **Kozlowski PA**, **Black KP**, **Shen L**, **Jackson S**. 1995. High prevalence of serum IgA HIV-1 infection-enhancing antibodies in HIV-infected persons. Masking by IgG. J Immunol **154**:6163–6173.

93. **Janoff EN**, **Wahl SM**, **Thomas K**, **Smith PD**. 1995. Modulation of human immunodeficiency virus type 1 infection of human monocytes by IgA. J Infect Dis **172**:855–858.

94. **Cerutti A**. 2008. The regulation of IgA class switching. Nat Rev Immunol **8**:421–

434.

95. **Eisen HN**. 2014. Affinity enhancement of antibodies: how low-affinity antibodies produced early in immune responses are followed by high-affinity antibodies later and in memory B-cell responses. Cancer Immunol Res **2**:381–392.

96. **Eisen HN**, **Siskind GW**. 2002. Variations in Affinities of Antibodies during the Immune Response *. Biochemistry **3**:996–1008.

97. **Muramatsu M**, **Kinoshita K**, **Fagarasan S**, **Yamada S**, **Shinkai Y**, **Honjo T**. 2000. Class switch recombination and hypermutation require activation-induced cytidine deaminase (AID), a potential RNA editing enzyme. Cell **102**:553–563.

98. **Weigert MG**, **Cesari IM**, **Yonkovich SJ**, **Cohn M**. 1970. Variability in the lambda light chain sequences of mouse antibody. Nature **228**:1045–1047.

99. **Mesin L**, **Ersching J**, **Victora GD**. 2016. Germinal Center B Cell Dynamics. Immunity **45**:471–482.

100. **Cyster JG**. 2010. B cell follicles and antigen encounters of the third kind. Nat Immunol **11**:989–996.

101. **Gonzalez SF**, **Degn SE**, **Pitcher LA**, **Woodruff M**, **Heesters BA**, **Carroll MC**. 2011. Trafficking of B cell antigen in lymph nodes. Annu Rev Immunol **29**:215–233.

102. **Schwickert TA**, **Lindquist RL**, **Shakhar G**, **Livshits G**, **Skokos D**, **Kosco-Vilbois MH**, **Dustin ML**, **Nussenzweig MC**. 2007. In vivo imaging of germinal centres reveals a dynamic open structure. Nature **446**:83–87.

103. **Crotty S**. 2015. A brief history of T cell help to B cells. Nat Rev Immunol **15**:185–189.

104. **Crotty S**. 2014. T follicular helper cell differentiation, function, and roles in disease. Immunity **41**:529–542.

105. **Kepler TB**, **Perelson AS**. 1993. Cyclic re-entry of germinal center B cells and the efficiency of affinity maturation. Immunol Today **14**:412–415.

106. **Victora GD**, **Nussenzweig MC**. 2012. Germinal centers. Annu Rev Immunol **30**:429–457.

107. **Allen CDC**, **Okada T**, **Cyster JG**. 2007. Germinal-center organization and cellular dynamics. Immunity **27**:190–202.

108. **Allen CDC**, **Ansel KM**, **Low C**, **Lesley R**, **Tamamura H**, **Fujii N**, **Cyster JG**. 2004. Germinal center dark and light zone organization is mediated by CXCR4 and CXCR5. Nat Immunol **5**:943–952.

109. **Victora GD**, **Schwickert TA**, **Fooksman DR**, **Kamphorst AO**, **Meyer-Hermann M**, **Dustin ML**, **Nussenzweig MC**. 2010. Germinal center dynamics revealed by multiphoton microscopy with a photoactivatable fluorescent reporter. Cell **143**:592–605.

110. **Goenka R**, **Matthews AH**, **Zhang B**, **O'Neill PJ**, **Scholz JL**, **Migone T-S**, **Leonard WJ**, **Stohl W**, **Hershberg U**, **Cancro MP**. 2014. Local BLyS production by T follicular cells mediates retention of high affinity B cells during affinity maturation. J Exp Med **211**:45–56.

111. **Victora GD**, **Mouquet H**. 2018. What Are the Primary Limitations in B-Cell Affinity Maturation, and How Much Affinity Maturation Can We Drive with Vaccination? Lessons from the Antibody Response to HIV-1. Cold Spring Harb Perspect Biol **10**.

112. **Paus D**, **Phan TG**, **Chan TD**, **Gardam S**, **Basten A**, **Brink R**. 2006. Antigen recognition strength regulates the choice between extrafollicular plasma cell and germinal center B cell differentiation. Journal of Experimental Medicine **203**:1081–1091.

113. **Phan TG**, **Paus D**, **Chan TD**, **Turner ML**, **Nutt SL**, **Basten A**, **Brink R**. 2006. High affinity germinal center B cells are actively selected into the plasma cell compartment. Journal of Experimental Medicine **203**:2419–2424.

114. **Smith KG**, **Light A**, **Nossal GJ**, **Tarlinton DM**. 1997. The extent of affinity maturation differs between the memory and antibody-forming cell compartments in the primary immune response. The EMBO Journal **16**:2996–3006.

115. **Shinnakasu R**, **Inoue T**, **Kometani K**, **Moriyama S**, **Adachi Y**, **Nakayama M**, **Takahashi Y**, **Fukuyama H**, **Okada T**, **Kurosaki T**. 2016. Regulated selection of germinal-center cells into the memory B cell compartment. Nat Immunol **17**:861–869.

116. **Weisel FJ**, **Zuccarino-Catania GV**, **Chikina M**, **Shlomchik MJ**. 2016. A Temporal Switch in the Germinal Center Determines Differential Output of Memory B and Plasma Cells. Immunity **44**:116–130.

117. **Klein F**, **Diskin R**, **Scheid JF**, **Gaebler C**, **Mouquet H**, **Georgiev IS**, **Pancera M**, **Zhou T**, **Incesu R-B**, **Fu BZ**, **Gnanapragasam PNP**, **Oliveira TY**, **Seaman MS**, **Kwong PD**, **Bjorkman PJ**, **Nussenzweig MC**. 2013. Somatic mutations of the immunoglobulin framework are generally required for broad and potent HIV-1 neutralization. Cell **153**:126–138.

118. **Kepler TB**, **Liao HX**, **Alam SM**, **Bhaskarabhatla R**, **Zhang R**, **Yandava C**, **Stewart S**, **Anasti K**, **Kelsoe G**, **Parks R**, **Lloyd KE**, **Stolarchuk C**, **Pritchett J**, **Solomon E**, **Friberg E**, **Morris L**, **Karim SSA**, **Cohen MS**, **Walter E**, **Moody MA**, **Wu X**, **Altae-Tran HR**, **Georgiev IS**, **Kwong PD**, **Boyd SD**, **Fire AZ**, **Mascola JR**, **Haynes BF**. 2014. Immunoglobulin gene insertions and deletions in the affinity maturation of HIV-1 broadly reactive neutralizing antibodies. Cell Host Microbe **16**:304–313.

119. **Takahashi Y**, **Dutta PR**, **Cerasoli DM**, **Kelsoe G**. 1998. In Situ Studies of the Primary Immune Response to (4-Hydroxy-3-Nitrophenyl)Acetyl. V. Affinity Maturation Develops in Two Stages of Clonal Selection. Journal of Experimental Medicine **187**:885–895.

120. **Salcedo TW**. 1993. Physical and functional association of p56lck with Fc gamma RIIIA (CD16) in natural killer cells. Journal of Experimental Medicine **177**:1475–1480.

121. **Ghazizadeh S**, **Bolen JB**, **Fleit HB**. 1994. Physical and functional association of Src-related protein tyrosine kinases with Fc gamma RII in monocytic THP-1 cells. J Biol Chem **269**:8878–8884.

122. **Falasca M**, **Logan SK**, **Lehto VP**, **Baccante G**, **Lemmon MA**, **Schlessinger J**. 1998. Activation of phospholipase C gamma by PI 3-kinase-induced PH domain-mediated membrane targeting. The EMBO Journal **17**:414–422.

123. **O'Neill SK**, **Getahun A**, **Gauld SB**, **Merrell KT**, **Tamir I**, **Smith MJ**, **Dal Porto JM**, **Li Q-Z**, **Cambier JC**. 2011. Monophosphorylation of CD79a and CD79b ITAM motifs initiates a SHIP-1 phosphatase-mediated inhibitory signaling cascade required for B cell anergy. Immunity **35**:746–756.

124. **Ono M**, **Bolland S**, **Tempst P**, **Ravetch JV**. 1996. Role of the inositol phosphatase SHIP in negative regulation of the immune system by the receptor Fc(gamma)RIIB. Nature **383**:263–266.

125. **Ono M**, **Okada H**, **Bolland S**, **Yanagi S**, **Kurosaki T**, **Ravetch JV**. 1997. Deletion of SHIP or SHP-1 reveals two distinct pathways for inhibitory signaling. Cell **90**:293–301.

126. **Ravetch JV**, **Bolland S**. 2001. IgG Fc receptors. Annu Rev Immunol **19**:275–290.

127. **Igietseme JU**, **Zhu X**, **Black CM**. 2014. Fc Receptor-Dependent Immunity, pp. 269–281. *In* Antibody Fc. Elsevier.

128. **Lindorfer MA**, **Köhl J**, **Taylor RP**. 2014. Interactions Between the Complement System and Fcγ Receptors, pp. 49–74. *In* Antibody Fc. Elsevier.

129. **Monteiro RC**, **van de Winkel JGJ**. 2003. IgA Fc receptors. Annu Rev Immunol **21**:177–204.

130. **Geissmann F**, **Launay P**, **Pasquier B**, **Lepelletier Y**, **Leborgne M**, **Lehuen A**, **Brousse N**, **Monteiro RC**. 2001. A Subset of Human Dendritic Cells Expresses IgA Fc Receptor (CD89), Which Mediates Internalization and Activation Upon Cross-Linking by IgA Complexes. J Immunol **166**:346–352.

131. **Heystek HC**, **Moulon C**, **Woltman AM**, **Garonne P**, **van Kooten C**. 2002. Human Immature Dendritic Cells Efficiently Bind and Take up Secretory IgA Without the Induction of Maturation. J Immunol **168**:102–107.

132. **van Egmond M**, **van Garderen E**, **van Spriel AB**, **Damen CA**, **van Amersfoort ES**, **van Zandbergen G**, **van Hattum J**, **Kuiper J**, **van de Winkel JG**. 2000. FcalphaRI-positive liver Kupffer cells: reappraisal of the function of immunoglobulin A in immunity. Nat Cell Biol **6**:680–685.

133. **Monteiro RC**. 1990. Cellular distribution, regulation, and biochemical nature of an Fc alpha receptor in humans. Journal of Experimental Medicine **171**:597–613.

134. **Pfefferkorn LC**, **Yeaman GR**. 1994. Association of IgA-Fc receptors (Fc alpha R) with Fc epsilon RI gamma 2 subunits in U937 cells. Aggregation induces the tyrosine phosphorylation of gamma 2. J Immunol **153**:3228–3236.

135. **Lang ML**, **Shen L**, **Wade WF**. 1999. Gamma-chain dependent recruitment of tyrosine kinases to membrane rafts by the human IgA receptor Fc alpha R. J Immunol **163**:5391–5398.

136. **Gulle H**, **Samstag A**, **Eibl MM**, **Wolf HM**. 1998. Physical and functional association of Fc alpha R with protein tyrosine kinase Lyn. Blood **91**:383–391.

137. **Park RK**, **Izadi KD**, **Deo YM**, **Durden DL**. 1999. Role of Src in the modulation of multiple adaptor proteins in FcalphaRI oxidant signaling. Blood **94**:2112–2120.

138. **Launay P**, **Lehuen A**, **Kawakami T**, **Blank U**, **Monteiro RC**. 1998. IgA Fc receptor (CD89) activation enables coupling to syk and Btk tyrosine kinase pathways: differential signaling after IFN-γ or phorbol ester stimulation. J Leukoc Biol **63**:636–642.

139. **Lang ML**, **Kerr MA**. 2000. Characterization of FcαR-Triggered Ca2+ Signals: Role in Neutrophil NADPH Oxidase Activation. Biochem Biophys Res Commun **276**:749–755.

140. **Otten MA**, **van Egmond M**. 2004. The Fc receptor for IgA (FcalphaRI, CD89). Immunol Lett **92**:23–31.

141. **van der Boog PJM**, **van Zandbergen G**, **de Fijter JW**, **Klar-Mohamad N**, **van Seggelen A**, **Brandtzaeg P**, **Daha MR**, **van Kooten C**. 2002. Fc RI/CD89 Circulates in Human Serum Covalently Linked to IgA in a Polymeric State. J Immunol **168**:1252–1258.

142. **van Egmond M**, **van Vuuren AJ**, **Morton HC**, **van Spriel AB**, **Shen L**, **Hofhuis FM**, **Saito T**, **Mayadas TN**, **Verbeek JS**, **van de Winkel JG**. 1999. Human immunoglobulin A receptor (FcalphaRI, CD89) function in transgenic mice requires both FcR gamma chain and CR3 (CD11b/CD18). Blood **93**:4387–4394.

143. **Pasquier B**, **Launay P**, **Kanamaru Y**, **Moura IC**, **Pfirsch S**, **Ruffié C**, **Hénin D**, **Benhamou M**, **Pretolani M**, **Blank U**, **Monteiro RC**. 2005. Identification of FcalphaRI as an inhibitory receptor that controls inflammation: dual role of FcRgamma ITAM. Immunity **22**:31–42.

144. **Pfirsch-Maisonnas S**, **Aloulou M**, **Xu T**, **Claver J**, **Kanamaru Y**, **Tiwari M**, **Launay P**, **Monteiro RC**, **Blank U**. 2011. Inhibitory ITAM signaling traps activating receptors with the phosphatase SHP-1 to form polarized “inhibisome” clusters. Science Signaling **4**:ra24–ra24.

145. **Launay P**, **Patry C**, **Lehuen A**, **Pasquier B**, **Blank U**, **Monteiro RC**. 1999. Alternative endocytic pathway for immunoglobulin A Fc receptors (CD89) depends on the lack of FcRgamma association and protects against degradation of bound ligand. J Biol Chem **274**:7216–7225.

146. **Herr AB**, **White CL**, **Milburn C**, **Wu C**, **Bjorkman PJ**. 2003. Bivalent binding of

IgA1 to FcalphaRI suggests a mechanism for cytokine activation of IgA phagocytosis. J Mol Biol **327**:645–657.

147. **Stockert RJ**, **Kressner MS**, **Collins JC**, **Sternlieb I**, **Morell AG**. 1982. IgA interaction with the asialoglycoprotein receptor. PNAS **79**:6229–6231.

148. **Stockert RJ**. 1995. The asialoglycoprotein receptor: relationships between structure, function, and expression. Physiol Rev **75**:591–609.

149. **Moura IC**, **Centelles MN**, **Arcos-Fajardo M**, **Malheiros DM**, **Collawn JF**, **Cooper MD**, **Monteiro RC**. 2001. Identification of the transferrin receptor as a novel immunoglobulin (Ig)A1 receptor and its enhanced expression on mesangial cells in IgA nephropathy. Journal of Experimental Medicine **194**:417–425.

150. **Lamkhioued B**, **Gounni AS**, **Gruart V**, **Pierce A**, **Capron A**, **Capron M**. 1995. Human eosinophils express a receptor for secretory component. Role in secretory IgA-dependent activation. Eur J Immunol **25**:117–125.

151. **Abu-Ghazaleh RI**, **Fujisawa T**, **Mestecky J**, **Kyle RA**, **Gleich GJ**. 1989. IgA-induced eosinophil degranulation. J Immunol **142**:2393–2400.

152. **Iikura M**, **Yamaguchi M**, **Fujisawa T**, **Miyamasu M**, **Takaishi T**, **Morita Y**, **Iwase T**, **Moro I**, **Yamamoto K**, **Hirai K**. 1998. Secretory IgA induces degranulation of IL-3-primed basophils. J Immunol **161**:1510–1515.

153. **Vaysburd M**, **Watkinson RE**, **Cooper H**, **Reed M**, **O'Connell K**, **Smith J**, **Cruickshanks J**, **James LC**. 2013. Intracellular antibody receptor TRIM21 prevents fatal viral infection. Proc Natl Acad Sci USA **110**:12397–12401.

154. **Rhodes DA**, **Trowsdale J**. 2007. TRIM21 is a trimeric protein that binds IgG Fc via the B30.2 domain. Mol Immunol **44**:2406–2414.

155. **Mallery DL**, **McEwan WA**, **Bidgood SR**, **Towers GJ**, **Johnson CM**, **James LC**. 2010. Antibodies mediate intracellular immunity through tripartite motif-containing 21 (TRIM21). Proc Natl Acad Sci USA **107**:19985–19990.

156. **Watkinson RE**, **Tam JCH**, **Vaysburd MJ**, **James LC**. 2013. Simultaneous neutralization and innate immune detection of a replicating virus by TRIM21. J Virol **87**:7309–7313.

157. **Anthony RM**, **Kobayashi T**, **Wermeling F**, **Ravetch JV**. 2011. Intravenous gammaglobulin suppresses inflammation through a novel T(H)2 pathway. Nature **475**:110–113.

158. **Ehrhardt GRA**, **Hsu JT**, **Gartland L**, **Leu C-M**, **Zhang S**, **Davis RS**, **Cooper MD**. 2005. Expression of the immunoregulatory molecule FcRH4 defines a distinctive tissue-based population of memory B cells. Journal of Experimental Medicine **202**:783–791.

159. **Stavnezer J**, **Guikema JEJ**, **Schrader CE**. 2008. Mechanism and regulation of class switch recombination. Annu Rev Immunol **26**:261–292.

160. **Collins AM**. 2016. IgG subclass co-expression brings harmony to the quartet model of murine IgG function. Immunol Cell Biol **94**:949–954.

161. **Wines BD**, **Ramsland PA**, **Trist HM**, **Gardam S**, **Brink R**, **Fraser JD**, **Hogarth PM**. 2011. Interaction of Human, Rat, and Mouse Immunoglobulin A (IgA) with Staphylococcal Superantigen-like 7 (SSL7) Decoy Protein and Leukocyte IgA Receptor. J Biol Chem **286**:33118–33124.

162. **Musich T**, **Demberg T**, **Morgan IL**, **Estes JD**, **Franchini G**, **Robert-Guroff M**. 2015. Purification and functional characterization of mucosal IgA from vaccinated and SIV-infected rhesus macaques. Clinical Immunology **158**:127–139.

163. **Huang J**, **Guerrero A**, **Parker E**, **Strum JS**, **Smilowitz JT**, **German JB**, **Lebrilla CB**. 2015. Site-Specific Glycosylation of Secretory Immunoglobulin A from Human Colostrum. J Proteome Res **14**:1335–1349.

164. **Jacobsen FW**, **Padaki R**, **Morris AE**, **Aldrich TL**, **Armitage RJ**, **Allen MJ**, **Lavallee JC**, **Arora T**. 2011. Molecular and functional characterization of cynomolgus monkey IgG subclasses. J Immunol **186**:341–349.

165. **Scinicariello F**, **Engleman CN**, **Jayashankar L**, **McClure HM**, **Attanasio R**. 2004. Rhesus macaque antibody molecules: sequences and heterogeneity of alpha and gamma constant regions. Immunology **111**:66–74.

166. **Warncke M**, **Calzascia T**, **Coulot M**, **Balke N**, **Touil R**, **Kolbinger F**, **Heusser C**. 2012. Different adaptations of IgG effector function in human and nonhuman primates and implications for therapeutic antibody treatment. J Immunol **188**:4405–4411.

167. **Boesch AW**, **Osei-Owusu NY**, **Crowley AR**, **Chu TH**, **Chan YN**, **Weiner JA**, **Bharadwaj P**, **Hards R**, **Adamo ME**, **Gerber SA**, **Cocklin SL**, **Schmitz JE**, **Miles AR**, **Eckman JW**, **Belli AJ**, **Reimann KA**, **Ackerman ME**. 2016. Biophysical and Functional Characterization of Rhesus Macaque IgG Subclasses. Front Immunol, 4 ed. **7**:220–16.

168. **Nguyen DC**, **Sanghvi R**, **Scinicariello F**, **Pulit-Penaloza J**, **Hill N**, **Attanasio R**. 2014. Cynomolgus and pigtail macaque IgG subclasses: characterization of IGHG genes and computational analysis of IgG/Fc receptor binding affinity. Immunogenetics **66**:361–377.

169. **Calvas P**, **Apoil P**, **Fortenfant F**, **Roubinet F**, **Andris J**, **Capra D**, **Blancher A**. 1999. Characterization of the three immunoglobulin G subclasses of macaques. Scand J Immunol **49**:595–610.

170. **Sumiyama K**, **Saitou N**, **Ueda S**. 2002. Adaptive evolution of the IgA hinge region in primates. Mol Biol Evol **19**:1093–1099.

171. **Scinicariello F**, **Attanasio R**. 2001. Intraspecies heterogeneity of immunoglobulin alpha-chain constant region genes in rhesus macaques. Immunology **103**:441–448.

172. **Proctor M**, **Manning PJ**. 1990. Production of immunoglobulin A protease by Streptococcus pneumoniae from animals. Infect Immun **58**:2733–2737.

173. **Reinholdt J**, **Kilian M**. 1991. Lack of cleavage of immunoglobulin A (IgA) from rhesus monkeys by bacterial IgA1 proteases. Infect Immun **59**:2219–2221.

174. **Mestas J**, **Hughes CCW**. 2004. Of Mice and Not Men: Differences between Mouse and Human Immunology. J Immunol **172**:2731–2738.

175. **Moldt B**, **Hessell AJ**. 2014. FcγRs Across Species, pp. 145–157. *In* Antibody Fc. Elsevier.

176. **Sakamoto N**, **Shibuya K**, **Shimizu Y**, **Yotsumoto K**, **Miyabayashi T**, **Sakano S**, **Tsuji T**, **Nakayama E**, **Nakauchi H**, **Shibuya A**. 2001. A novel Fc receptor for IgA and IgM is expressed on both hematopoietic and non-hematopoietic tissues. Eur J Immunol **31**:1310–1316.

177. **Shibuya A**, **Sakamoto N**, **Shimizu Y**, **Shibuya K**, **Osawa M**, **Hiroyama T**, **Eyre HJ**, **Sutherland GR**, **Endo Y**, **Fujita T**, **Miyabayashi T**, **Sakano S**, **Tsuji T**, **Nakayama E**, **Phillips JH**, **Lanier LL**, **Nakauchi H**. 2000. Fc alpha/mu receptor mediates endocytosis of IgM-coated microbes. Nat Immunol **1**:441–446.

178. **Rogers KA**, **Jayashankar L**, **Scinicariello F**, **Attanasio R**. 2008. Nonhuman Primate IgA: Genetic Heterogeneity and Interactions with CD89. J Immunol **180**:4816–4824.

179. **Morton HC**, **Pleass RJ**, **Storset AK**, **Brandtzaeg P**, **Woof JM**. 2005. Cloning and characterization of equine CD89 and identification of the CD89 gene in chimpanzees and rhesus macaques. Immunology **115**:74–84.

180. **Rogers KA**, **Scinicariello F**, **Attanasio R**. 2004. Identification and characterization of macaque CD89 (immunoglobulin A Fc receptor). Immunology **113**:178–186.

181. **Mestecky J**. 1987. The common mucosal immune system and current strategies for induction of immune responses in external secretions. J Clin Immunol **7**:265–276.

182. **Phillips-Quagliata JM**, **Roux ME**, **Arny M**, **Kelly-Hatfield P**, **McWilliams M**, **Lamm ME**. 1983. Migration and regulation of B-cells in the mucosal immune system. Annals of the New York Academy of Sciences **409**:194–203.

183. **Kuper CF**, **Koornstra PJ**, **Hameleers DM**, **Biewenga J**, **Spit BJ**, **Duijvestijn AM**, **van Breda Vriesman PJ**, **Sminia T**. 1992. The role of nasopharyngeal lymphoid tissue. Immunol Today **13**:219–224.

184. **Boyaka PN**, **McGhee JR**, **Czerkinsky C**, **Mestecky J**. 2005. Chapter 47 - Mucosal Vaccines: An Overview, pp. 855–874. *In* Mestecky, J, Lamm, ME, McGhee, JR, Bienenstock, J, Mayer, L, Strober, W (eds.), Mucosal Immunology (Third Edition). Academic Press, Burlington.

185. **Boyaka PN**. 2017. Inducing Mucosal IgA: A Challenge for Vaccine Adjuvants and Delivery Systems. J Immunol **199**:9–16.

186. **Azizi A**, **Ghunaim H**, **Diaz-Mitoma F**, **Mestecky J**. 2010. Mucosal HIV vaccines: A holy grail or a dud? Vaccine **28**:4015–4026.

187. **Neutra MR**, **Kozlowski PA**. 2006. Mucosal vaccines: the promise and the challenge. Nat Rev Immunol **6**:148–158.

188. **Sabin AB**. 1957. Present status of attenuated live virus poliomyelitis vaccine. Bull N Y Acad Med **33**:17–39.

189. **Sabin AB**. 1957. Properties and behavior of orally administered attenuated poliovirus vaccine. J Am Med Assoc **164**:1216–1223.

190. **Ogra PL**, **Karzon DT**. 1969. Distribution of poliovirus antibody in serum, nasopharynx and alimentary tract following segmental immunization of lower alimentary tract with poliovaccine. J Immunol **102**:1423–1430.

191. **Block SL**, **Yi T**, **Sheldon E**, **Dubovsky F**, **Falloon J**. 2011. A randomized, double-blind noninferiority study of quadrivalent live attenuated influenza vaccine in adults. Vaccine **29**:9391–9397.

192. **Bhuiyan TR**, **Choudhury FK**, **Khanam F**, **Saha A**, **Sayeed MA**, **Salma U**, **Lundgren A**, **Sack DA**, **Svennerholm A-M**, **Qadri F**. 2014. Evaluation of immune responses to an oral typhoid vaccine, Ty21a, in children from 2 to 5 years of age in Bangladesh. Vaccine **32**:1055–1060.

193. **Clemens JD**, **Sack DA**, **Harris JR**, **Chakraborty J**, **Khan MR**, **Stanton BF**, **Kay BA**, **Khan MU**, **Yunus M**, **Atkinson W**. 1986. Field trial of oral cholera vaccines in Bangladesh. The Lancet **2**:124–127.

194. **Holmgren J**, **Svennerholm AM**, **Lönnroth I**, **Fall-Persson M**, **Markman B**, **Lundbeck H**. 1977. Development of improved cholera vaccine based on subunit toxoid. Nature **269**:602–604.

195. **World Health Organization**. 2012. Weekly epidemiological record, Cholera 2012.

196. **Joensuu J**, **Koskenniemi E**, **Pang XL**, **Vesikari T**. 1997. Randomised placebo-controlled trial of rhesus-human reassortant rotavirus vaccine for prevention of severe rotavirus gastroenteritis. The Lancet **350**:1205–1209.

197. **Midthun K**, **Kapikian AZ**. 1996. Rotavirus vaccines: an overview. Clin Microbiol Rev **9**:423–434.

198. **Azegami T**, **Yuki Y**, **Kiyono H**. 2014. Challenges in mucosal vaccines for the control of infectious diseases. Int Immunol **26**:517–528.

199. **Su F**, **Patel GB**, **Hu S**, **Chen W**. 2016. Induction of mucosal immunity through systemic immunization: Phantom or reality? Hum Vaccin Immunother **12**:1070–1079.

200. **Underdown BJ**, **Strober W**. 2015. Chapter 70 - Parenteral Immunization and Protection from Mucosal Infection, pp. 1391–1402. *In* Mestecky, J, Strober, W, Russell, MW, Kelsall, BL, Cheroutre, H, Lambrecht, BN (eds.), Mucosal Immunology (Fourth Edition)Fourth Edition. Academic Press, Boston.

201. **Tarkowski A**, **Lue C**, **Moldoveanu Z**, **Kiyono H**, **McGhee JR**, **Mestecky J**. 1990.

Immunization of humans with polysaccharide vaccines induces systemic, predominantly polymeric IgA2-subclass antibody responses. J Immunol **144**:3770–3778.

202. **Engström P-E**, **Gustafson R**, **Granberg M**, **Engström GN**. 2009. Specific IgA subclass responses in serum and saliva: a 12-month follow-up study after parenteral booster immunization with tetanus toxoid. Acta Odontologica Scandinavica **60**:198–202.

203. **Nieminen T**, **Käyhty H**, **Leroy O**, **Eskola J**. 1999. Pneumococcal conjugate vaccination in toddlers: mucosal antibody response measured as circulating antibody-secreting cells and as salivary antibodies. Pediatr Infect Dis J **18**:764–772.

204. **Murdin AD**, **Barreto L**, **Plotkin S**. 1996. Inactivated poliovirus vaccine: past and present experience. Vaccine **14**:735–746.

205. **Blackwelder WC**, **Storsaeter J**, **Olin P**, **Hallander HO**. 1991. Acellular pertussis vaccines. Efficacy and evaluation of clinical case definitions. Am J Dis Child **145**:1285–1289.

206. **Gorse GJ**, **Otto EE**, **Powers DC**, **Chambers GW**, **Eickhoff CS**, **Newman FK**. 1996. Induction of mucosal antibodies by live attenuated and inactivated influenza virus vaccines in the chronically ill elderly. J Infect Dis **173**:285–290.

207. **Moldoveanu Z**, **Clements ML**, **Prince SJ**, **Murphy BR**, **Mestecky J**. 1995. Human immune responses to influenza virus vaccines administered by systemic or mucosal routes. Vaccine **13**:1006–1012.

208. **Clements ML**, **Betts RF**, **Tierney EL**, **Murphy BR**. 1986. Serum and nasal wash antibodies associated with resistance to experimental challenge with influenza A wild-type virus. J Clin Microbiol **24**:157–160.

209. **Brokstad KA**, **Cox RJ**, **Olofsson J**, **Jonsson R**, **Haaheim LR**. 1995. Parenteral influenza vaccination induces a rapid systemic and local immune response. J Infect Dis **171**:198–203.

210. **Brokstad KA**, **Eriksson J-C**, **Cox RJ**, **Tynning T**, **Olofsson J**, **Jonsson R**, **Davidsson A**. 2002. Parenteral vaccination against influenza does not induce a local antigen-specific immune response in the nasal mucosa. J Infect Dis **185**:878–884.

211. **Demberg T**, **Robert-Guroff M**. 2009. Mucosal immunity and protection against HIV/SIV infection: strategies and challenges for vaccine design. Int Rev Immunol **28**:20–48.

212. **McHugh KJ**, **Guarecuco R**, **Langer R**, **Jaklenec A**. 2015. Single-injection vaccines: Progress, challenges, and opportunities. Journal of Controlled Release **219**:596–609.

213. **Cleland JL**. 1999. Single-administration vaccines: controlled-release technology to mimic repeated immunizations. Trends Biotechnol **17**:25–29.

214. **Conn J Jr**, **Oyasu R**, **Welsh M**, **Beal JM**. 1974. Vicryl (polyglactin 910) synthetic

absorbable sutures. The American Journal of Surgery **128**:19–23.

215. **Austin PE**, **Dunn KA**, **Eily-Cofield K**, **Brown CK**, **Wooden WA**, **Bradfield JF**. 1995. Subcuticular sutures and the rate of inflammation in noncontaminated wounds. Ann Emerg Med **25**:328–330.

216. **Ulery BD**, **Nair LS**, **Laurencin CT**. 2011. Biomedical Applications of Biodegradable Polymers. J Polym Sci B Polym Phys **49**:832–864.

217. **Tam HH**, **Melo MB**, **Kang M**, **Pelet JM**, **Ruda VM**, **Foley MH**, **Hu JK**, **Kumari S**, **Crampton J**, **Baldeon AD**, **Sanders RW**, **Moore JP**, **Crotty S**, **Langer R**, **Anderson DG**, **Chakraborty AK**, **Irvine DJ**. 2016. Sustained antigen availability during germinal center initiation enhances antibody responses to vaccination. Proc Natl Acad Sci USA **113**:E6639–E6648.

218. **Kemp JM**, **Kajihara M**, **Nagahara S**, **Sano A**, **Brandon M**, **Lofthouse S**. 2002. Continuous antigen delivery from controlled release implants induces significant and anamnestic immune responses. Vaccine **20**:1089–1098.

219. **Kanchan V**, **Katare YK**, **Panda AK**. 2009. Memory antibody response from antigen loaded polymer particles and the effect of antigen release kinetics. Biomaterials **30**:4763–4776.

220. **Sharp FA**, **Ruane D**, **Claass B**, **Creagh E**, **Harris J**, **Malyala P**, **Singh M**, **O'Hagan DT**, **Pétrilli V**, **Tschopp J**, **O'Neill LAJ**, **Lavelle EC**. 2009. Uptake of particulate vaccine adjuvants by dendritic cells activates the NALP3 inflammasome. Proc Natl Acad Sci USA **106**:870–875.

221. **Cleland JL**, **Lim A**, **Daugherty A**, **Barron L**, **Desjardin N**, **Duenas ET**, **Eastman DJ**, **Vennari JC**, **Wrin T**, **Berman P**, **Murthy KK**, **Powell MF**. 1998. Development of a single-shot subunit vaccine for HIV-1. 5. Programmable in vivo autoboost and long lasting neutralizing response. J Pharm Sci **87**:1489–1495.

CHAPTER 2:

Common features of mucosal and peripheral antibody responses elicited by candidate HIV-1 vaccines in rhesus monkeys

This chapter is based on the peer-review publication:

Li H*, Stephenson KE*, Kang Z-H*, Lavine CL, Seaman MS, Barouch DH. 2014. Common features of mucosal and peripheral antibody responses elicited by candidate HIV-1 vaccines in rhesus monkeys. *J Virol* 88:13510–13515.

*Authors contributed equally to publication

ACKNOWLEDGMENTS

We thank G. Tomaras, P. Kozlowski, M. Beck, J. Kramer, G. Russo, J. Nkolola, and L. Parenteau for their generous advice and assistance. We acknowledge support from National Institutes of Health grants AI078526, AI084794, AI095985, AI096040 (D.H.B.), and AI060354 (K.E.S.) and the Ragon Institute of MGH, MIT, and Harvard (D.H.B.).

ABSTRACT

Human immunodeficiency virus type 1 (HIV-1) vaccines that elicit protective antibody responses at mucosal sites would be highly desirable. Here, we report that intramuscular immunization of candidate HIV-1 vaccine vectors and purified Env proteins elicited potent and durable humoral immune responses in colorectal mucosa in rhesus monkeys. The kinetics, isotypes, functionality, and epitope specificity of these mucosal antibody responses were similar to those of peripheral responses in serum. These data suggest a close immunological relationship between mucosal and systemic antibody responses following vaccination in primates.

INTRODUCTION

Human mucosal surfaces represent the major portal of entry for human immunodeficiency virus type 1 (HIV-1) (1). Thus, a prophylactic vaccine will likely need to elicit protective antibody responses at mucosal sites of virus exposure. However, mucosal humoral immune responses following vaccination are poorly characterized. The RV144 clinical trial suggested that vaccine-elicited HIV-1 envelope (Env) -specific humoral immune responses may have contributed to the partial protection observed for vaccines (2), but mucosal immune responses were not assessed in that trial. In contrast, previous studies have shown that immunization with peptide, DNA, protein, or attenuated bacterial or viral vector-based vaccines through parental or mucosal routes may elicit antigen-specific humoral immune responses at mucosal sites in mice, nonhuman primates, and humans (3-7). However, the characteristics, functionality, and epitope specificity of vaccine-elicited mucosal antibody responses have not been fully explored. Moreover, whether mucosal antibody responses reflect distinct populations compared with those for peripheral antibody responses remains to be determined. We therefore assessed the magnitude, durability, isotype, neutralizing activity, and epitope specificity of mucosal and peripheral antibody responses in rhesus monkeys elicited by adenovirus (Ad) vector-based and protein- based HIV-1 vaccine candidates.

MATERIALS AND METHODS

Elution of Weck Cels

300uL of elution buffer (1X PBS, 0.25% w/v BSA, 0.5% v/v Igepal, 1XProtease inhibitor cocktail) was incubated with thawed Weck Cel sponges in a Spin-X filter column (Corning Costar) for 5 minutes on ice. The filter column was centrifuged for 5 minutes at 16,000g at 4°C. This process was repeated again with another 300uL of elution buffer.

The average volume of eluates from 8 experimental (used) and 8 unused Weck Cel sponges were calculated respectively. To calculate the dilution factor of eluted colorectal secretions, we used the following formula:

$$dilution\ factor = \frac{experimental\ sponge\ eluate\ volume}{experiment\ sponge\ eluate\ volume - unused\ sponge\ eluate\ volume}$$

ELISA

Quantitative IgG and IgA concentration – Total IgG or IgA concentrations were determined using monkey IgG or IgA enzyme-linked immunosorbent assay (ELISA) kits respectively (Alpha Diagnostic International).

Serum Env-specific IgG – Serum binding IgG antibody titers against HIV-1 Env were determined by endpoint ELISAs as previously described. (8). Briefly, 96-well Maxisorp ELISA plates (Thermo Fisher Scientific) were coated overnight with 100 uL per well of HIV-1 Env at a concentration of 1 ug/mL in PBS, and subsequently blocked for 4 h with PBS containing 2% BSA (Sigma) and 0.05% Tween-20 (Sigma). Serum was serially diluted and incubated for 1 h at room temperature. Plates were washed 3 times with PBS containing 0.05% Tween-20 and were incubated for 1 h with HRP-conjugated anti-IgG (Jackson ImmunoResearch Laboratories Inc.). The plates were washed 3 times and developed with SureBlue tetramethylbenzidine microwell peroxidase (KPL Research Products), stopped by

the addition of stop solution (KPL research Products), and analyzed at 450nm/550nm on a Spectramax Plus ELISA plate reader (Molecular Devices) using Softmax Pro-4.7.1 software.

All other Env-specific ELISAs – For all other ELISAs, following sample incubation, plates were incubated with a biotin-conjugated secondary antibody (IgG and IgA: Alpha Diagnostic International; IgG1 and IgG3: NIH Non-human Primate Reagent Resource) for 1 h at 37C, washed 3 times, incubated with streptavidin-HRP for 1h before developing.

IgA α chain-specific and secretory component- (SC-) specific ELISAs – Plates were coated with an anti-IgA antibody (Alpha Diagnostics International). Following incubation with sample, plates were incubated with a biotin-conjugated α-specific or SC-specific antibody for 1 h at 37C, washed 3 times, incubated with streptavidin-HRP for 1h before developing.

Neutralizing Antibody Assay in TZM.bl Cells

Neutralizing antibody responses against $SIV_{mac251.15}$ Env pseudovirions were measured using luciferase-based virus neutralization assays in TZM.bl cells (8-13). These assays measure the reduction in luciferase reporter gene expression in TZM.bl cells following a single round of virus infection. The ID50 was calculated as the serum dilution that resulted in a 50% reduction in relative luminescence units compared with the virus control wells after the subtraction of cell control relative luminescence units. Threefold serial dilutions of serum samples were performed in duplicate (96-well flat-bottomed plate) in 10% DMEM growth medium (100 uL per well). Virus was then added to each well and the plates were incubated for 1 h at 37°C. TZM.bl cells were then added (1×10^4 per well in 100 uL volume) in 10% DMEM growth medium containing diethylaminoethyl- dextran (Sigma) at a final

concentration of 11 ug/mL. Murine leukemia virus (MuLV) was used as a negative controls in all assays.

Peptide microarrays

Microarray slides were incubated with purified antibody (14). Serum was diluted 1/200 in SuperBlock T20 (TBS) Blocking Buffer (Thermo Scientific), and incubated for 1h at 30°C with the peptide microarray slide. Slides were then washed with 5mL of TBS-Buffer + 0.1% Tween-20 for 3 min on a shaker at room temperature for 5 washes. Next, slides were placed in the individual chambers of a Sarstedt Quadriperm Dish and incubated with Alexa-Fluor 647-conjugated AffiniPure Mouse Anti-Human IgG (H+L) (Jackson ImmunoResearch Laboratories) for 1 hour at room temperature. Slides were then washed 5 times with TBS-Buffer + 0.1% Tween-20 and 5 times with deionized water. To dry, slides were placed in a 50mL Falcon tube, and spun at 1400rpm for 5 minutes. A control slide incubated with secondary antibodies alone without sample was also ran to determine background.

Microarray image analysis

Slides were scanned with a GenePix 4300A scanner (Molecular Devices), using 635nm and 532nm lasers at 500 PMT and 100 Power settings. Images were saved as TIF files. The fluorescence intensity for each feature (peptide spot) was calculated using GenePix Pro 7 software and GenePix Array List (GAL) file. We then calculated the mean fluorescent intensity across the triplicate sub-arrays using a custom- designed R script and R software package 2.15.2. The threshold value used to define a minimum positive fluorescent intensity was calculated for each slide using the computational tool rapmad and a custom-designed R script. Data from each individual slide was combined with data from the control slide to

create two distributions of data (noise and signal). The threshold values for positivity were defined as 5 standard deviations above the mean of the noise distribution (SD.noise*5).

An antibody epitope was defined to be 5-15 amino acid long (with the minimum epitope for antibody binding to be 5 amino acids long), the breadth to be the number of amino acid regions within any given HIV-1 protein (e.g. Env, Gag, Pol) region (e.g. V1, V2 etc. for HIV-1 Env) spanning an 11 amino acid stretch. We defined the depth to be the number of unique sequences within an overlapping region of 5 to 15 amino acids (14).

RESULTS

Total IgG and IgA antibody responses in serum and mucosal secretions elicited following protein or Adenovirus vector immunization

We first collected blood and colorectal mucosal secretions using Weck-Cel sponges from 8 healthy adult rhesus monkeys. Using sera and mucosal secretions eluted from Weck-Cel sponges (15), we assessed the amount of total IgG and IgA. As expected, we found that the amount of IgG in serum was significantly higher than that of IgA ($P = 0.0039$; paired t test), whereas the amount of IgA in colorectal mucosal secretions was significantly higher than that of IgG ($P = 0.0337$; paired t test) (Fig 2.1A). Nevertheless, the total amounts of both IgG and IgA in mucosal secretions were substantially lower than those found in serum. To confirm that the antibodies collected from mucosal sites actually represented mucosal antibodies, we assessed mucosal and serum IgA for the IgA α-chain (α-specific responses) and IgA secretory component (SC-specific responses). The α-specific responses represent both monomeric and polymeric IgA, whereas SC-specific IgA is only found in secretory IgA (sIgA) in mucosal secretions (7, 16). Serum samples showed high α-specific IgA and no detectable SC-specific IgA, as expected. In contrast, mucosal secretions showed both α-specific and SC-specific IgA (Figure 2.1B). SC-specific anti-IgA antibody proved specific for sIgA, with minimal cross-reactivity to monomeric and polymeric IgA (Figure 2.1C). These results confirm that the IgA from mucosal secretions was largely sIgA and not serum contamination.

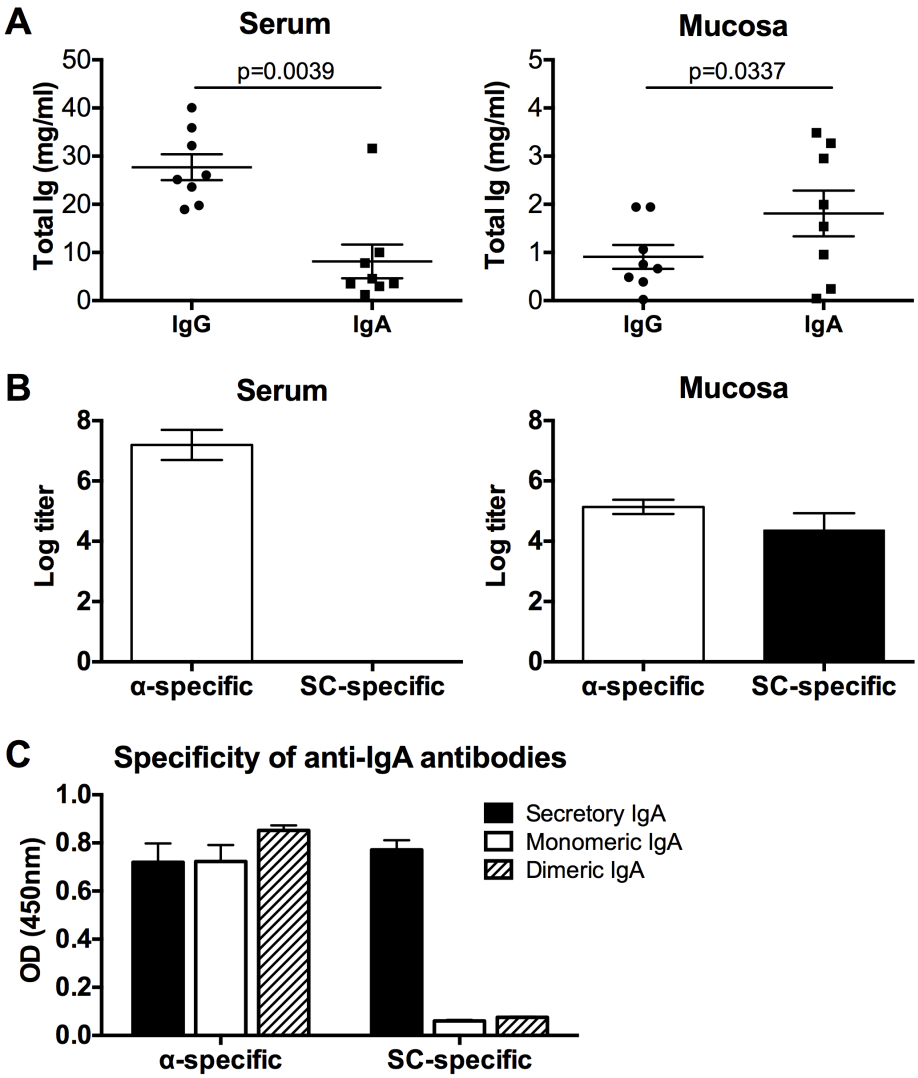

Figure 2.1 – Total mucosal IgG and IgA in rhesus monkeys

Sera and colorectal mucosal secretions were collected from 8 healthy adult rhesus monkeys.

(A) The amount of total IgG and IgA was determined by quantitative ELISA.

(B) The amount of serum and mucosal IgA containing the α-chain (α-specific) or the secretory component (SC-specific) was also determined. Means and standard deviations (SD) of endpoint titers are shown.

(C) Responses of α-specific and SC-specific anti-IgA antibodies to recombinant monomeric and dimeric IgA, as well as the sIgA standard, were determined by ELISA. Means and SD of the optical density (OD; 450 nm) from 4 replicates are shown.

Env-specific serum or mucosal IgG and IgA antibody responses elicited following protein or Adenovirus vector immunization

We next assessed Env-specific IgG and IgA responses in colorectal secretions and sera from 24 rhesus monkeys immunized with candidate HIV-1 vaccines. Sixteen adult rhesus monkeys were immunized intramuscularly (i.m.) with 2 X 10^{10} viral particles of adenovirus serotype 35 (Ad35) at week 0 and 2 X 10^{10} viral particles of Ad26 (10) at week 24 (Ad/Ad). Both Ad vectors encoded simian immunodeficiency virus $SIVS_{ME543}$ Env-Gag-Pol antigens (17). Eight additional adult rhesus monkeys were immunized i.m. with 0.25 mg recombinant HIV-1 clade C CZA97.012 Env gp140 (18) with adjuvant at weeks 0, 4, 8, 12, 16, and 20. IgG and IgA responses specific to SIV Env (SIV_{mac251} gp120; Immune Technology Corp.) and HIV-1 clade C CZA97.012 Env gp140 (8) were determined for both sera and colorectal mucosal secretions by ELISA 2 to 4 weeks and 20 to 24 weeks following the final immunization. Responses were defined as positive if the absorbance was greater than the mean plus 3 standard deviations of the absorbance of negative controls. The cutoff absorbance was generally 0.05 for IgG responses and 0.1 for IgA responses. Both Ad/Ad and protein immunizations elicited high titers of Env-specific IgG and IgA responses in sera and mucosal secretions at the peak time point ($P < 0.01$; paired t test), and these responses declined by approximately 0.5 log (range, 0.17 to 0.57 log; median, 0.54) by 20 to 24 weeks following the final immunization (Figure 2.2A). Consistent with prior reports (5), mucosal antibody titers were 1 to 2 logs lower than those found in serum. Moreover, Env-specific IgG titers were approximately 1.5 logs (range, 1.29 to 1.69 logs; median, 1.59) higher than Env-specific IgA titers in both serum and mucosal secretions. Env-specific IgA in mucosal secretions but not in serum exhibited SC-specific responses (data not shown), consistent with the data shown in Figure 2.1B. Env-specific mucosal IgG and IgA responses correlated with Env-specific systemic IgG and IgA responses at both the peak time point ($P = 0.002$ for IgG;

P = 0.0001 for IgA) and later time points (P = 0.02 for IgG; P = 0.03 for IgA) (Figure 2.2B and C), suggesting that intra-muscular immunization of Ad-vectored and protein HIV-1 candidate vaccines elicited immunologically coordinated antibody responses in the periphery and at mucosal sites.

Figure 2.2 – Vaccine-elicited mucosal antibody responses in rhesus monkeys

Rhesus monkeys were immunized i.m. with Ad35 (at week 0) and Ad26 (at week 24) encoding SIV Gag-Env-Pol (Ad/Ad; n = 16 monkeys) or recombinant HIV-1 Env protein trimer at weeks 0, 4, 8, 12, 16, and 20 (Protein; n = 8).

(A) Env-specific IgG and IgA antibody titers were determined for both serum and colorectal mucosal secretions by ELISA at baseline and 2 to 4 weeks (Ad/Ad: week 26; Protein: week 24) and 20 to 26 weeks (Ad/Ad: week 52; Protein: week 44) after the final immunization. Means and standard deviations of endpoint ELISA titers are shown.

Correlations between Env-specific IgG (left) and IgA (right) responses in sera and mucosal secretions at **(B)** 2 to 4 weeks and **(C)** 20 to 26 weeks after the final immunization were analyzed using Spearman rank-correlation tests. Filled circles, monkeys from the Ad/Ad group; open circles, monkeys from the protein group.

(figure on next page)

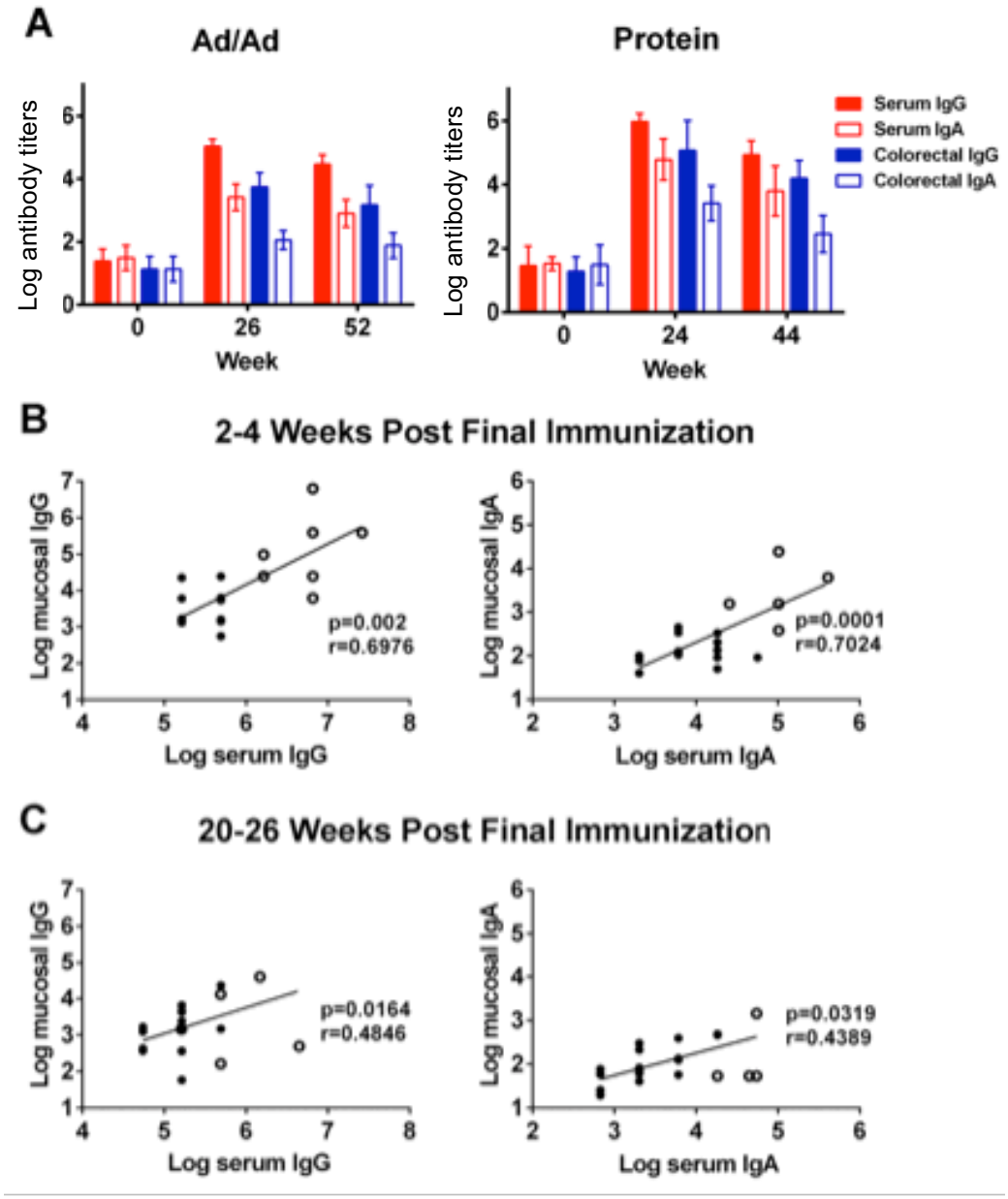

Figure 2.2 – Vaccine-elicited mucosal antibody responses in rhesus monkeys (continued)

Evaluation of Env-specific IgG subclasses and neutralizing activity of vaccine-elicited and serum mucosal antibodies

Follow-up studies of RV144 suggested that vaccine-elicited Env-specific IgG3 titers may correlate with protective efficacy (19, 20). Rhesus IgG1, IgG2, IgG3, and IgG4 sequences are 88.0% to 90.1% identical to the corresponding human IgG subclasses, although our understanding of the biology of rhesus IgG subclasses remains incomplete (21). To dissect subclasses of Env-specific IgG responses elicited in rhesus monkeys, we performed ELISAs for 6 monkeys from each group using secondary antibodies specific for rhesus IgG1 and IgG3 (kindly provided by K. Reimann, NIH Non-human Primate Reagent Resource). Both Ad/Ad and protein vaccines elicited IgG1 and IgG3 responses in serum and mucosal secretions. The Ad vectors elicited comparable titers of IgG3 and IgG1 responses in both sera and mucosal secretions, whereas the protein vaccine elicited approximately 1 log higher titers of IgG3 than IgG1 (Figure 2.3A and B), although mucosal responses were lower than serum responses for both subclasses. The anti-IgG1 and anti-IgG3 monoclonal antibodies exhibited minimal cross-reactivity to the other rhesus IgG subclasses (Figure 2.3E).

To determine if vaccine-elicited mucosal antibodies were functional, we performed neutralization assays using mucosal secretions collected at 2 weeks after the final immunization from monkeys that received the Ad/Ad vaccines compared with eight additional control monkeys that received a sham vaccine. Mucosal secretions and sera from vaccinated monkeys exhibited significantly greater neutralizing activity against the TCLA strain of $SIV_{mac251.15}$ compared to that of the sham group ($P < 0.001$ for sera and $P < 0.01$ for mucosal secretions; unpaired t test) (Figure 2.3C and D). Thus, these vaccine vectors elicited functional neutralizing antibodies in colorectal secretions, although titers in mucosal secretions were around 2 logs lower than those found in serum. These data suggest that IgG isotypes and functionality of vaccine-elicited, Env-specific mucosal antibody responses are

similar to those of antibodies in peripheral blood, despite the overall predominance of IgA in mucosal secretions.

Figure 2.3 IgG subclasses and neutralizing activity of vaccine-elicited mucosal antibodies

(A) Env-specific IgG1 and IgG3 titers were determined for sera from Ad/Ad (left)- and protein (right)-immunized monkeys by ELISA.

(B) Env-specific IgG1 and IgG3 titers were also determined for mucosal secretions.

(A and B): ns, not significant; **: $P < 0.01$ (paired t test).

(C) Pseudovirus neutralizing assays were performed using tissue culture-adapted strain SIVmac251.15. The 50% infective dose (ID50) titers were determined for sera from monkeys immunized with Ad/Ad at 2 weeks after the final immunization.

(D) ID50 titers were also determined for mucosal secretions from these monkeys. Samples from sham-immunized monkeys were used as controls.

(C and D): **: $P < 0.01$; ***: $P < 0.001$ (unpaired t test).

(E) Reactivity of anti-IgG1 and anti-IgG3 monoclonal antibodies to recombinant rhesus IgG1, IgG2, IgG3, and IgG4 were determined by ELISA. Means and SD of the OD (450 nm) from 6 replicates are shown.

(figure on next page)

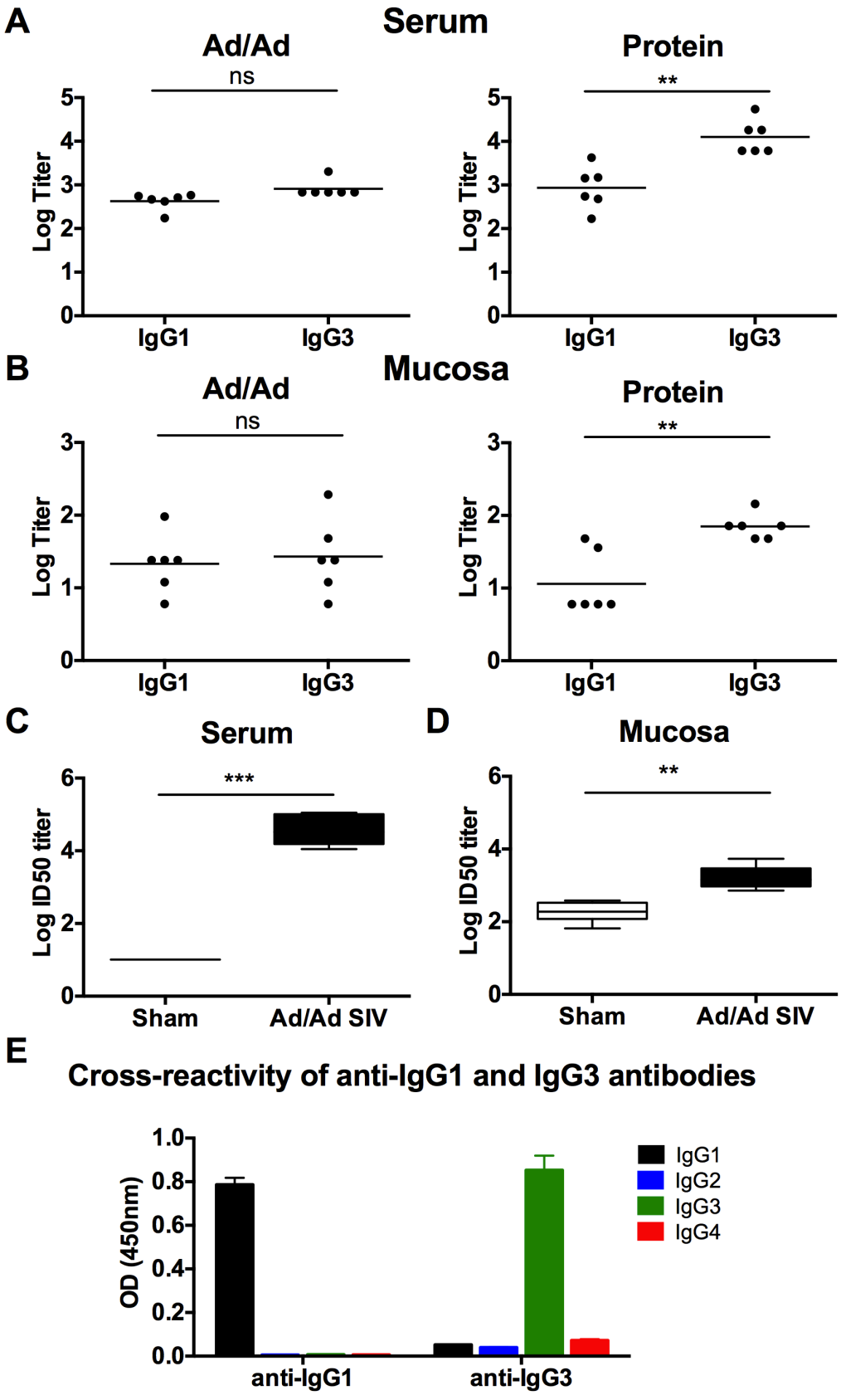

Figure 2.3 – IgG subclasses and neutralizing activity of vaccine-elicited mucosal antibodies (continued)

Mapping of linear Env epitopes bound by mucosal and serum IgG following vaccination

To determine if vaccine-elicited antibodies at mucosal sites had epitope specificities similar to those of vaccine-elicited antibodies in serum, we assessed paired mucosal and serum samples for Env-specific IgG linear epitope profiling from 5 monkeys immunized with the Env protein using peptide microarrays (JPT Peptide Technology). As a negative control, we also evaluated mucosal and serum samples from two naive unvaccinated monkeys, the results of which proved negligible (22, 23). Microarrays consisted of 3 identical subarrays containing 3,882 linear Env peptides covering 57% of global HIV-1 Env sequences in the Los Alamos National Laboratory database (24). Mucosal and serum samples were incubated with microarrays and a labeled secondary antibody, and the signal intensity (SI) of peptide binding was measured by a Genepix 4300A scanner. The threshold value used to define a minimum positive signal was calculated for each slide using the computational tool rapmad (robust alignment of peptide microarray data) (25) and was established as 5 standard deviations above the mean of the noise distribution. To calculate the breadth of antibody responses, we evaluated the number of Env peptide responses for each animal, and we aligned the reactive peptide sequences to eliminate overlap. If any reactive peptide sequences shared 5 or more amino acids, we assumed that the peptides were recognized by the same antigen-binding site on a single antibody; these overlapping sequences were conservatively defined as a single positive "binding site." If the first and last overlapping peptide in a string of overlapping peptides shared 4 or fewer amino acids, we assumed that the peptides were recognized by a minimum of two antibody binding sites. To calculate the depth of antibody responses, we evaluated the overlapping sequences of each binding site and determined the number of unique sequence variations for each binding site. We then calculated the median number of variations/binding site for each animal.

The pattern of IgG binding to linear Env peptides appeared strikingly similar between serum and mucosal samples, with both serum and mucosal antibodies binding predominantly to V3 linear peptides, followed by V1/V2 and V4 peptides (Figure 2.4A and B). Within compartments, there was some variability between animals in the binding to V1/V2 peptides, but V3 binding was universal (data not shown). For individual monkeys, a mean of 97% of serum responses overlapped by ≥ 5 amino acids with mucosal responses, whereas a mean of 81% of mucosal responses over- lapped by 5 amino acids with serum responses. There was a significant positive correlation between the mean signal intensity of mucosal and serum IgG peptide binding ($P < 0.0001$, Spearman rank-correlation test) (Figure 2.4C). Of note, both mucosal and serum IgG from protein-immunized monkeys showed binding to peptides within the V1/V2 region of Env (positions 120 to 204) (2). In addition, there was no difference between the breadth and depth of IgG binding to linear Env peptides between the mucosal and serum compartments (Figure 2.4D). These results suggest that Env-specific mucosal and serum IgG generally share similar epitope specificities.

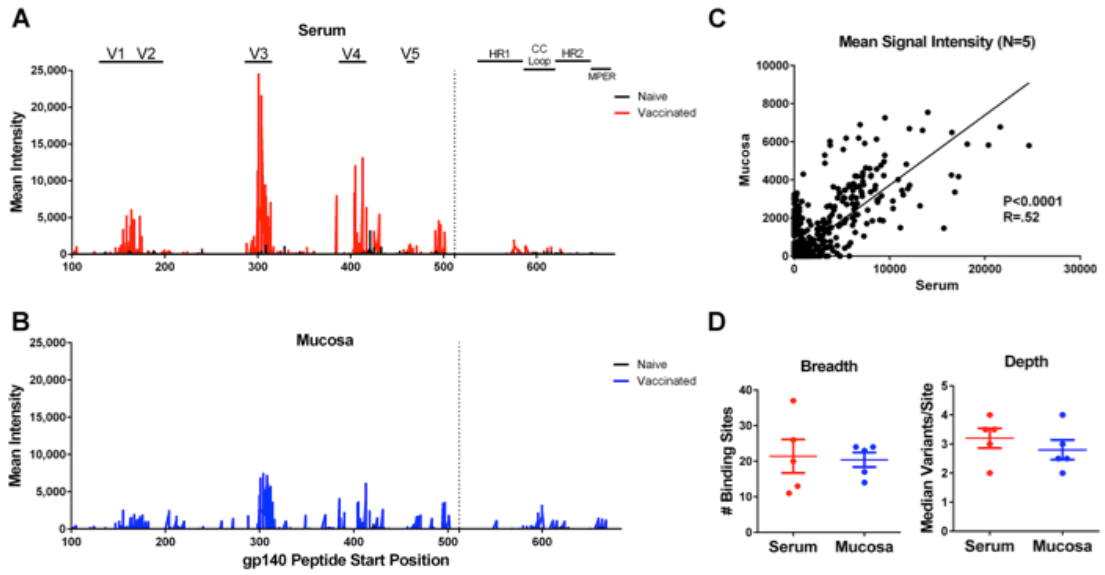

Figure 2.4 Mucosal and serum IgG binding to linear Env peptides by peptide microarrays

IgG binding to 3,882 linear Env peptides was assessed by peptide microarrays using serum and mucosal secretions from 5 monkeys immunized with the Env protein vaccine 16 weeks after the final immunization as well as 2 naive control monkeys.

(A) Mean signal intensity of binding is plotted by the peptide gp140 start position for serum.

(B) Mean signal intensity of binding is plotted for mucosal samples.

(C) Mean signal intensity of mucosal peptide binding is plotted against mean signal intensity of serum peptide binding for the 5 immunized monkeys. Correlations were analyzed using the Spearman rank-correlation test.

(D) The breadth (number of binding sites) and depth (median number of epitope variants/binding site) for each immunized monkey are plotted for serum and mucosal samples. Mean responses and standard errors of the means (SEM) are depicted.

DISCUSSION

HIV-1 infects humans primarily through mucosal surfaces, and therefore it is likely that a prophylactic vaccine would elicit protective antibodies both at mucosal surfaces and in the systemic circulation. For optimal induction of mucosal immune responses, several studies have suggested that vaccines should be administered through mucosal routes (3, 26). However, other studies have demonstrated that vaccines given parentally can also induce mucosal antibody responses in certain settings (27, 28). A comparative evaluation of intranasal (i.n.) and parental (i.m.) immunization of an HIV-1 peptide-based immunogen with adjuvant in cynomolgus monkeys showed that antibody responses at the nasal and genital mucosa were highest in animals immunized parentally (29). Individual mucosal compartments also display differences with respect to antibody isotypes and densities, as well as origins of cells involved in innate and adaptive immunity.

In this study, we demonstrate that intramuscular immunization with both Ad-vectored and protein-based candidate HIV-1 vaccines elicited potent and durable Env-specific antibody responses in colorectal mucosa and that the kinetics, isotype, functionality, and epitope specificity of mucosal antibodies generally mirror those found in serum. These data suggest that vaccine-elicited peripheral and mucosal humoral immune responses are likely immunologically coordinated. The remarkable degree of similarity also raises the possibility that mucosal and peripheral antibodies elicited by vaccination may originate from the common B cell populations, although a detailed study of mucosal B cells is beyond the scope of this study. Previous studies suggest that mucosal IgA is largely synthesized locally and transported through epithelial cells into the lumen (30). The degree to which mucosal IgG and IgA elicited by vaccination reflects peripheral versus local B cells requires additional investigation.

REFERENCES

1. **Hladik F**, **McElrath MJ**. 2008. Setting the stage: host invasion by HIV. Nat Rev Immunol **8**:447–457.

2. **Haynes BF**, **Gilbert PB**, **McElrath MJ**, **Zolla-Pazner S**, **Tomaras GD**, **Alam SM**, **Evans DT**, **Montefiori DC**, **Karnasuta C**, **Sutthent R**, **Liao HX**, **DeVico AL**, **Lewis GK**, **Williams C**, **Pinter A**, **Fong Y**, **Janes H**, **DeCamp A**, **Huang Y**, **Rao M**, **Billings E**, **Karasavvas N**, **Robb ML**, **Ngauy V**, **de Souza MS**, **Paris R**, **Ferrari G**, **Bailer RT**, **Soderberg KA**, **Andrews C**, **Berman PW**, **Frahm N**, **De Rosa SC**, **Alpert MD**, **Yates NL**, **Shen X**, **Koup RA**, **Pitisuttithum P**, **Kaewkungwal J**, **Nitayaphan S**, **Rerks-Ngarm S**, **Michael NL**, **Kim JH**. 2012. Immune-correlates analysis of an HIV-1 vaccine efficacy trial. N Engl J Med **366**:1275–1286.

3. **Devito C**, **Zuber B**, **Schroder U**, **Benthin R**, **Okuda K**, **Broliden K**, **Wahren B**, **Hinkula J**. 2004. Intranasal HIV-1-gp160-DNA/gp41 Peptide Prime-Boost Immunization Regimen in Mice Results in Long-Term HIV-1 Neutralizing Humoral Mucosal and Systemic Immunity. J Immunol **173**:7078–7089.

4. **Oliveira AF**, **Cardoso SA**, **Almeida FBDR**, **de Oliveira LL**, **Pitondo-Silva A**, **Soares SG**, **Hanna ES**. 2012. Oral immunization with attenuated Salmonella vaccine expressing Escherichia coli O157:H7 intimin gamma triggers both systemic and mucosal humoral immunity in mice. Microbiol Immunol **56**:513–522.

5. **Buffa V**, **Klein K**, **Fischetti L**, **Shattock RJ**. 2012. Evaluation of TLR agonists as potential mucosal adjuvants for HIV gp140 and tetanus toxoid in mice. **7**:e50529.

6. **Kozlowski PA**, **Williams SB**, **Lynch RM**, **Flanigan TP**, **Patterson RR**, **Cu-Uvin S**, **Neutra MR**. 2002. Differential Induction of Mucosal and Systemic Antibody Responses in Women After Nasal, Rectal, or Vaginal Immunization: Influence of the Menstrual Cycle. J Immunol **169**:566–574.

7. **Patterson LJ**, **Kuate S**, **Daltabuit-Test M**, **Li Q**, **Xiao P**, **McKinnon K**, **DiPasquale J**, **Cristillo A**, **Venzon D**, **Haase A**, **Robert-Guroff M**. 2012. Replicating adenovirus-simian immunodeficiency virus (SIV) vectors efficiently prime SIV-specific systemic and mucosal immune responses by targeting myeloid dendritic cells and persisting in rectal macrophages, regardless of immunization route. Clin Vaccine Immunol **19**:629–637.

8. **Nkolola JP**, **Peng H**, **Settembre EC**, **Freeman M**, **Grandpre LE**, **Devoy C**, **Lynch DM**, **La Porte A**, **Simmons NL**, **Bradley R**, **Montefiori DC**, **Seaman MS**, **Chen B**, **Barouch DH**. 2010. Breadth of neutralizing antibodies elicited by stable, homogeneous clade A and clade C HIV-1 gp140 envelope trimers in guinea pigs. J Virol **84**:3270–3279.

9. **Permar SR**, **Wilks AB**, **Ehlinger EP**, **Kang HH**, **Mahlokozera T**, **Coffey RT**, **Carville A**, **Letvin NL**, **Seaman MS**. 2010. Limited contribution of mucosal IgA to Simian immunodeficiency virus (SIV)-specific neutralizing antibody response and virus envelope evolution in breast milk of SIV-infected, lactating rhesus monkeys. J Virol **84**:8209–8218.

10. **Li M**, **Gao F**, **Mascola JR**, **Stamatatos L**, **Polonis VR**, **Koutsoukos M**, **Voss G**, **Goepfert P**, **Gilbert P**, **Greene KM**, **Bilska M**, **Kothe DL**, **Salazar-Gonzalez JF**, **Wei X**, **Decker JM**, **Hahn BH**, **Montefiori DC**. 2005. Human immunodeficiency virus type 1 env clones from acute and early subtype B infections for standardized assessments of vaccine-elicited neutralizing antibodies. J Virol **79**:10108–10125.

11. **Sarzotti-Kelsoe M**, **Bailer RT**, **Turk E**, **Lin C-L**, **Bilska M**, **Greene KM**, **Gao H**, **Todd CA**, **Ozaki DA**, **Seaman MS**, **Mascola JR**, **Montefiori DC**. 2014. Optimization and validation of the TZM-bl assay for standardized assessments of neutralizing antibodies against HIV-1. J Immunol Methods **409**:131–146.

12. **Mascola JR**, **D'Souza P**, **Gilbert P**, **Hahn BH**, **Haigwood NL**, **Morris L**, **Petropoulos CJ**, **Polonis VR**, **Sarzotti M**, **Montefiori DC**. 2005. Recommendations for the Design and Use of Standard Virus Panels To Assess Neutralizing Antibody Responses Elicited by Candidate Human Immunodeficiency Virus Type 1 Vaccines. J Virol **79**:10103–10107.

13. **Li M**, **Gao F**, **Mascola JR**, **Stamatatos L**, **Polonis VR**, **Koutsoukos M**, **Voss G**, **Goepfert P**, **Gilbert P**, **Greene KM**, **Bilska M**, **Kothe DL**, **Salazar-Gonzalez JF**, **Wei X**, **Decker JM**, **Hahn BH**, **Montefiori DC**. 2005. Human immunodeficiency virus type 1 env clones from acute and early subtype B infections for standardized assessments of vaccine-elicited neutralizing antibodies. J Virol **79**:10108–10125.

14. **Stephenson KE**, **Neubauer GH**, **Reimer U**, **Pawlowski N**, **Knaute T**, **Zerweck J**, **Korber BT**, **Barouch DH**. 2014. Quantification of the epitope diversity of HIV-1-specific binding antibodies by peptide microarrays for global HIV-1 vaccine development. J Immunol Methods.

15. **Kozlowski PA**, **Lynch RM**, **Patterson RR**, **Cu-Uvin S**, **Flanigan TP**, **Neutra MR**. 2000. Modified wick method using Weck-Cel sponges for collection of human rectal secretions and analysis of mucosal HIV antibody. **24**:297–309.

16. **Brandtzaeg P**. 1995. Molecular and cellular aspects of the secretory immunoglobulin system*. APMIS **103**:1–19.

17. **Abbink P**, **Lemckert AAC**, **Ewald BA**, **Lynch DM**, **Denholtz M**, **Smits S**, **Holterman L**, **Damen I**, **Vogels R**, **Thorner AR**, **O'Brien KL**, **Carville A**, **Mansfield KG**, **Goudsmit J**, **Havenga MJE**, **Barouch DH**. 2007. Comparative seroprevalence and immunogenicity of six rare serotype recombinant adenovirus vaccine vectors from subgroups B and D. J Virol **81**:4654–4663.

18. **Barouch DH**, **Liu J**, **Li H**, **Maxfield LF**, **Abbink P**, **Lynch DM**, **Iampietro MJ**, **Sanmiguel A**, **Seaman MS**, **Ferrari G**, **Forthal DN**, **Ourmanov I**, **Hirsch VM**, **Carville A**, **Mansfield KG**, **Stablein D**, **Pau MG**, **Schuitemaker H**, **Sadoff JC**, **Billings EA**, **Rao M**, **Robb ML**, **Kim JH**, **Marovich MA**, **Goudsmit J**, **Michael NL**. 2012. Vaccine protection against acquisition of neutralization-resistant SIV challenges in rhesus monkeys. Nature **482**:89–93.

19. **Chung AW**, **Ghebremichael M**, **Robinson H**, **Brown E**, **Choi I**, **Lane S**, **Dugast A-S**, **Schoen MK**, **Rolland M**, **Suscovich TJ**, **Mahan AE**, **Liao L**, **Streeck H**,

Andrews C, **Rerks-Ngarm S**, **Nitayaphan S**, **de Souza MS**, **Kaewkungwal J**, **Pitisuttithum P**, **Francis D**, **Michael NL**, **Kim JH**, **Bailey-Kellogg C**, **Ackerman ME**, **Alter G**. 2014. Polyfunctional Fc-effector profiles mediated by IgG subclass selection distinguish RV144 and VAX003 vaccines. Sci Transl Med **6**:228ra38–228ra38.

20. **Yates NL**, **Liao HX**, **Fong Y**, **DeCamp A**, **Vandergrift NA**, **Williams WT**, **Alam SM**, **Ferrari G**, **Yang Z-Y**, **Seaton KE**, **Berman PW**, **Alpert MD**, **Evans DT**, **O'Connell RJ**, **Francis D**, **Sinangil F**, **Lee C**, **Nitayaphan S**, **Rerks-Ngarm S**, **Kaewkungwal J**, **Pitisuttithum P**, **Tartaglia J**, **Pinter A**, **Zolla-Pazner S**, **Gilbert PB**, **Nabel GJ**, **Michael NL**, **Kim JH**, **Montefiori DC**, **Haynes BF**, **Tomaras GD**. 2014. Vaccine-induced Env V1-V2 IgG3 correlates with lower HIV-1 infection risk and declines soon after vaccination. Sci Transl Med **6**:228ra39–228ra39.

21. **Scinicariello F**, **Engleman CN**, **Jayashankar L**, **McClure HM**, **Attanasio R**. 2004. Rhesus macaque antibody molecules: sequences and heterogeneity of alpha and gamma constant regions. Immunology **111**:66–74.

22. **Nahtman T**, **Jernberg A**, **Mahdavifar S**, **Zerweck J**, **Schutkowski M**, **Maeurer M**, **Reilly M**. 2007. Validation of peptide epitope microarray experiments and extraction of quality data. J Immunol Methods **328**:1–13.

23. **Masch A**, **Zerweck J**, **Reimer U**, **Wenschuh H**, **Schutkowski M**. 2010. Antibody signatures defined by high-content peptide microarray analysis. Methods Mol Biol **669**:161–172.

24. **Stephenson KE**, **Pawlowski N**, **Hoegen Von P**, **Reimer U**, **Rosenberg ES**, **Barouch DH**. HIV-1 antibody epitope mapping of individuals treated with antiretroviral therapy during acute/early HIV-1-infection. *In*. Barcelona, Spain.

25. **Renard BY**, **Löwer M**, **Kühne Y**, **Reimer U**, **Rothermel A**, **Türeci O**, **Castle JC**, **Sahin U**. 2011. rapmad: Robust analysis of peptide microarray data. BMC Bioinformatics **12**:324.

26. **Mapletoft JW**, **Latimer L**, **Babiuk LA**, **Littel-van den Hurk SVD**. 2010. Intranasal Immunization of Mice with a Bovine Respiratory Syncytial Virus Vaccine Induces Superior Immunity and Protection Compared to Those by Subcutaneous Delivery or Combinations of Intranasal and Subcutaneous Prime-Boost Strategies. Clin Vaccine Immunol **17**:23–35.

27. **Shoji M**, **Katayama K**, **Tachibana M**, **Tomita K**, **Sakurai F**, **Kawabata K**, **Mizuguchi H**. 2012. Intramuscular DNA immunization with in vivo electroporation induces antigen-specific cellular and humoral immune responses in both systemic and gut-mucosal compartments. Vaccine **30**:7278–7285.

28. **Krause A**, **Whu WZ**, **Xu Y**, **Joh J**, **Crystal RG**, **Worgall S**. 2011. Protective anti-Pseudomonas aeruginosa humoral and cellular mucosal immunity by AdC7-mediated expression of the P. aeruginosa protein OprF. Vaccine **29**:2131–2139.

29. **Egan MA**, **Chong SY**, **Hagen M**, **Megati S**, **Schadeck EB**, **Piacente P**, **Ma B-J**,

Montefiori DC, **Haynes BF**, **Israel ZR**, **Eldridge JH**, **Staats HF**. 2004. A comparative evaluation of nasal and parenteral vaccine adjuvants to elicit systemic and mucosal HIV-1 peptide-specific humoral immune responses in cynomolgus macaques. Vaccine **22**:3774–3788.

30. **Mestecky J**, **Moro I**, **Kerr MA**, **Woof JM**. 2005. Chapter 9 - Mucosal Immunoglobulins, pp. 153–182. *In* Mestecky, J, Lamm, ME, McGhee, JR, Bienenstock, J, Mayer, L, Strober, W (eds.), Mucosal Immunology (Third Edition)Third Edition. Academic Press, Burlington.

CHAPTER 3:

Similar epitope specificities of IgG and IgA antibodies elicited by Ad26 vector prime, Env protein boost immunizations in rhesus monkeys

This chapter is based on the peer-review publication:

Kang, Z-H, C.A. Bricault, E.N. Borducchi, K.E. Stephenson, M.S. Seaman, M. Pau, H. Schuitemaker, D. van Manen, F. Wegmann, and D.H. Barouch. Similar epitope specificities of IgG and IgA antibodies elicited by Ad26 vector prime, Env protein boost immunizations in rhesus monkeys. In press, *Journal of Virology*

ACKNOWLEDGEMENTS

We thank A. Badamchi, L. Parenteau, M. Shetty, K. Smith and L. Peter for their generous advice and assistance. A32 was obtained through the AIDS NIH Reagent Program. We acknowledge support from: National Institutes of Health grants AI096040, AI124377, AI126603, AI128751.

ABSTRACT

Vaccine-elicited immunoglobulin G (IgG) has been shown to be important for protection against simian/human immunodeficiency virus (SHIV) infection in rhesus monkeys. However, it remains unclear whether vaccine-elicited IgA responses are beneficial or detrimental for protection. In this study, we evaluated the kinetics, magnitude, breadth, and linear epitope specificities of vaccine-elicited IgG and IgA responses in serum and mucosal secretions following intramuscular immunization with Ad26 prime, Env protein boost vaccination regimens. The systemic and mucosal antibody responses exhibited similar kinetics but lower titers than serum antibody responses. Moreover, IgG and IgA responses were correlated, both in terms of the magnitude of responses and in terms of antibody specificities against linear HIV-1 Env, Gag and Pol epitopes. These data suggest that IgG and IgA responses are highly coordinated in both peripheral blood and mucosal compartments following Ad26/Env vaccination in rhesus monkeys.

INTRODUCTION

HIV-1 infection in humans is mainly transmitted via the mucosal route (1). It is therefore likely that a prophylactic vaccine will need to elicit protective antibody responses at the mucosal sites of infection (2). However, mucosal IgG and IgA responses following vaccination remain poorly characterized. Cervico-vaginal secretions generally contain higher levels of IgG than IgA, whereas gastrointestinal secretions and saliva typically contain more IgA (3, 4).

The RV144 vaccine trial demonstrated 31.2% efficacy in preventing HIV-1 infection (5). Follow-up studies showed that while plasma IgG directed against the variable loop 1 and 2 (V1/V2) region in Env correlated directly with protection, plasma IgA binding to Env inversely correlated with protection (6). It has been hypothesized that IgA directed against the C1 region of Env, may have interfered with the antibody-dependent cellular cytotoxicity effector (ADCC) function of the protective IgG responses (7).

However, HIV-specific IgA responses have also been previously linked to protection in certain models. In HIV-1 exposed, persistently seronegative individuals, HIV-specific IgA antibodies were detected in both the serum and mucosal secretions (8-11), and mucosal and plasma IgA purified from these seronegative individuals inhibited HIV mucosal transcytosis *in vitro* (8, 9). In rhesus macaques that were passively immunized with IgA1, IgA2, and IgG1 versions of a neutralizing monoclonal human antibody HGN194, IgA1 provided the best protection against a SHIV challenge, and only IgA1 blocked transcytosis of cell-free virus across the epithelial layer *in vitro*, even though all three versions had similar neutralizing activities (12).

Thus, it remains unclear whether vaccine-induced peripheral and mucosal IgA responses are beneficial or detrimental for protection against infection. The Ad26 prime, Env protein boost (Ad26/Env) vaccine has previously been shown to provide partial protection

against SIVmac251 and SHIV-SF162P3 challenges (13), and this vaccine has recently been advanced into a phase 2b proof-of-concept study in humans (HVTN705, HPX2008). In this study, we evaluated the magnitude and epitope specificity of IgG and IgA elicited by Ad26/Env vaccination in rhesus monkeys.

MATERIALS AND METHODS

Animals and immunizations

20 adult rhesus monkeys (Macaca mulatta) were housed in the Alphagenesis Inc. Animal Research Facility. All studies were approved by the Alphagenesis Inc. Institutional Animal Care and Use Committee (IACUC). Priming immunizations at weeks 0 and 12 involved IM injections of $1X10^{10}$ viral particles (v.p.) of non-replicating recombinant adenovirus 26 (Ad26) vector expressing HIV mosaic Gag, Pol, and Env immunogens (Ad26.Gag-Pol and Ad26.Env) (14, 15). Animals were subsequently boosted IM at weeks 24 and 48 with either clade C gp140Fd trimer protein immunogen alone (250ug/animal), or in combination with Ad26.Gag-Pol and Ad26.Env ($1X10^{10}$v.p./animal). Clade C gp140 trimer protein immunizations were adjuvanted with either Adju-Phos (850ug) or Matrix M (60ug). The antigens were formulated in a dose volume of 500uL, and administered via IM injections in the quadriceps muscles. Immunization regimens are detailed in Table 1.

Antibody purification

IgG purification – IgG was purified from serum using a protein G-agarose column (2mL of protein G-agarose beads). Columns were washed with Protein G IgG binding buffer (Thermo Scientific #21019) and bound IgG was subsequently eluted with 0.1M glycine (pH 2-3) and immediately neutralized with 1M Tris (pH 8). The different IgG eluate fractions were then pooled together and buffer exchanged with 1X PBS using a Amicon Ultra 10K Device Spin column.

IgA purification – IgA was purified from IgG-depleted serum with a peptide M-agarose column (2mL of peptide M-agarose beads). Columns were washed with Peptide M IgA binding buffer (10mM sodium phosphate, 150mM sodium chloride, pH7.2), and bound IgA

subsequently eluted with 0.1M glycine (pH2-3) and immediately neutralized with 1M Tris (pH 8). The different IgA eluate fractions were then pooled together, run over a protein G-agarose column again to remove any contaminating IgG, and subsequently buffer exchanged with 1X PBS using a Amicon Ultra 10K Device Spin column.

ELISA

Serum IgG and IgA – Serum binding antibody titers against HIV-1 Env were determined by endpoint ELISAs as previously described. (16). Briefly, 96-well Maxisorp ELISA plates (Thermo Fisher Scientific) were coated overnight with 100 uL per well of HIV-1 Env at a concentration of 1 ug/mL in PBS, and subsequently blocked for 4 h with PBS containing 2% BSA (Sigma) and 0.05% Tween-20 (Sigma). Serum serially diluted and incubated for 1 h at room temperature. Plates were washed 3 times with PBS containing 0.05% Tween-20 and were incubated for 1 h with HRP-conjugated anti-IgG (Jackson ImmunoResearch Laboratories Inc.), or biotin-conjugated anti-IgA (Alpha Diagnostic International). Plates incubated with biotin-conjugated anti-IgA were washed 3 times and subsequently incubated with streptavidin-HRP. The plates were washed 3 times and developed with SureBlue tetramethylbenzidine microwell peroxidase (KPL Research Products), stopped by the addition of stop solution (KPL research Products), and analyzed at 450nm/550nm on a Spectramax Plus ELISA plate reader (Molecular Devices) using Softmax Pro-4.7.1 software.

Total IgG and IgA concentrations were determined using a kit from Alpha Diagnostic International.

Mucosal IgG and IgA – For monkey mucosal secretion ELISAs, plates were instead incubated with a biotin-conjugated secondary antibody (Alpha Diagnostic International) for 1 h at 37°C, washed 3 times, incubated with streptavidin-HRP for 1h before developing.

ELISA endpoint titers were defined as the highest reciprocal serum or mucosal secretion dilution that yielded absorbance greater than 2-fold background (IgG responses) or 3-fold background (IgA responses).

Neutralizing Antibody Assay in TZM.bl Cells

Neutralizing antibody responses against HIV-1 Env pseudovirions were measured using luciferase-based virus neutralization assays in TZM.bl cells (16-19). These assays measure the reduction in luciferase reporter gene expression in TZM.bl cells following a single round of virus infection. The ID50 was calculated as the serum dilution that resulted in a 50% reduction in relative luminescence units compared with the virus control wells after the subtraction of cell control relative luminescence units. Threefold serial dilutions of serum samples were performed in duplicate (96-well flat-bottomed plate) in 10% DMEM growth medium (100 uL per well). Virus was then added to each well and the plates were incubated for 1 h at 37°C. TZM.bl cells were then added (1×10^4 per well in 100 uL volume) in 10% DMEM growth medium containing diethylaminoethyl- dextran (Sigma) at a final concentration of 11 ug/mL. Murine leukemia virus (MuLV) was used as a negative controls in all assays. HIV-1 Env pseudoviruses, including clade A (DJ263.8), clade B (SF162.LS and BaL.26), and clade C (MW965.26) isolates were prepared as previously described (19)

Peptide microarrays

Microarray slides were incubated with purified antibody (20). 1ug/mL of purified IgG and 5ug/mL of purified IgA was diluted 1/10 in SuperBlock T20 (TBS) Blocking Buffer (Thermo Scientific), and incubated for 1h at 30C with the peptide microarray slide. Slides were then washed with 5mL of TBS-Buffer + 0.1% Tween-20 for 3 min on a shaker at room temperature for 5 washes. Next, slides were placed in the individual chambers of a Sarstedt

Quadriperm Dish and incubated with Alexa-Fluor 647-conjugated AffiniPure Mouse Anti-Human IgG (H+L) (Jackson ImmunoResearch Laboratories) and biotin-conjugated anti-Monkey IgA (Alpha-Diagnostics International) for 1 hour at room temperature. Slides were then washed 5 times with TBS-Buffer + 0.1% Tween-20. Cy3-conjugated Strepavidin (Jackson ImmunoResearch Laboratories) was added to the slide and incubated in the dark for 1 h at room temperature. Slides were then washed 5 times with TBS-Buffer + 0.1% Tween-20 and 5 times with deionized water. To dry, slides were placed in a 50mL Falcon tube, and spun at 1400rpm for 5 minutes. A control slide incubated with secondary antibodies alone without sample was also ran to determine background.

Microarray image analysis

Slides were scanned with a GenePix 4300A scanner (Molecular Devices), using 635nm and 532nm lasers at 500 PMT and 100 Power settings. Images were saved as TIF files. The fluorescent intensity for each feature (peptide spot) was calculated using GenePix Pro 7 software and GenePix Array List (GAL) file. We then calculated the mean fluorescent intensity across the triplicate sub-arrays using a custom- designed R script and R software package 2.15.2. The threshold value used to define a minimum positive fluorescent intensity was calculated for each slide using the computational tool rapmad and a custom-designed R script. Data from each individual slide was combined with data from the control slide to create two distributions of data (noise and signal). The threshold values for positivity were defined as 5 standard deviations above the mean of the noise distribution (SD.noise*5). As different fluorophores and lasers were used to detect IgG and IgA, the mean signal fluorescent intensity (MFI) values of reactive peptides for each monkey were normalized to a scale of a 100.

An antibody epitope was defined to be 5-15 amino acid long (with the minimum epitope for antibody binding to be 5 amino acids long), the breadth to be the number of amino acid regions within any given HIV-1 protein (e.g. Env, Gag, Pol) region (e.g. V1, V2 etc. for HIV-1 Env) spanning an 11 amino acid stretch. We defined the depth to be the number of unique sequences within an overlapping region of 5 to 15 amino acids (20).

Comparison of IgG vs IgA epitopes: To compare the common vs. unique linear epitopes targeted by IgG and IgA, we compared the lists of reactive peptides sequences targeted by both IgG and IgA (or both) within each animal. The reactive peptide sequences for IgG and IgA in the same animal were aligned against each other to eliminate overlap. If any reactive peptide sequences shared 5 or more amino acids, we conservatively assumed that the peptides reflected the same epitopes. If the first and last overlapping peptide in a string of overlapping peptides shared 4 or fewer amino acids, we assumed that the peptides were recognized by a minimum of two antibody-binding sites. The list of unique linear epitope sequences for IgG was then compared to the list of unique sequences for IgA to determine which sequences were common (versus unique) to both IgG and IgA.

Competition ELISA

96 well Maxisorp plates were coated overnight with 1ug/mL of Mos1 (100uL per well). They were washed with PBS containing 0.05% Tween-20 and subsequently blocked for 3h with PBS containing 1% BSA and 0.05% Tween-20. Purified serum IgG and IgA were then added in serial dilutions (with a starting concentration of 1620ug/mL and 20ug/mL respectively) and incubated for 1 h at room temperature. The plates were washed and incubated for 1 h with biotinylated A32 (biotinylation kit: EX-Link Micro NHS-PEG4-Biotinylation). The amount of A32-biotin added was previously determined by choosing a

concentration of A32-biotin with 0.28ug/mL of streptavidin-HRP that will give a OD of about 1. The plates were then washed and incubated with 0.28ug/mL of streptavidin-HRP for an hour, and developed with SureBlue tetramethylbenzidine microwell peroxidase (KPL Research Products), stopped by the addition of stop solution (KPL research Products), and analyzed at 450nm/550nm on a Spectramax Plus ELISA plate reader (Molecular Devices) using Softmax Pro-4.7.1 software.

RESULTS

Vaccination regimens

We utilized a study originally designed to test five different Adenovirus 26 (Ad26) vector and Env protein immunization regimens (Table 3.1) for a detailed evaluation of IgG and IgA antibody responses. 20 rhesus macaques (Macaca mulatta) were primed intramuscularly (IM) with either a 3- or 4- valent Ad26 vector regimen at week 0 and 12, and then were boosted by Env gp140 protein at weeks 24 and 48, either alone or in combination with Ad26 vectors. Two groups (N=8) also received an additional Env gp140 boost at week 76, whereas three groups (N=12) did not receive an Env gp140 boost at week 76.

These regimens all induced a similar magnitude of Env-specific binding antibodies by ELISA at weeks 28 and 53 (Figure 1A). To evaluate vaccine-induced IgG and IgA responses, we pooled animals that either did (N=8) or did not (N=12) receive the week 76 Env gp140 boost for subsequent analyses. Animals that received different regimens shared similar magnitudes and kinetics of binding antibody responses within these two groups (Figure 3.1A).

Table 3.1 – Immunization regimens of rhesus macaques

$1X10^{10}$ viral particles (v.p.) of Ad26 vectors, 250ug of a C97ZA012 gp140 (Clade C) envelope protein, 60ug of the adjuvant Matrix M, or 850ug of the adjuvant Adju-Phos, were administered intramuscularly (IM) in the quadriceps of rhesus macaques (n = 4 per group) as detailed in the table above. Animals were immunized on weeks 0, 12, 24, 48 and 76.

Each Ad26 vector carries mosaic Gag-Pol transgene sequences and mosaic Env transgene sequences. These mosaic sequences have been bioinformatically designed to optimize cellular immunologic coverage of the global HIV-1 sequence diversity (14, 15).

		Immunization Schedule		
		Week 0, 12	**Week 24, 48**	**Week 76**
Groups	**1**	Ad26.Mos1.GagPol Ad26.Mos2.GagPol Ad26.Mos1.Env Ad26.Mos2.Env	Clade C gp140Env + Adju-Phos	Adju-Phos
	2	Ad26.Mos1.GagPol Ad26.Mos2.GagPol Ad26.Mos1.Env Ad26.Mos2.Env	Ad26.Mos1.GagPol Ad26.Mos2.GagPol Ad26.Mos1.Env Ad26.Mos2.Env Clade C gp140Env + Adju-Phos	MosM gp140Env + Adju-Phos
	3	Ad26.Mos1.GagPol Ad26.Mos2.GagPol Ad26.Mos1.Env Ad26.Mos2.Env	Ad26.Mos1.GagPol Ad26.Mos2.GagPol Ad26.Mos1.Env Ad26.Mos2.Env Clade C gp140Env + Matrix M	PBS
	4	Ad26.Mos1.GagPol Ad26.Mos2.GagPol Ad26.Mos1.Env	Ad26.Mos1.GagPol Ad26.Mos2.GagPol Ad26.Mos1.Env Clade C gp140Env + Adju-Phos	MosM gp140Env + Adju-Phos
	5	Ad26.Mos1.GagPol Ad26.Mos2.GagPol Ad26.Mos1.Env Ad26.Mos3.Env	Ad26.Mos1.GagPol Ad26.Mos2.GagPol Ad26.Mos1.Env Ad26.Mos3.Env Clade C gp140Env + Adju-Phos	PBS

Serum and mucosal binding antibody titers are correlated following vaccination

To assess Env-specific binding antibody titers from serum and colorectal secretions, we assessed samples from 4 weeks after each Env immunization (weeks 28, 53, 80) by ELISA. Consistent with our previous observations (21), Env-specific IgG and IgA responses were elicited in both serum and mucosal compartments, and the kinetics of mucosal antibody titers closely mimicked those in serum (Figures 3.1A, B). However, mucosal antibody titers were 1.5-2.0 logs lower than those found in serum (median: 2.051 logs for Mos1; 1.574 logs for C97), and Env-specific IgA titers were 0.5-1.0 log lower than Env-specific IgG titers (median: 0.953 logs for serum responses; 0.477 logs for mucosal responses). Antibody titers at week 80 were higher in the groups that received the additional week 76 boost compared with the groups that did not receive the week 76 boost ($p<0.005$ for all serum responses; $p<0.05$ for mucosal responses, except C97-specific IgG mucosal response: $p=0.0516$) (Figure 3.1B).

IgG versus IgA antibody titers were tightly correlated in both serum and mucosal compartments (serum: $r=0.8427$, mucosal: $r=0.8285$ for Mos1; serum: $r=0.7908$, mucosal: $r=0.9095$ for C97; $p<0.0001$, Spearman rank-correlation test) (Figure 2A). Serum IgG versus mucosal IgG antibody titers were also significantly correlated ($r=0.2865$, $p=0.0265$ for Mos1-specific responses; $r=0.4733$, $p=0.0001$ for C97-specific responses), as were serum IgA versus mucosal IgA antibody titers ($r=0.4824$, $p<0.0001$ for Mos1; $r=0.4998$, $p<0.0001$ for C97) (Figure 3.2B). These data extend previous findings showing that Env-specific mucosal antibody responses correlated with the systemic antibody responses following vaccination (22). This correlation was observed at multiple time points (data not shown), suggesting that responses are immunologically coordinated.

To investigate whether the Env-specific IgA in colorectal secretions represented transudation of serum IgA into the colorectal mucosa, we assessed mucosal Mos1-specific IgA for the presence of IgA-containing secretory component region (SC region), which is present on secretory IgA in mucosal secretions (23). There was no detectable SC region in Mos1-specific IgA in colorectal samples (Figure 3.2C). However, total IgA containing the SC region was readily detected in colorectal secretions, while no SC-region specific IgA was detected in serum as expected (Figure 3.2D). The IgA:IgG ratio was different in the serum and mucosal compartments, suggesting that there was little to no contamination of these mucosal samples by serum. These data are consistent with a model in which the majority of Env-specific IgA in mucosal secretions reflects transudation of serum IgA rather than locally produced IgA.

Figure 3.1 – Envelope-specific IgG and IgA antibody responses elicited following IM vaccination in serum and colorectal secretions

Rhesus monkeys were immunized IM with either a 3- or 4-valent Ad26 prime-boost regimen, as detailed in Table 3.1, on weeks 0, 12, 24 and 48. On week 76, animals were subsequently either sham boosted, or boosted with a clade C envelope protein (C97ZA012 gp140).

Serum and colorectal (CR) samples were assessed for Env-specific IgG and IgA binding antibody responses by endpoint ELISA, using clade C (C97ZA012) and mosaic (Mos1) Env coating proteins at weeks 0, 28, 53, 76 and 80. Horizontal broken lines represent assay threshold. Serum samples from 24 naïve monkeys were used to establish a baseline for Env-specific IgA responses in serum.

(A) Antibody responses are shown for individual immunization regimen groups. Mean and standard error of mean (SEM) values are shown.

(B) Antibody responses for animals that did (red, N=8) or did not (black, N=12) receive the week 76 Env protein boost were pooled together. Median for endpoint ELISA titers is shown.

(figure on next page)

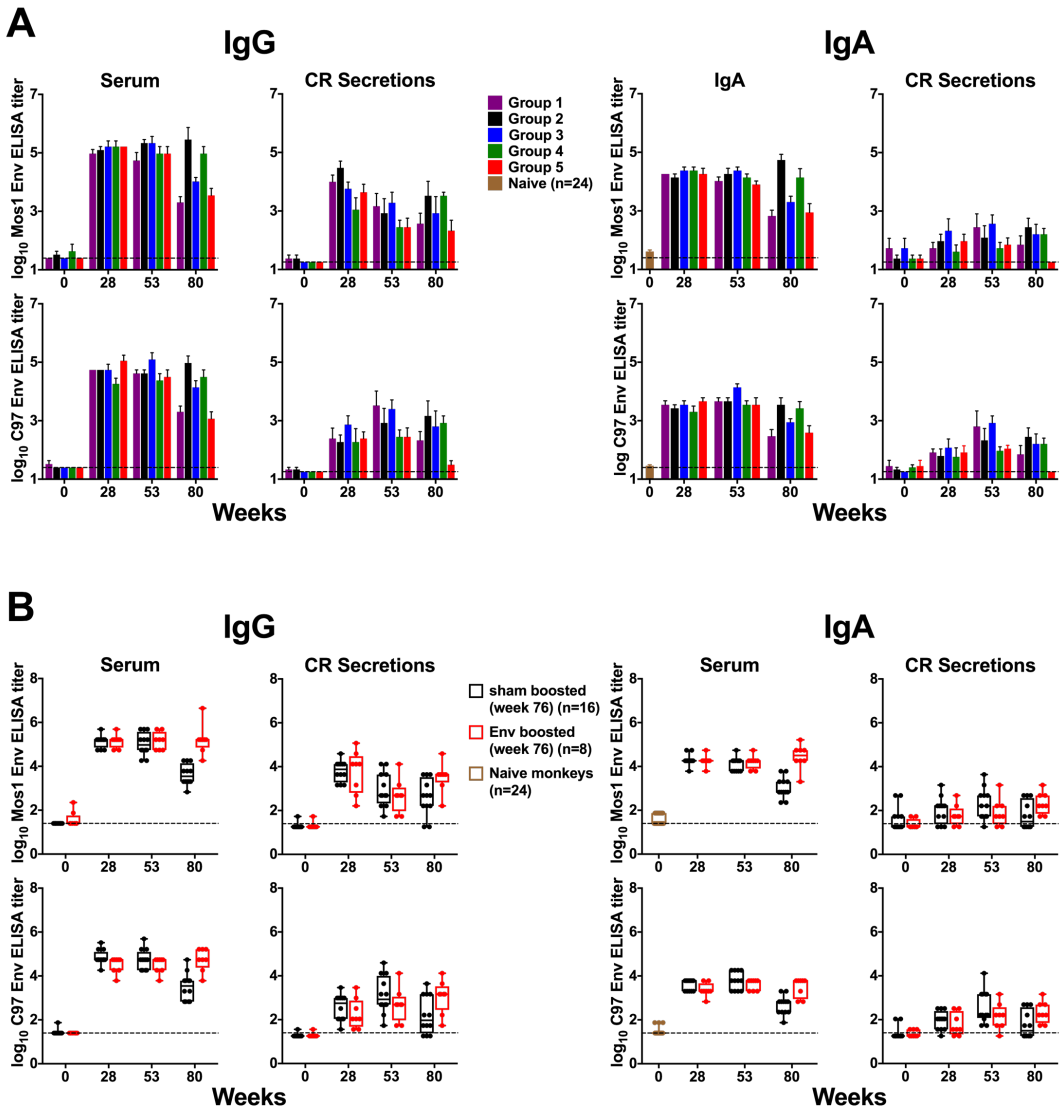

Figure 3.1 – Envelope-specific IgG and IgA antibody responses elicited following IM vaccination in serum and colorectal secretions (continued)

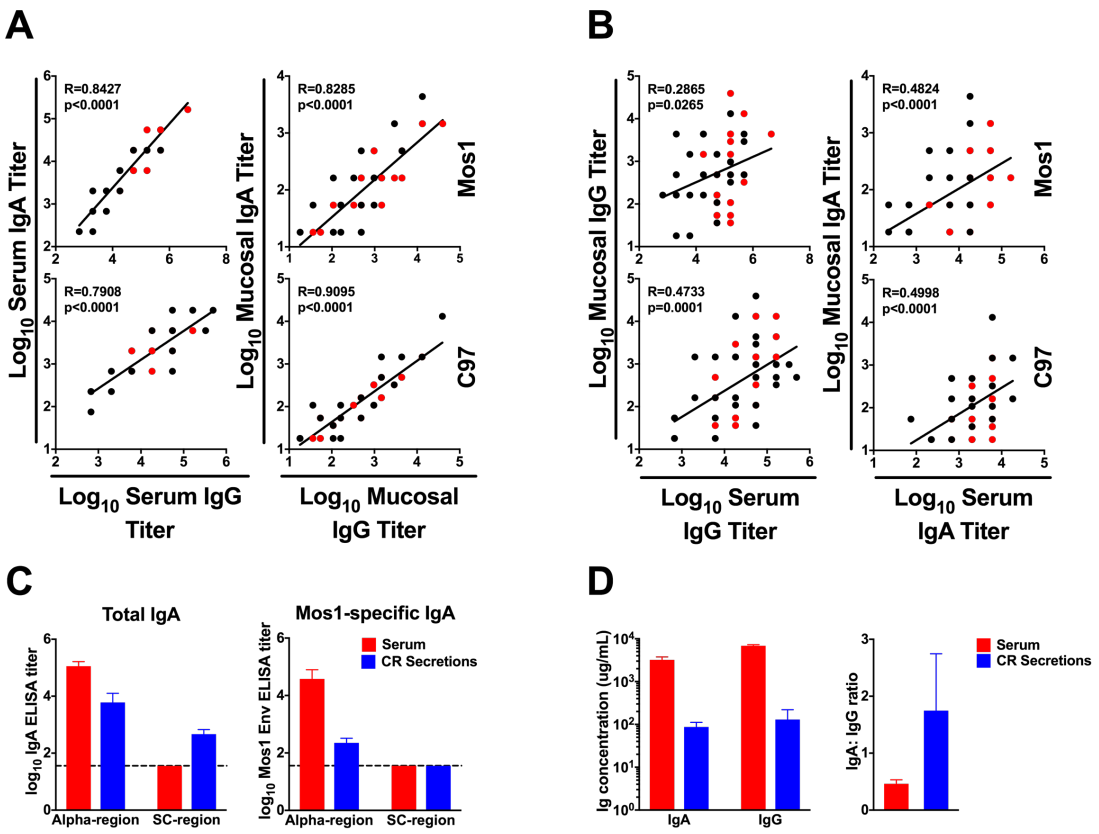

Figure 3.2 – Analysis of vaccine-elicited Env-specific IgG and IgA binding antibody responses in serum and colorectal secretions

(A-B) Correlations between C97 or Mos1 Env-specific IgG and IgA binding antibody titers in serum and colorectal samples were evaluated for weeks 28, 53 and 80. **(A)** Correlations between C97 or Mos1 Env-specific IgG and IgA responses in serum (left) and mucosal secretions (right). **(B)** Correlations between C97 or Mos1 Env-specific serum and mucosal antibody titers for IgG (left) and IgA (right). Correlations were analyzed using the Spearman rank-correlation tests.

(C-D) Week 80 serum and colorectal secretion samples from monkeys boosted 4 weeks earlier with the Env protein (n=3) were then evaluated for: **(C)** the presence of secretory component (SC) region in total and Mos1 Env-specific IgA **(D)** Total IgG and IgA concentrations and the IgA: IgG ratio. Mean and SEM values are shown.

Neutralizing antibody titers are correlated with binding antibody titers following vaccination

To determine the neutralizing capacity of antibodies elicited by the different immunization regimens, neutralizing antibody responses (NAb) from serum samples were analyzed across a panel of Tier 1A (highly sensitive) and Tier 1B (less sensitive) pseudoviruses using the TZM.bl neutralization assay (17, 18). As previously reported, these vaccines do not induce Tier 2 NAb responses (13). Higher neutralizing antibody titers were elicited against Tier 1A pseudoviruses (MW965.26 and SF162.LS) as compared to the Tier 1B pseudoviruses (DJ263.8 and BaL.26), and neutralizing antibody responses generally increased in magnitude following each immunization (Figure 3.3A). At week 80, only those animals that were boosted at week 76 (red bars) showed an increase in the magnitude of their neutralizing antibody titers, as expected (Figure 3.3A). We were unable to assess neutralizing antibody responses in colorectal secretions due to insufficient sample volume. C97 and Mos1 Env-specific mucosal and serum binding IgG and IgA titers correlated with the Tier 1A neutralizing antibody responses (Figure 3.3B and 3.3C, respectively; $r>0.65$, $p<0.0001$ for all IgG correlations; $r>0.34$, $p<0.005$ for all IgA correlations; Spearman-rank correlation tests). Weaker correlations between binding antibody titers and neutralizing antibody titers were observed against Tier 1B pseudoviruses (data not shown), likely due to the low Tier 1B responses.

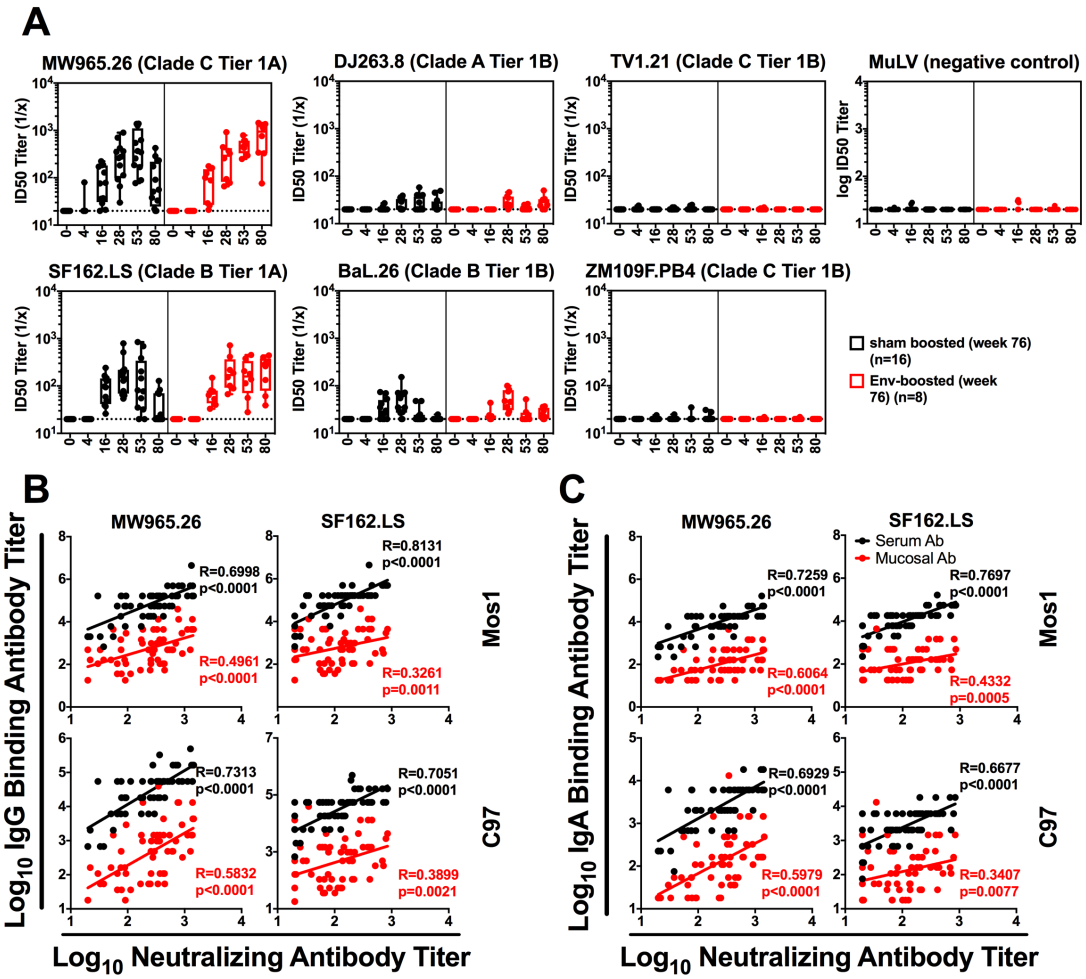

Figure 3.3 – Peripheral neutralizing antibody responses elicited by systemic IM immunizations.

Rhesus monkeys were immunized IM with either a 3- or 4-valent Ad26 prime-boost regimen, as detailed in Table 1, on weeks 0, 12, 24, and 48. On week 76, animals were subsequently either sham boosted (black, n=12), or boosted with a clade C envelope protein (red, n=8).

(A) Serum neutralizing antibody responses were analyzed across a panel of Tier 1A (MW965.26 and SF162.LS) and Tier 1B (DJ263.8, BaL.26, TV1.21, ZM109F.PB4) pseudoviruses and the 50% infective dose (ID_{50}) was determined. Murine Leukemia Virus (MuLV) was used as a negative control. Horizontal broken lines represent assay threshold. Median for neutralizing endpoint titers is shown.

(B-C) Correlations between Mos1 Env-specific and C97 Env-specific binding IgG **(B)** and IgA **(C)** antibody responses in either serum (black) or mucosal (red) samples, and neutralizing antibody responses to MW965.26, SF162.LS pseudoviruses, for weeks 28, 53 and 80 after the first immunization. Correlations were analyzed using the Spearman rank-correlation tests.

IgG and IgA elicited by vaccination have similar linear antibody epitope breadth and depth

IgG and IgA were separately purified from week 80 serum samples using a protein G-agarose column (IgG), and a peptide M-agarose column (IgA), respectively (24). A SDS/PAGE gel was subsequently ran to determine the purity of samples (Figure 3.4A). Purified IgG showed similar reactivity as seen on ELISAs (data not shown).

To determine the diversity of the linear epitopes targeted by vaccine-elicited IgG or IgA, purified IgG and IgA samples from week 80 serum were assessed by peptide microarrays containing 6564 HIV-1 15 amino acid long peptides as previously described (20), using the groups that were boosted at week 76, with the highest binding and neutralizing antibody responses.

Purified serum IgG and IgA linear binding antibody responses were analyzed for Env, Gag and Pol. The pattern of IgG and IgA binding against linear Env peptides was overall similar, with both IgG and IgA responses predominantly directed against V1/V2, V3, C4, C5 and HR2 epitopes, although there was more IgG binding to the V3 region, and more IgA binding to C4 region (Figure 3.4B). Only minimal IgA responses were directed to C1, which have been reported to be a target for IgA that interferes with IgG-mediated ADCC activity (7). There was also a correlation between the normalized mean signal fluorescent intensity (MFI) of IgG versus IgA ($r=0.2856$, $p<0.0001$; Spearman-rank correlation test) (Figure 3.4C), consistent with the ELISA data (Figure 3.2A). The breadth and depth of IgG binding to linear Env, Gag and Pol peptides were similar to the breadth and depth of IgA binding to these regions (Figure 3.4D-F). IgG trended towards a slightly greater breadth of peptide binding than IgA, and its depth against Env linear epitopes was slightly higher than IgA ($p=0.011$) (Figure 3.4D), but overall IgG and IgA showed comparable profiles.

For individual Env regions, we similarly observed a trend of IgG recognizing a slightly greater breadth and depth of epitopes than IgA, particularly in the C1, C2 (breadth) and C1, C2, V2, V3 and HR2 regions (depth) (Figure 3.4D). However, these differences were sporadic and modest and likely reflects the overall higher magnitude of IgG responses. Similarly, we observed similar IgG and IgA breadth and depth of antibody responses within individual Gag (Figure 3.4E) and Pol (Figure 3.4F) regions. The protease region in Pol was not included in the Ad vectors, and thus no binding was observed for protease epitopes as expected (Figure 3.4F).

Figure 3.4 – Purified IgG and IgA binding to linear Env, Gag and Pol peptides by peptide microarray

IgG and IgA binding to Env, Gag or Pol linear 15-mer peptides was analyzed by peptide microarray, using purified IgG and IgA from week 80 serum samples from monkeys boosted 4 weeks earlier with a clade C Env protein (C97ZA012 gp140) (Groups 2 and 4, n=8).

(A) Representative Coomassie-stained SDS-PAGE gels of purified IgG and IgA. Each lane represents purified IgG or IgA antibody from an individual animal.

(B) The normalized mean fluorescence intensity (MFI) of the IgG (black, top) and IgA (red, bottom) responses against Env linear peptides is plotted against the Env peptide start position (HXB2 numbering). MFI values for the IgG or IgA responses for each animal were normalized to a scale of 100 AU, based on the highest MFI value for each monkey. The MFI values of all 8 monkeys are depicted.

(C) Correlation between IgG and IgA normalized MFI values for Env peptides. Correlations were analyzed using the Spearman rank-correlation tests.

(D-F) The breadth (number of binding sites per region) and depth (the number of epitope variants per region) for each immunized monkey is plotted for purified IgG (black) and IgA (red) responses against **(D)** Env, **(E)** Gag, and **(F)** Pol linear peptides. The breadth and depth of the antibody responses against peptides from the entire Gag, Pol or Env protein (left), or individual regions within each protein (right) are both depicted. Horizontal bars depict median for breadth or depth. Statistical significance was analyzed using the Mann Whitney test (*: $p \leq 0.05$, **: $p \leq 0.01$, ***: $p \leq 0.001$).

(figure on next page)

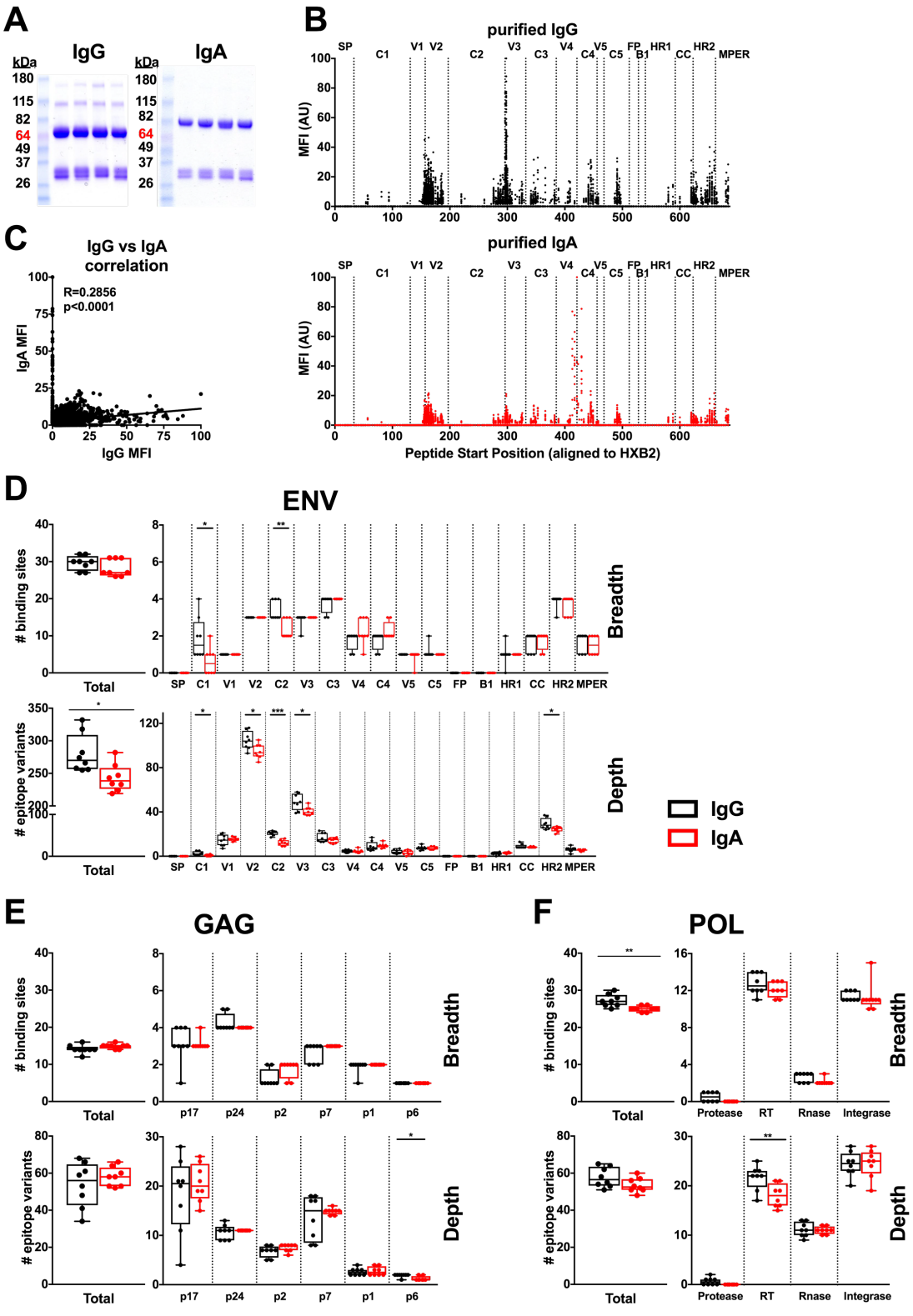

Figure 3.4 – Purified IgG and IgA binding to linear Env, Gag and Pol peptides by peptide microarray (continued)

IgG and IgA from vaccinated monkeys target similar linear epitopes

We next explored the extent to which IgG and IgA targeted similar linear epitopes in Env, Gag, and Pol. IgG and IgA responses appeared to recognize similar linear Env, Gag and Pol peptides, with the majority of epitopes targeted by both IgG and IgA (Figure 3.5) (mean: Env: 67.1%, Gag: 67.33%, Pol: 69.5%). However, there was a minority of epitopes that were targeted uniquely by either IgG (mean: Env: 19.72%, Gag: 12.91%, Pol: 19.92%) or IgA (mean: Env: 4.31%, Gag: 19.76%, Pol: 10.57%). Unique epitopes are peptide sequences that differ by at least 1 amino acid, and are found across the antigen, in regions of high density of epitopes common to both IgG and IgA. There were slightly more unique linear Env ($p=0.002$) and Pol ($p=0.0393$) epitopes targeted by IgG compared with IgA (Figure 3.5). This finding is consistent with the observation that the breadth and depth of IgG responses were slightly higher than those of IgA responses (Figure 3.4D-F).

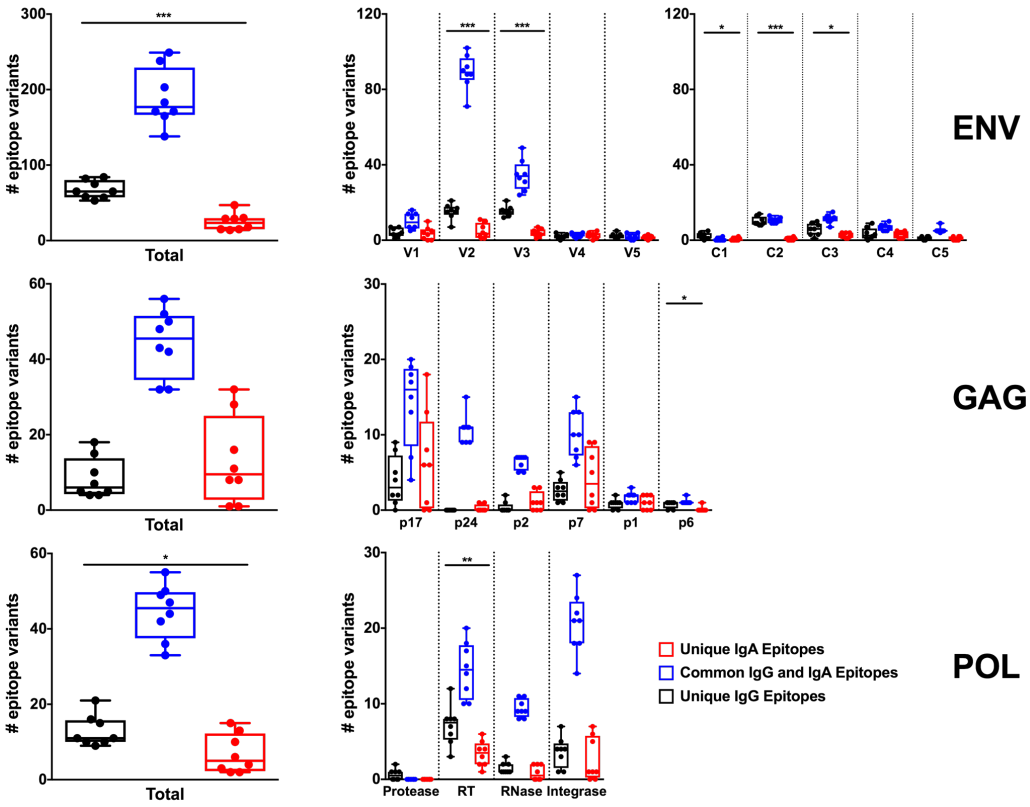

Figure 3.5 – Comparison of IgG and IgA linear epitope binding

Env (V1-V5 and C1-C5 regions only), Gag, and Pol linear epitopes targeted by purified IgA and IgG from serum were compared for sequence similarity. Blue bars depict common sequences that are targeted by both IgA and IgG responses, while the black or red bars depict sequences that are uniquely targeted by either IgG or IgA respectively. Horizontal bars represent the median number of targeted sequences. Sequences were compared for individual regions within Env, Gag and Pol (right), as well as for each protein in general. Only the V1-V5 and C1-C5 regions of Env were analyzed. Statistical significance was analyzed using the Mann Whitney test (*: $p \leq 0.05$, **: $p \leq 0.01$, ***: $p \leq 0.001$).

Purified IgG from vaccinated monkeys only weakly targets the A32 epitope

To determine whether purified IgA samples from this study bound the C1 conformational epitope that was previously found to interfere with the ADCC function of IgG (7), a competition ELISA was performed using the monoclonal antibody (mAb) A32. A32 binds a C1 conformational epitope (25), and was previously used to identify the C1 binding epitope of IgG-mediated ADCC in the RV144 trial (26). Using a competition ELISA against the Mos1 antigen, low concentrations of purified IgG (up to 6.67 ug/mL) did not compete with A32 binding, but,high concentrations of purified IgG competed with A32 binding. Purified IgA does not compete against A32 binding up to a concentration of 20ug/mL (Figure 3.6). We were unable to use higher concentrations of IgA. These data demonstrate that IgA responses induced by the Ad26/Env vaccine were unable to compete with A32 binding.

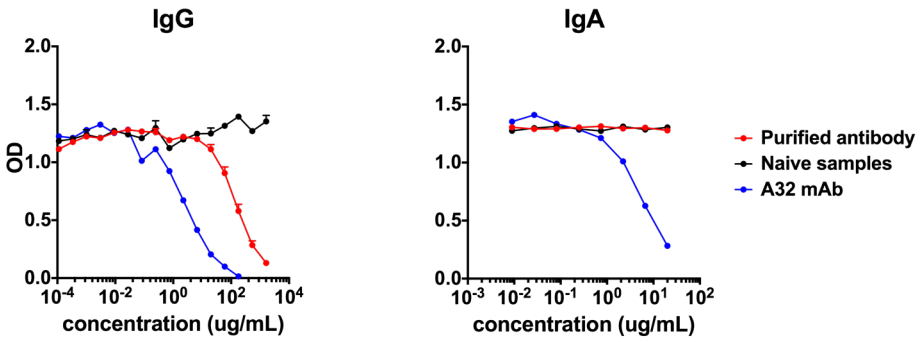

Figure 3.6 – Competition ELISA with the A32 mAb

Purified IgG and IgA (n=8) from week 80 serum samples from monkeys boosted 4 weeks earlier with a Clade C Env protein (C97ZA012 gp140) were used in a competition ELISA to block binding of the A32 mAb to Mos1 Env. A32 mAb was used as a positive control, and purified IgG and IgA from naïve monkeys (n=3) were used as a negative control. Mean and standard error of mean are shown.

DISCUSSION

Mucosal surfaces represent the critical portals for HIV-1 entry, and thus it is likely that mucosal antibody responses will be required to be generated by a prophylactic HIV-1 vaccine. While immunization via a mucosal route is optimal to generate mucosal antibody responses in certain models, it is also clear that parenteral immunizations can effectively induce both systemic and mucosal immune responses in animal models (27-29), and in humans (30-32).

In this study, we showed that intramuscularly administered Ad26/Env vaccines induced both serum and mucosal Env-specific IgG and IgA antibodies in rhesus macaques. The kinetics and magnitude of mucosal antibody responses were similar to that of serum responses. Moreover, IgG and IgA responses were correlated in both anatomic compartments (Figures 3.1 and 3.2A). These data suggest that systemic and mucosal antibody responses are immunologically coordinated, with mucosal antibodies likely reflecting transudation of serum antibodies into mucosal compartments (21, 33, 34). These findings confirm and extend prior studies. In monkeys that were systemically injected with monomeric or dimeric IgA forms of the broadly neutralizing antibody b12, both forms of IgA were found in mucosal compartments (34). Bound polymeric immunoglobulin receptor (pIgR) is subsequently cleaved to form the secretory component (SC). It is possible that the Env-specific IgA found in colorectal secretions of our vaccinated monkeys are transudated from serum, given the absence of SC region-containing Env-specific IgA (Figure 3.2C).

IgA is the major antibody isotype present in mucosal secretions (1), and is important in protective responses against viral infections. However, it remains unclear whether HIV-1-specific IgA responses are beneficial or detrimental (35). Serum anti-Env IgA titers were inversely correlated with reduced acquisition risk in the RV144 clinical trial (6, 7), and the mechanism of this effect has been hypothesized to involve C1-specific IgA that reduces the

ADCC function of Env-specific IgG (7). However, it has so been suggested that Env-specific HIV-1 IgA responses are possibly markers of correlates of risk of infection, rather than have a direct mechanistic effect on protective humoral responses (36). Additionally, it is unlikely that IgA correlations from a canarypox ALVAC /gp120 monomeric Env immunization regimen would be expected to be relevant to an Ad26/Env immunization regimen. We utilized the high-throughput peptide microarray as a tool to study vaccine-elicited IgA antibody responses in greater detail, with the limitation that conformational epitopes are not evaluated in this assay. Peptide microarrays were utilized to assess antibody diversity against HIV-1 linear epitopes (6, 37). We detected consistent systemic and mucosal IgA responses, generally with lower titers than IgG responses. Purified IgG and IgA samples from our vaccinated monkeys bound to similar regions within the Env protein, predominantly in the V1-V3 and C4, C5 regions (Figure 3.4B), with minimal to no linear IgG and IgA responses directed against the C1 linear epitope. The mAb A32 blocks ADCC and binds a conformational C1 epitope (26, 38). By competition ELISA, high concentrations of purified IgG (above 20 ug/mL), but not IgA, blocked A32 binding (Figure 3.6).

Class switch recombination is mediated by activation-induced cytidine deaminase, and results in the expression of one of the downstream isotypes (IgA, IgG, or IgE) from the expression of IgM or IgD on naïve B cells. IgA is formed by class switching from either IgM or IgG intermediaries (39, 40), and it has been shown *in vitro* that IgA is preferentially formed by sequential switching through IgG intermediaries (41). Our results showing that IgG and IgA targeted similar Env, Gag and Pol linear peptide sequences (Figure 3.5), suggests that vaccine-elicited IgA and IgG reflected common B cell precursors, and it is possible that IgA could have been elicited via class switching through a IgG intermediary. As IgG and IgA class switching are regulated by the local microenvironment such as cytokines (42), these data raise interesting questions about how and when class switching

occurs following immunization, and how this may affect protection against subsequent infection.

Our findings demonstrate that IgG and IgA responses in peripheral blood and colorectal secretions are tightly correlated following Ad26/Env vaccination, both in terms of overall magnitude as well as individual epitopes targeted. The Ad26/Env vaccine is currently being evaluated in a phase 2b clinical efficacy trial, and thus whether vaccine-elicited IgA contributes to, or detracts from, protective efficacy is an important question that warrants further evaluation.

REFERENCES:

1. **Hladik F**, **McElrath MJ**. 2008. Setting the stage: host invasion by HIV. Nat Rev Immunol **8**:447–457.

2. **Xiao P**, **Patterson LJ**, **Kuate S**, **Brocca-Cofano E**, **Thomas MA**, **Venzon D**, **Zhao J**, **DiPasquale J**, **Fenizia C**, **Lee EM**, **Kalisz I**, **Kalyanaraman VS**, **Pal R**, **Montefiori D**, **Keele BF**, **Robert-Guroff M**. 2012. Replicating Adenovirus-Simian Immunodeficiency Virus (SIV) Recombinant Priming and Envelope Protein Boosting Elicits Localized, Mucosal IgA Immunity in Rhesus Macaques Correlated with Delayed Acquisition following a Repeated Low-Dose Rectal SIV mac251Challenge. J Virol **86**:4644–4657.

3. **Mestecky J**, **Moldoveanu Z**, **Russell MW**. 2005. Immunologic uniqueness of the genital tract: challenge for vaccine development. Am J Reprod Immunol **53**:208–214.

4. **Mestecky J**, **Moro I**, **Kerr MA**, **Woof JM**. 2005. Chapter 9 - Mucosal Immunoglobulins, pp. 153–182. In Mestecky, J, Lamm, ME, McGhee, JR, Bienenstock, J, Mayer, L, Strober, W (eds.), Mucosal Immunology (Third Edition)Third Edition. Academic Press, Burlington.

5. **Rerks-Ngarm S**, **Pitisuttithum P**, **Nitayaphan S**, **Kaewkungwal J**, **Chiu J**, **Paris R**, **Premsri N**, **Namwat C**, **de Souza M**, **Adams E**, **Benenson M**, **Gurunathan S**, **Tartaglia J**, **McNeil JG**, **Francis DP**, **Stablein D**, **Birx DL**, **Chunsuttiwat S**, **Khamboonruang C**, **Thongcharoen P**, **Robb ML**, **Michael NL**, **Kunasol P**, **Kim JH**, **MOPH-TAVEG Investigators**. 2009. Vaccination with ALVAC and AIDSVAX to prevent HIV-1 infection in Thailand. N Engl J Med **361**:2209–2220.

6. **Haynes BF**, **Gilbert PB**, **McElrath MJ**, **Zolla-Pazner S**, **Tomaras GD**, **Alam SM**, **Evans DT**, **Montefiori DC**, **Karnasuta C**, **Sutthent R**, **Liao HX**, **DeVico AL**, **Lewis GK**, **Williams C**, **Pinter A**, **Fong Y**, **Janes H**, **DeCamp A**, **Huang Y**, **Rao M**, **Billings E**, **Karasavvas N**, **Robb ML**, **Ngauy V**, **de Souza MS**, **Paris R**, **Ferrari G**, **Bailer RT**, **Soderberg KA**, **Andrews C**, **Berman PW**, **Frahm N**, **De Rosa SC**, **Alpert MD**, **Yates NL**, **Shen X**, **Koup RA**, **Pitisuttithum P**, **Kaewkungwal J**, **Nitayaphan S**, **Rerks-Ngarm S**, **Michael NL**, **Kim JH**. 2012. Immune-correlates analysis of an HIV-1 vaccine efficacy trial. N Engl J Med **366**:1275–1286.

7. **Tomaras GD**, **Ferrari G**, **Shen X**, **Alam SM**, **Liao HX**, **Pollara J**, **Bonsignori M**, **Moody MA**, **Fong Y**, **Chen X**, **Poling B**, **Nicholson CO**, **Zhang R**, **Lu X**, **Parks R**, **Kaewkungwal J**, **Nitayaphan S**, **Pitisuttithum P**, **Rerks-Ngarm S**, **Gilbert PB**, **Kim JH**, **Michael NL**, **Montefiori DC**, **Haynes BF**. 2013. Vaccine-induced plasma IgA specific for the C1 region of the HIV-1 envelope blocks binding and effector function of IgG. Proc Natl Acad Sci USA **110**:9019–9024.

8. **Devito C**, **Hinkula J**, **Kaul R**, **Kimani J**, **Kiama P**, **Lopalco L**, **Barass C**, **Piconi S**, **Trabattoni D**, **Bwayo JJ**, **Plummer F**, **Clerici M**, **Broliden K**. 2002. Cross-clade HIV-1-specific neutralizing IgA in mucosal and systemic compartments of HIV-1-exposed, persistently seronegative subjects. J Acquir Immune Defic Syndr **30**:413–420.

9. **Broliden K**, **Hinkula J**, **Devito C**, **Kiama P**, **Kimani J**, **Trabbatoni D**, **Bwayo JJ**, **Clerici M**, **Plummer F**, **Kaul R**. 2001. Functional HIV-1 specific IgA antibodies in

HIV-1 exposed, persistently IgG seronegative female sex workers. **79**:29–36.

10. **Mazzoli S**, **Trabattoni D**, **Caputo Lo S**, **Piconi S**, **Blé C**, **Meacci F**, **Ruzzante S**, **Salvi A**, **Semplici F**, **Longhi R**, **Fusi ML**, **Tofani N**, **Biasin M**, **Villa ML**, **Mazzotta F**, **Clerici M**. 1997. HIV-specific mucosal and cellular immunity in HIV-seronegative partners of HIV-seropositive individuals. Nat Cell Biol **3**:1250–1257.

11. **Mazzoli S**, **Lopalco L**, **Salvi A**, **Trabattoni D**, **Caputo Lo S**, **Semplici F**, **Biasin M**, **Bl C**, **Cosma A**, **Pastori C**, **Meacci F**, **Mazzotta F**, **Villa ML**, **Siccardi AG**, **Clerici M**. 1999. Human immunodeficiency virus (HIV)-specific IgA and HIV neutralizing activity in the serum of exposed seronegative partners of HIV-seropositive persons. J Infect Dis **180**:871–875.

12. **Watkins JD**, **Sholukh AM**, **Mukhtar MM**, **Siddappa NB**, **Lakhashe SK**, **Kim M**, **Reinherz EL**, **Gupta S**, **Forthal DN**, **Sattentau QJ**, **Villinger F**, **Corti D**, **Ruprecht RM**, **CAVD Project Group**. 2013. Anti-HIV IgA isotypes: differential virion capture and inhibition of transcytosis are linked to prevention of mucosal R5 SHIV transmission. AIDS **27**:F13–20.

13. **Barouch DH**, **Alter G**, **Broge T**, **Linde C**, **Ackerman ME**, **Brown EP**, **Borducchi EN**, **Smith KM**, **Nkolola JP**, **Liu J**, **Shields J**, **Parenteau L**, **Whitney JB**, **Abbink P**, **Ng'ang'a DM**, **Seaman MS**, **Lavine CL**, **Perry JR**, **Li W**, **Colantonio AD**, **Lewis MG**, **Chen B**, **Wenschuh H**, **Reimer U**, **Piatak M**, **Lifson JD**, **Handley SA**, **Virgin HW**, **Koutsoukos M**, **Lorin C**, **Voss G**, **Weijtens M**, **Pau MG**, **Schuitemaker H**. 2015. Protective efficacy of adenovirus/protein vaccines against SIV challenges in rhesus monkeys. Science **349**:320–324.

14. **Fischer W**, **Perkins S**, **Theiler J**, **Bhattacharya T**, **Yusim K**, **Funkhouser R**, **Kuiken C**, **Haynes B**, **Letvin NL**, **Walker BD**, **Hahn BH**, **Korber BT**. 2007. Polyvalent vaccines for optimal coverage of potential T-cell epitopes in global HIV-1 variants. Nat Cell Biol **13**:100–106.

15. **Barouch DH**, **O'Brien KL**, **Simmons NL**, **King SL**, **Abbink P**, **Maxfield LF**, **Sun Y-H**, **La Porte A**, **Riggs AM**, **Lynch DM**, **Clark SL**, **Backus K**, **Perry JR**, **Seaman MS**, **Carville A**, **Mansfield KG**, **Szinger JJ**, **Fischer W**, **Muldoon M**, **Korber B**. 2010. Mosaic HIV-1 vaccines expand the breadth and depth of cellular immune responses in rhesus monkeys. Nat Med **16**:319–323.

16. **Nkolola JP**, **Peng H**, **Settembre EC**, **Freeman M**, **Grandpre LE**, **Devoy C**, **Lynch DM**, **La Porte A**, **Simmons NL**, **Bradley R**, **Montefiori DC**, **Seaman MS**, **Chen B**, **Barouch DH**. 2010. Breadth of neutralizing antibodies elicited by stable, homogeneous clade A and clade C HIV-1 gp140 envelope trimers in guinea pigs. J Virol **84**:3270–3279.

17. **Sarzotti-Kelsoe M**, **Bailer RT**, **Turk E**, **Lin C-L**, **Bilska M**, **Greene KM**, **Gao H**, **Todd CA**, **Ozaki DA**, **Seaman MS**, **Mascola JR**, **Montefiori DC**. 2014. Optimization and validation of the TZM-bl assay for standardized assessments of neutralizing antibodies against HIV-1. J Immunol Methods **409**:131–146.

18. **Mascola JR**, **D'Souza P**, **Gilbert P**, **Hahn BH**, **Haigwood NL**, **Morris L**,

Petropoulos CJ, **Polonis VR**, **Sarzotti M**, **Montefiori DC**. 2005. Recommendations for the Design and Use of Standard Virus Panels To Assess Neutralizing Antibody Responses Elicited by Candidate Human Immunodeficiency Virus Type 1 Vaccines. J Virol **79**:10103–10107.

19. **Li M**, **Gao F**, **Mascola JR**, **Stamatatos L**, **Polonis VR**, **Koutsoukos M**, **Voss G**, **Goepfert P**, **Gilbert P**, **Greene KM**, **Bilska M**, **Kothe DL**, **Salazar-Gonzalez JF**, **Wei X**, **Decker JM**, **Hahn BH**, **Montefiori DC**. 2005. Human immunodeficiency virus type 1 env clones from acute and early subtype B infections for standardized assessments of vaccine-elicited neutralizing antibodies. J Virol **79**:10108–10125.

20. **Stephenson KE**, **Neubauer GH**, **Reimer U**, **Pawlowski N**, **Knaute T**, **Zerweck J**, **Korber BT**, **Barouch DH**. 2014. Quantification of the epitope diversity of HIV-1-specific binding antibodies by peptide microarrays for global HIV-1 vaccine development. J Immunol Methods.

21. **Li H**, **Stephenson KE**, **Kang Z-H**, **Lavine CL**, **Seaman MS**, **Barouch DH**. 2014. Common features of mucosal and peripheral antibody responses elicited by candidate HIV-1 vaccines in rhesus monkeys. J Virol **88**:13510–13515.

22. **Li H**, **Rhee EG**, **Masek-Hammerman K**, **Teigler JE**, **Abbink P**, **Barouch DH**. 2012. Adenovirus Serotype 26 Utilizes CD46 as a Primary Cellular Receptor and Only Transiently Activates T Lymphocytes following Vaccination of Rhesus Monkeys. J Virol **86**:10862–10865.

23. **Johansen FE**, **Braathen R**, **Brandtzaeg P**. 2000. Role of J chain in secretory immunoglobulin formation. Scand J Immunol **52**:240–248.

24. **Musich T**, **Demberg T**, **Morgan IL**, **Estes JD**, **Franchini G**, **Robert-Guroff M**. 2015. Purification and functional characterization of mucosal IgA from vaccinated and SIV-infected rhesus macaques. Clinical Immunology **158**:127–139.

25. **Wyatt R**, **Moore J**, **Accola M**, **Desjardin E**, **Robinson J**, **Sodroski J**. 1995. Involvement of the V1/V2 variable loop structure in the exposure of human immunodeficiency virus type 1 gp120 epitopes induced by receptor binding. J Virol **69**:5723–5733.

26. **Ferrari G**, **Pollara J**, **Kozink D**, **Harms T**, **Drinker M**, **Freel S**, **Moody MA**, **Alam SM**, **Tomaras GD**, **Ochsenbauer C**, **Kappes JC**, **Shaw GM**, **Hoxie JA**, **Robinson JE**, **Haynes BF**. 2011. An HIV-1 gp120 envelope human monoclonal antibody that recognizes a C1 conformational epitope mediates potent antibody-dependent cellular cytotoxicity (ADCC) activity and defines a common ADCC epitope in human HIV-1 serum. J Virol **85**:7029–7036.

27. **Taylor G**, **Bruce C**, **Barbet AF**, **Wyld SG**, **Thomas LH**. 2005. DNA vaccination against respiratory syncytial virus in young calves. Vaccine **23**:1242–1250.

28. **Zhang F**, **LI Y-H**, **FAN M-W**, **JIA R**, **XU Q-A**, **GUO J-H**, **YU F**, **TIAN Q-W**. 2007. Enhanced efficacy of CTLA-4 fusion anti-caries DNA vaccines in gnotobiotic hamsters. Acta Pharmacol Sin **28**:1236–1242.

29. **Joo HM**, **He Y**, **Sundararajan A**, **Huan L**, **Sangster MY**. 2010. Quantitative analysis of influenza virus-specific B cell memory generated by different routes of inactivated virus vaccination. Vaccine **28**:2186–2194.

30. **Yang K**, **Wang S**, **Chang KO**, **Lu S**, **Saif LJ**, **Greenberg HB**, **Brinker JP**, **Herrmann JE**. 2001. Immune responses and protection obtained with rotavirus VP6 DNA vaccines given by intramuscular injection. Vaccine **19**:3285–3291.

31. **Nardelli-Haefliger D**, **Wirthner D**, **Schiller JT**, **Lowy DR**, **Hildesheim A**, **Ponci F**, **De Grandi P**. 2003. Specific Antibody Levels at the Cervix During the Menstrual Cycle of Women Vaccinated With Human Papillomavirus 16 Virus-Like Particles. JNCI Journal of the National Cancer Institute **95**:1128–1137.

32. **Baden LR**, **Liu J**, **Li H**, **Johnson JA**, **Walsh SR**, **Kleinjan JA**, **Engelson BA**, **Peter L**, **Abbink P**, **Milner DA**, **Golden KL**, **Viani KL**, **Stachler MD**, **Chen BJ**, **Pau MG**, **Weijtens M**, **Carey BR**, **Miller CA**, **Swann EM**, **Wolff M**, **Loblein H**, **Seaman MS**, **Dolin R**, **Barouch DH**. 2015. Induction of HIV-1-specific mucosal immune responses following intramuscular recombinant adenovirus serotype 26 HIV-1 vaccination of humans. Journal of Infectious Diseases **211**:518–528.

33. **Scherpenisse M**, **Mollers M**, **Schepp RM**, **Meijer CJLM**, **de Melker HE**, **Berbers GAM**, **van der Klis FRM**. 2014. Detection of systemic and mucosal HPV-specific IgG and IgA antibodies in adolescent girls one and two years after HPV vaccination. Hum Vaccin Immunother **9**:314–321.

34. **Fouda GG**, **Eudailey J**, **Kunz EL**, **Amos JD**, **Liebl BE**, **Himes J**, **Boakye-Agyeman F**, **Beck K**, **Michaels AJ**, **Cohen-Wolkowiez M**, **Haynes BF**, **Reimann KA**, **Permar SR**. 2017. Systemic administration of an HIV-1 broadly neutralizing dimeric IgA yields mucosal secretory IgA and virus neutralization. Mucosal Immunol **10**:228–237.

35. **Zhou M**, **Ruprecht RM**. 2014. Are anti-HIV IgAs good guys or bad guys? Retrovirology, 3rd ed. **11**:64–11.

36. **Chung AW**, **Kumar MP**, **Arnold KB**, **Yu WH**, **Schoen MK**, **Dunphy LJ**, **Suscovich TJ**, **Frahm N**, **Linde C**, **Mahan AE**, **Hoffner M**, **Streeck H**, **Ackerman ME**, **McElrath MJ**, **Schuitemaker H**, **Pau MG**, **Baden LR**, **Kim JH**, **Michael NL**, **Barouch DH**, **Lauffenburger DA**, **Alter G**. 2015. Dissecting Polyclonal Vaccine-Induced Humoral Immunity against HIV Using Systems Serology. Cell **163**:988–998.

37. **Nahtman T**, **Jernberg A**, **Mahdavifar S**, **Zerweck J**, **Schutkowski M**, **Maeurer M**, **Reilly M**. 2007. Validation of peptide epitope microarray experiments and extraction of quality data. J Immunol Methods **328**:1–13.

38. **Bonsignori M**, **Pollara J**, **Moody MA**, **Alpert MD**, **Chen X**, **Hwang K-K**, **Gilbert PB**, **Huang Y**, **Gurley TC**, **Kozink DM**, **Marshall DJ**, **Whitesides JF**, **Tsao C-Y**, **Kaewkungwal J**, **Nitayaphan S**, **Pitisuttithum P**, **Rerks-Ngarm S**, **Kim JH**, **Michael NL**, **Tomaras GD**, **Montefiori DC**, **Lewis GK**, **DeVico A**, **Evans DT**, **Ferrari G**, **Liao HX**, **Haynes BF**. 2012. Antibody-dependent cellular cytotoxicity-mediating antibodies from an HIV-1 vaccine efficacy trial target multiple epitopes and

preferentially use the VH1 gene family. J Virol **86**:11521–11532.

39. **Deenick EK**, **Hasbold J**, **Hodgkin PD**. 1999. Switching to IgG3, IgG2b, and IgA is division linked and independent, revealing a stochastic framework for describing differentiation. J Immunol **163**:4707–4714.

40. **Iwasato T**, **Arakawa H**, **Shimizu A**, **Honjo T**, **Yamagishi H**. 1992. Biased distribution of recombination sites within S regions upon immunoglobulin class switch recombination induced by transforming growth factor beta and lipopolysaccharide. Journal of Experimental Medicine **175**:1539–1546.

41. **Brinkmann V**, **Heusser CH**. 1993. T cell-dependent differentiation of human B cells into IgM, IgG, IgA, or IgE plasma cells: high rate of antibody production by IgE plasma cells, but limited clonal expansion of IgE precursors. Mol Immunol **152**:323–332.

42. **Cerutti A**. 2008. The regulation of IgA class switching. Nat Rev Immunol **8**:421–434.

CHAPTER 4:

Evaluating novel delivery methods of vaccination that may improve induction of antigen-specific antibodies.

This chapter represents an on-going study with final experiments in progress for finalization of a manuscript at the time of thesis submission.

ACKNOWLEDGEMENTS

Protein production and immunogenicity studies by Z. H. Kang. Formulation of microspheres and *in vitro* characterization studies by S. Tzeng, R. Guarecuco, R. Langer, A. Jaklenec. Experimental discussions and recommendations provided by S. Tzeng, C. Bricault, A. Jaklenec, R. Langer, and D. Barouch. Technical support and assistance provided by J. Iampietro and E. Blass.

ABSTRACT

Poly (D, L-lactic-co-glycolic acid) (PLGA) microspheres are widely studied as a delivery method for antigen. In this study, we formulated 8 different microsphere formulations, encapsulating the HIV-1 envelope trimer protein (Env), using 2 different formulation methods, and co-encapsulating 3 different adjuvants. These PLGA microsphere formulations degraded and released the encapsulated Env antigen over a period of about 5 weeks. We evaluated the immunogenicity of these microspheres in mice. Encapsulated Env induced significantly higher antibody responses than soluble protein with comparable doses, while empty PLGA microspheres did not appear to have a similar adjuvant effect. Furthermore, it appears that immunization with these encapsulated Env formulations could increase antibody diversity. Encapsulated Env formulations also induced higher neutrophil chemoattractants, and the levels of these cytokines were correlated with subsequent antibody titers. These data suggest that these PLGA formulations are effective vaccine delivery systems that warrant further investigation.

INTRODUCTION

Biodegradable microspheres (size of between 1-1000um) have long been studied as a delivery system for vaccines. Biodegradable polymers, which can be either synthetic or natural, are coupled to the vaccine antigen. One of the more common polymers used is PLGA (poly (D, L-lactic-co-glycolic acid)), which is hydrolyzed to form lactic acid and glycolic acid, releasing the encapsulated antigen. The administration of vaccines via such systems is advantageous, as microspheres can be easily ingested or injected, and can be engineered such they target different organs or cell types, or to release the encapsulated antigen in a continuous or pulsatile fashion for periods of weeks to months. Encapsulation of the antigen could also protect it from degradation, increasing its half-life. Additionally, they have been reported to have an adjuvant effect on the immune system (1, 2). Modulation of the microparticle's properties is done by changing the particle size, shape, and elastic properties, and these in turn are determined by the formulation conditions.

Continuous antigen delivery has been suggested to induce a strong immune response (7). In particular, immunizations with encapsulated antigen have been shown to induce a stronger systemic antibody response, as compared to immunizations with soluble antigen alone (1, 8). Although it is possible that persistent expression of antigen might induce tolerance, this could be dose dependent (9).

Two methods of formulating microspheres are the single spontaneous emulsification solvent diffusion method (3) and the double emulsion formulation method(4). The spontaneous emulsification method utilizes a single-phase solvent system, where both protein and polymer are soluble. The particles form spontaneously, circumventing the need for high energy mixing. This may reduce aggregation and improve protein stability (5). We also expect there to be a

homogenous distribution of protein within the microspheres, as the protein is in the same phase as the polymer, allowing a more continuous release of protein during degradation, without a large initial burst. It is also expected to be easily scaled up. Microspheres formed by the double emulsion process results in droplets that are dispersed within other droplets. They form spheres with a greater range in size. The formulation process also allows hydrophobic and hydrophilic molecules to be encapsulated (6).

We aim to formulate microparticles that release encapsulated protein antigen continuously over a period of weeks. We hypothesize that immunizations with microspheres with a sustained antigen release profile would result in a more immunogenic profile compared to one that result from a traditional pulsatile (prime-boost) release profile. In particular, we hope that this would result in increased antigen-specific antibody responses at mucosal sites.

MATERIALS AND METHODS

Protein production

HIV-1 envelope C97ZA012.1 gp140Fd trimer (C97 Env) was produced as described in (10). Briefly, 293T cell lines stably transfected with the envelope construct were grown in DMEM containing 10% FBS to confluence, and the media was then changed to Freestyle 293 expression medium (Invitrogen). Supernatant was harvested at 96-108 h after medium change. C97gp140Fd Env was purified from the supernatant by HisTrap Ni-NTA (Qiagen) columns. Ni-NTA columns were washed with 20mM imidazole and protein was eluted with 300mM imidazole. Fractions containing Env were pooled, concentrated, and further purified using gel filtration chromatography on Superose6 (GE Healthcare). Purified proteins were concentrated using CentriPrep YM-50 concentrators (Millipore), flash frozen in liquid nitrogen, and stored at -80°C.

Microsphere fabrication

Single emulsion microspheres

Microspheres encapsulating C97 Env and Adju-Phos (Brenntag) were fabricated using a spontaneous single emulsion method. 200 uL of C97 Env (17.04 mg/mL) and 100 uL of Adju-Phos (5.05 mg/mL), MPLA or CpG (1mg/mL) were added to 200 mg of PLGA RG 502H dissolved in 10mL of co-solvent (CH_2Cl_2:TFE : 1:4), forming a clear, single phase solution, which was then added to 200 mL of non-solvent (5% PVA). The emulsion formed spontaneously and was allowed to stir at room temperature for 3 h. The microspheres were collected by centrifugation, washed 3 times with distilled water and lyophilised. Microspheres were stored at 4°C until use.

Double emulsion microspheres

C97 Env and adjuvants (Adju-Phos, CpG, MPLA; or PBS for control) were co-encapsulated in PLGA microspheres by the double emulsion method (as previously described in (11)). PLGA was dissolved in 100mg/mL dichloromethane (o1). C97 Env protein was then mixed with the adjuvant of interest in an aqueous solution (w1). The protein/adjuvant solution was then added to the PLGA solution. The mixture was then vortexed to form the first emulsion. The second emulsion was formed by adding heavy mineral oil with 3% Span 80 (o2) to the first emulsion at a 1:1 volumetric ratio of o1:o2 and vortexing at 3,500 rpm for 5 s. The emulsion was stirred at 250 rpm at room temperature in a stirring bath for 3 h to allow DCM evaporation. The hardened microspheres were then pelleted by centrifugation. The excess oil and surfactant were decanted, and the pellet was washed three times by resuspension in hexanes and centrifugation at 200 × g for 3 min at 4°C. After decanting the supernatant after the final wash, all residual hexanes and water were removed under vacuum for 1 h at room temperature. Microspheres were stored at 4°C until use.

Determination of encapsulation efficiency

5-10 mg of microspheres were incubated with 0.5 mL of 1 M NaOH at 60°C for 2 h. 0.5 mL of 1 M HCl was then added to neutralize the solution. The amount of protein released was quantitated using a micro BCA assay kit (Pierce). Samples were run in triplicate.

Determination of total amount of C97 Env released *in vitro*

Microsphere release studies were carried out in phosphate buffered saline (PBS, pH 7.2) at

37°C. 10 mg of microspheres were incubated with 1 mL PBS in capped tubes and placed on a rotator. At fixed time points, samples were centrifuged at 1500 RCF for 5 min, after which the supernatant was collected and stored at -80°C until analysis. Samples were then suspended in 1 mL of fresh PBS and returned to the incubator until the following time point.

Quantitative C97 Env ELISA

The amount of C97 Env in the supernatant was determined using a quantitative ELISA. 96-well Maxisorp ELISA plates were coated overnight with 100 uL per well of 5F3 monoclonal antibody (Polymun) at a concentration of 0.3 mg/mL in PBS. Plates were then washed and blocked in PBS containing Casein (ThermoScientific) for 2 hours at room temperature. Plates were then washed and 100 uL per well of pan-gp120 IgG monoclonal antibody added and incubated at room temperature for 1 h. Plates were washed and 100 uL per well of anti-mouse IgG-HRP added, and incubated at room temperature for 1 h. Plates were washed and then developed with 100 uL of SureBlue tetramethylbenzidine microwell peroxidase (KPL Research Products) for 3 min, and subsequently stopped by the addition of stop solution (KPL Research Products), and analyzed at 450 nm/550 nm on a Spectramax Plus ELISA plate reader (Molecular Devices) using Softmax Pro-4.7.1 software. All washes were performed 4 times with PBS containing 0.05% Tween-20 (Sigma). All samples were run in triplicate.

Animals and immunizations

Female C57B/6 mice (Jackson Labs) were housed at the Animal Research Facility of Beth Israel Deaconess Medical Centre under protocols approved by the Institutional Animal Care and Use Committee. Mice were immunized by bilateral intramuscular injections in the upper

quadriceps with soluble or microsphere-encapsulated C97 Env with or without adjuvant (Adju-Phos, MPLA, or CpG) at 10 or 12 week intervals (weeks 0 and 10, or weeks 0 and 12). Serum samples were obtained by submandibular bleeding of anesthetized animals. Colorectal (CR) secretions were obtained by placing an approximately 0.1mm by 0.9mm piece of Weck-Cel® cellulose sponge (Beaver-Visitec) in the rectal compartment of an anesthetized mouse for 5 min. CR secretions were eluted using a Corning Co-star Spin-X centrifuge tube filter (pore size: 0.45um), centrifuged at 16000g for 5 minutes at 4C, in 150uL of extraction buffer (PBS, 0.25% v/v BSA, 0.5% v/v Igepal CA-630 (Sigma), 0.1% v/v protease inhibitor cocktail (Sigma)).

Serum ELISAs

C97 Env-specific total IgG endpoint ELISAs

C97-specific IgG titers in serum and CR secretions were determined by endpoint ELISAs as previously described. (12). Briefly, 96-well Maxisorp ELISA plates (Thermo Fisher Scientific) were coated overnight with 100 uL per well of HIV-1 Env at a concentration of 1 ug/mL in PBS, and subsequently blocked for 3-4 h with PBS containing 2% BSA (Sigma) and 0.05% Tween-20 (Sigma). Serum or eluted mucosal secretions was then added in serial dilutions and incubated for 1 h at room temperature. The plates were washed 3 times with PBS containing 0.05% Tween-20 and were incubated for 1 h with a 1/1000 dilution of a HRP-conjugated IgG (Jackson ImmunoResearch Laboratories) for mouse serum, mouse eluted mucosal secretion ELISAs. The plates were washed 3 times and developed with SureBlue tetramethylbenzidine microwell peroxidase (KPL Research Products), stopped by the addition of stop solution (KPL research Products), and analyzed at 450nm/550nm on a Spectramax Plus ELISA plate reader (Molecular Devices) using Softmax Pro-4.7.1 software.

Peptide microarrays

Peptide microarray slides were used as described in (13). Briefly, mouse serum was diluted 1/200 in SuperBlock T20 (TBS) Blocking Buffer (Thermo Scientific), and incubated for 1h at 30°C with the peptide microarray slide. Slides were then washed with 5mL of TBS-Buffer + 0.1% Tween-20 for 3 min on a shaker at room temperature for 5 washes. Next, slides were placed in the individual chambers of a Sarstedt Quadriperm Dish and incubated with Alexa-Fluor 647-conjugated AffiniPure Anti-Mouse IgG (H+L) (Jackson ImmunoResearch Laboratories). Slides were then washed 5 times with TBS-Buffer + 0.1% Tween-20 and 5 times with deionized water. To dry, slides were placed in a 50mL Falcon tube, and spun at 1400rpm for 5 minutes. A control slide incubated with secondary antibodies alone without sample was also ran to determine background.

Microarray image analysis

Slides were scanned with a GenePix 4300A scanner (Molecular Devices), using 635nm and 532nm lasers at 500 PMT and 100 Power settings. Images were saved as TIF files. The fluorescent intensity for each feature (peptide spot) was calculated using GenePix Pro 7 software and GenePix Array List (GAL) file. We then calculated the mean fluorescent intensity across the triplicate sub-arrays using a custom-designed R script and R software package 2.15.2. The threshold value used to define a minimum positive fluorescent intensity was calculated for each slide using the computational tool rapmad and a custom-designed R script. Data from each individual slide was combined with data from the control slide to create two distributions of data (noise and signal). The threshold values for positivity were defined as 5 standard deviations

above the mean of the noise distribution (SD.noise*5). The mean signal fluorescent intensity (MFI) values of reactive peptides for each mouse were normalized to a scale of a 100.

An antibody epitope was defined to be 5-15 amino acid long (with the minimum epitope for antibody binding to be 5 amino acids long), the breadth to be the number of amino acid regions within any given HIV-1 protein (e.g. Env, Gag, Pol) region (e.g. V1, V2 etc. for HIV-1 Env) spanning an 11 amino acid stretch. We defined the depth to be the number of unique sequences within an overlapping region of 5 to 15 amino acids (13).

Comparison of reactive IgG epitopes between encapsulated and bolus groups: To compare the common vs. unique linear epitopes targeted by the different groups, we took the average of reactive Env peptides sequences targeted within each group. Reactive peptides were very similar between animals within the same group. Reactive peptide sequences between the encapsulated and bolus groups were aligned against each other to eliminate overlap. If any reactive peptide sequences shared 5 or more amino acids, we conservatively assumed that the peptides reflected the same epitopes. If the first and last overlapping peptide in a string of overlapping peptides shared 4 or fewer amino acids, we assumed that the peptides were recognized by a minimum of two antibody-binding sites. The list of unique linear epitope sequences for the encapsulated group was then compared to the list of unique sequences for the bolus group to determine which sequences were common (versus unique) to both groups.

Luminex assays

Serum samples were prepared using the Milliplex Mouse 32-plex premix (Millipore), according to the manufacturer;s protocol. Data was acquired on a Magpix instrument running xPONENT 4.2 (Luminex), with an 80% to 120% standard acceptance range.

RESULTS

Encapsulation of Env has an adjuvant effect, while immunization with empty microspheres does not

We first tested the immunogenicity of single emulsion (SE) microspheres in mice. Single emulsion microspheres containing either a clade C envelope protein ((C97ZA012.1 gp140Fd; from here on denoted as C97 Env) (microsphere is denoted as SE (C97)) or Adju-Phos (SE (Adju-Phos)) alone, or co-encapsulating both C97 Env and Adju-Phos (SE (C97+Adju-Phos)), were fabricated. Empty SE microspheres were also fabricated (SE (empty)). Mice were then immunized with 11 different combinations of soluble and/or encapsulated C97 Env and/or Adju-Phos (as described in Figure 4.1A). The amount of soluble C97 Env used for immunizations was matched to the amounts of C97 Env that was rencapsulated by 5mg of SE (C97 + Adju-Phos) microspheres (Table 4.1), while the amount of soluble Adju-Phos used was calculated by assuming a similar encapsulation efficiency for Adju-Phos as C97 Env. As a positive control, mice were immunized with 50ug soluble C97 Env and 100ug soluble Adju-Phos, which is a typical protein and adjuvant dose that is used in mice (Figure 4.1A).

Peak C97 Env-specific IgG responses were then evaluated at 6 weeks post-immunization. Mice that were immunized with encapsulated C97 Env, whether they were encapsulated alone, or co-encapsulated with Adju-Phos (Groups 1-4, range of log IgG titers: 2.11-2.47), elicited IgG titers that were comparable to mice that were immunized with the positive control (Group 12, log IgG titer: 2.23). Mice that were immunized with soluble C97 Env elicited no or low IgG responses (Groups 5-9, range of log IgG titers: 1.40-1.63). Additionally, the presence of empty microspheres did not have an adjuvant effect on soluble C97 Env (Groups 6, 7, 9).

A

Group	SE Microsphere administered (per mouse)	Soluble protein or adjuvant administered (per mouse)
1	5mg SE (4ug C97 + 0.6ug AP)	-
2	5mg SE (4ug C97)	0.6ug AP
3	5mg SE (4ug C97)	-
4	2.5mg SE (2ug C97) + 2.5mg SE (0.3ug AP)	-
5	-	4ug C97 + 0.6ug AP
6	5mg SE (empty)	4ug C97 + 0.6ug AP
7	5mg SE (0.6ug AP)	4ug C97
8	-	4ug C97
9	5mg SE (empty)	4ug C97
10	-	PBS (sham)
11	5mg SE (empty)	-
12		50ug C97 + 100ug AP

B

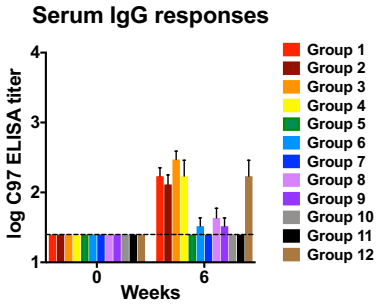

Figure 4.1 – Antibody responses elicited following IM immunizations with different combinations of encapsulated or soluble C97 Env and Adju-Phos

(A) C57B/6 mice were IM immunized at weeks 0 with 12 different groups of soluble or SE encapsulated C97 Env (C97) or Adju-Phos (AP). The values shown in parenthesis in each SE microsphere group represent the estimated amount of antigen and adjuvant that was released by the amount of microsphere injected into each mouse (n=4 per group)

(B) Peak serum C97 Env-specific IgG responses elicited 6 weeks post immunization was analyzed by endpoint ELISA. Horizontal broken lines represent assay threshold.

Encapsulated HIV-1 Env, in mice immunized with SE (Adju-Phos) elicited larger and more diverse antibody responses than soluble HIV-1 Env

We next investigated the diversity of the linear epitopes targeted by vaccine-elicited IgG antibodies. Mice were IM immunized at weeks 0 and 10 with either (i) 5mg SE (C97 + Adju-Phos) or with (ii) soluble 50ug C97 Env + 100ug Adju-Phos (Figure 4.2A). Comparable serum C97 Env-specific IgG responses were elicited in both groups (5mg SE (C97 Env + Adju-Phos): 4.10 logs; 50ug C97 + 100ug Adju-Phos: 4.74 logs) at 36 weeks post prime (Figure 4.2B), even though the amount of C97 Env that was released *in vitro* is significantly less (2ug of C97 Env) (Table 4.1).

To determine the diversity of Env linear epitopes targeted by IgG, week 36 serum was assessed peptide microarrays slides containing 6564 HIV-1 15 amino acid long peptides (JPT Peptide Technologies) as previously described (13, 14). The binding pattern of antibodies generated following immunization to linear HIV-1 Env peptides was then analyzed.

The pattern of IgG binding to linear Env peptides was mostly similar between the 2 groups, with most responses generated against the V1/V2, V3, C3, V4, FP, and CC/HR2 regions of Env. In general there was more epitope binding across all regions for the encapsulated group (Figure 4.2C). IgG from mice immunized with encapsulated C97 Env resulted in a more diverse antibody response that targets significantly greater breadth (mean: encapsulated Env: 49.0, soluble Env: 34.3; p=0.0007) and depth (mean: encapsulated Env: 419.3, soluble Env: 253.0; p=0.0043) of linear Env peptides. For individual Env regions, we similarly observed that encapsulated Env generated greater breadth and depth, especially in the C1, C2, and HR1 regions (breadth), and the C1-C5, V1, V3, V4, HR1, and MPER regions (depth). Immunization with encapsulated or

soluble C97 Env generated the greatest depth of antibody responses in the V2 region of Env, followed by the V3 region (Figure 4.2D).

We next explored the extent to which IgG from both groups targeted similar linear Env epitopes. Most of the epitope diversity generated by soluble C97 Env immunizations is a subset of, and similar to, that generated by encapsulated C97 Env immunizations. There were very few epitopes that were uniquely targeted by IgG from the soluble C97 Env group. Immunization with encapsulated C97 Env generated an antibody response that targeted more unique epitope variants, especially in the V1, V2 and V3 regions, that were not targeted by the antibody response from soluble C97 Env immunizations (Figure 4.2E).

Figure 4.2 – Evaluation of breadth and depth of antibody responses elicited following IM immunization with encapsulated or soluble C97 Env + Adju-Phos by peptide microarray

(A) Immunization regimen – C57B/6 mice were IM immunized at weeks 0 and 10, with 5mg SE (C97 Env + Adju-Phos), or with soluble 50ug C97 Env + 100ug Adju-Phos (a typical protein and adjuvant dose used in mice). N = 3 for each group

(B) Serum C97 Env-specific IgG responses elicited at week 36 were analyzed by endpoint ELISA.

(C) The normalized mean fluorescence intensity (MFI) of the IgG from the encapsulated C97 Env (red) and from the soluble C97 Env (black) groups against Env linear peptides is plotted against the Env peptide start position (HXB2 numbering). MFI values for each animal were normalized to a scale of 100 AU, based on the highest MFI value for each mouse. The MFI values of all 3 mice from each group are depicted.

(D) The breadth (number of binding sites per region) and depth (number of epitope variants per region) for each mouse is plotted for serum IgG responses against Env linear peptides (n=3). The breadth and depth of the antibody responses against peptides from individual regions within Env (left), or from the entire Env protein (right) are both depicted.

Means and SEMs are shown for **(C)** and **(D)**. Statistical significance was analyzed using the t-test (*: $p \leq 0.05$, **: $p \leq 0.01$, ***: $p \leq 0.001$).

(E) Linear Env epitopes targeted by serum IgG in encapsulated or soluble Env immunized mice were compared for sequence similarity. Blue bars depict common sequences targeted by both groups, while the red or black bars depict sequences that are uniquely targeted in the encapsulated or soluble Env groups respectively. The average depth response for each group was plotted.

(figure on next page)

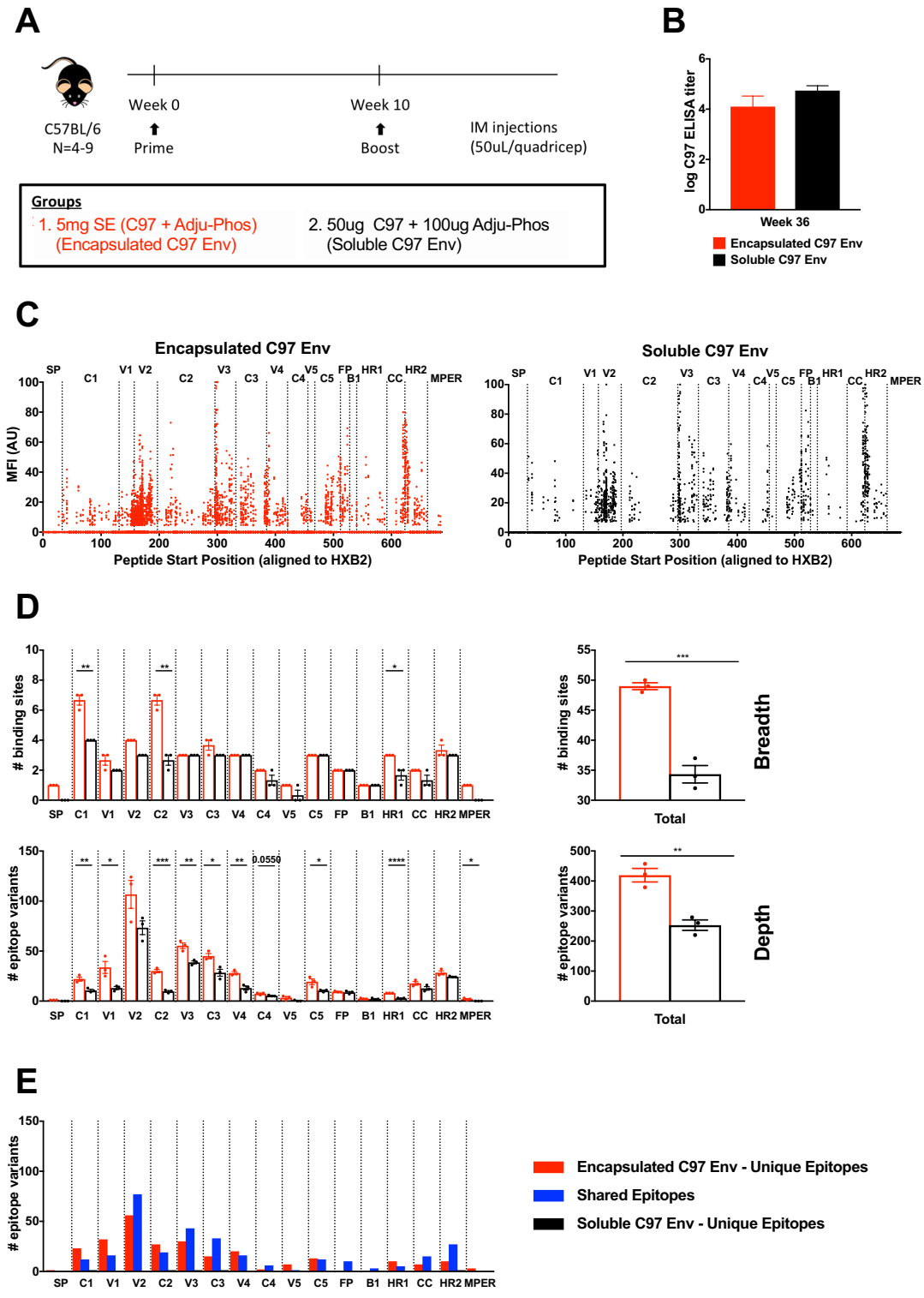

Figure 4.2 – Evaluation of breadth and depth of antibody responses elicited following IM immunization with encapsulated or soluble C97 Env + Adju-Phos by peptide microarray (continued)

Formulation and *in vitro* characterization of microspheres

We then decided to expand our evaluation on the immunogenicity of encapsulated Env in biodegradable PLGA microspheres, by using different formulation methods and having different adjuvants co-encapsulated. 8 different formulations of PLGA microspheres C97 Env were fabricated using either a spontaneous single emulsion (SE) process, or a double emulsion (DE) process (Table 4.1). The formulations contained either C97 Env alone, or had a co-encapsulated adjuvant (Adju-Phos, MPLA, or CpG).

The double emulsion formulation process increases encapsulation efficiency:

The encapsulation efficiency was determined using a micro bicinchoninic acid (BCA) assay, after dissolving the PLGA microspheres in 1M NaOH. The double emulsion formulation process encapsulated more C97 Env antigen, as compared with the single emulsion process. There was also a greater range of encapsulation efficiencies between different formulations in the microspheres that were fabricated using the single emulsion process. Double emulsion formulations have encapsulation efficiencies between 86.38% to 101.35%, while the encapsulation efficiencies of single emulsion formulations were lower, at a range of 4.94% to 81.08% (Table 4.1).

The type of adjuvant that was co-encapsulated with C97 Env affected the encapsulation efficiencies as well, especially in microspheres formulated using the single emulsion process (encapsulation efficiency for SE(C97+Adju-Phos): 4.94%; SE(C97+CpG): 35.19%; SE(C97+MPLA): 81.08%) (Table 4.1).

Greater amounts of HIV-1 C97 Env is released during degradation of double emulsion microspheres

In vitro release kinetics from these formulations were determined with a quantitative Env ELISA using antibodies against a linear gp41 epitope (5F3) and a conformational gp120 epitope (pan-gp120 IgG).

All microsphere formulations degraded within 7 weeks, with an initial burst of protein released in the first 2 days. Small amounts of C97 Env were continuously released over the next 3 weeks, after which the rate of protein release increased (Figure 4.3A). The total amount of C97 Env released is higher in double emulsion microspheres. Double emulsion microspheres co-encapsulating CpG had the highest amount of C97 Env released – 11.14ug of C97/mg of microsphere (Table 4.1). The cumulative percentage of C97 Env released was also less than the encapsulation efficiency, suggesting that some protein may have been degraded or denatured during the encapsulation process.

Double emulsion microspheres are smaller in size than single emulsion microspheres

Microspheres were imaged using a scanning electron microscope (SEM). Double emulsion microspheres were smaller in size, and ranged from 1-5 microns to about 20-30 microns. Single emulsion microspheres were larger, ranging from about 15-20 microns to about 40-50 microns. The larger size of the microspheres suggests that they are unlikely to be travelling far from the injection site. Additionally, the double emulsion microspheres appear to be very porous, although porosity did not appear to affect the encapsulation efficiency (Figure 4.3B).

Table 4.1 – Microsphere formulations

Eight different microsphere formulations were fabricated using either the single or double emulsion method. 17.04ug of C97ZA012 gp140Fd Env (C97 Env) and 2.525ug of adjuvant (Adju-Phos, MPLA, or CpG) was loaded per mg of microsphere. The amount of antigen encapsulated was determined using a micro bicinchoninic acid (BCA) assay, after dissolving the PLGA microspheres in 1M NaOH. The amount of antigen released was determined using a quantitative ELISA, and was the cumulative sum of antigen released into the supernatant as the PLGA microsphere formulation degraded in a PBS solution. Values in parenthesis represent standard deviation. (n=3)

MPLA - Monophosphoryl Lipid A

Formulation		Formulation method	Adjuvant	Antigen input	Antigen encapsulated		Antigen released	
					Amount encapsulated (ug /mg microsphere)	Percentage encapsulated (%)	Amount released (ug/mg microsphere)	Percentage released (%)
1	SE (C97)	Single emulsion	-	17.04 ug of C97 Env (per mg microsphere)	1.11 (±0.09)	6.54 (±0.53)	0.68 (±0.08)	4.00 (±0.45)
2	SE (C97 + Adju-Phos)		Adju-Phos		0.84 (±0.16)	4.94 (±0.10)	0.51 (±0.06)	2.98 (±0.33)
3	SE (C97 + MPLA)		MPLA		13.82 (±1.96)	81.08 (±11.50)	3.09 (±0.47)	18.15 (±2.76)
4	SE (C97 + CpG)		CpG		6.00 (±1.51)	35.19 (±8.83)	2.90 (±0.10)	17.02 (±2.08)
5	DE (C97)	Double emulsion	-		16.17 (±1.24)	94.87 (±7.30)	10.71 (±0.57)	62.84 (±3.37)
6	DE (C97 + Adju-Phos)		Adju-Phos		17.27 (±0.65)	101.35 (±3.83)	10.54 (±1.50)	61.84 (±8.78)
7	DE (C97 + MPLA)		MPLA		16.09 (±1.92)	94.41 (±11.28)	9.48 (±1.28)	55.65 (±7.54)
8	DE (C97 + CpG)		CpG		14.72 (±0.49)	86.38 (±2.90)	11.14 (±1.33)	65.40 (±7.81)

Figure 4.3 - *In vitro* characterization of single emulsion and double emulsion microspheres

Microspheres encapsulating C97 Env were formulated without adjuvant, with Adju-Phos, MPLA or CpG, using the single emulsion (SE) or double emulsion (DE) formulation method.

(A) The *in vitro* release kinetics was determined by allowing microspheres to degrade in PBS at 37C on a rotator. The amount of intact Env released was determined using a quantitative Env ELISA.

(B) SEM images of microspheres were taken at 150 and 700 times magnification.

(figure on next page)

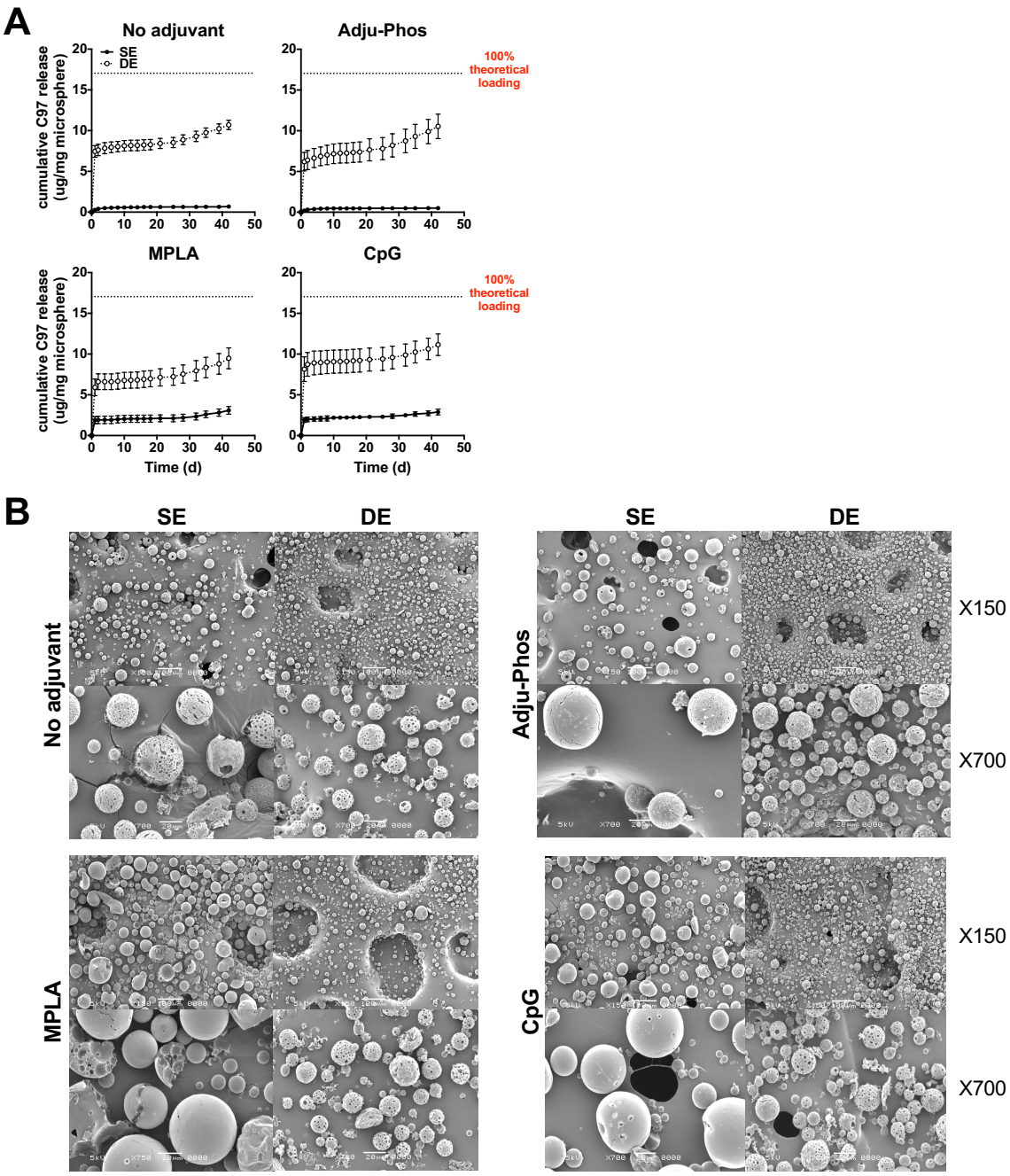

Figure 4.3 - *In vitro* characterization of single emulsion and double emulsion microspheres (continued)

Double emulsion microspheres co-encapsulating HIV-1 C97 Env and CpG are the most immunogenic

Female C57B/6 mice were IM immunized with decreasing doses (0.5mg, 0.05mg) of the 8 microsphere formulations, as well as corresponding soluble amounts of C97 Env and adjuvant (matched to the amounts of C97 Env and adjuvant loaded). Groups were also immunized with empty SE or DE microspheres, or PBS, as negative controls (Figure 4.4A).

The humoral immune response to each microsphere formulation was then assessed by ELISA. At 4-6 weeks post prime, C97 Env-specific IgG responses were elicited by all 8 formulations of microspheres, at both 0.5mg and 0.05mg doses. In comparison, only the highest dose of soluble C97 Env (8.5ug) elicited any detectable IgG titer (1.77-2.14 logs) (Figure 4.4B).

Antibody titers elicited by immunization with DE or SE microspheres co-encapsulating Adju-Phos, MPLA, or no adjuvant, were comparable to each other. DE (C97 + CpG). 0.5mg DE (C97 + CpG) elicited 1.5-2 logs higher IgG titers, compared to 0.5mg SE (C97 + CpG). Antibody titers generated by double emulsion microspheres co-encapsulating CpG also peaked later, at week 6, instead of week 4 for single emulsion microspheres or soluble C97 Env immunizations (data not shown).

After 4-6 weeks post boost, C97 Env-specific IgG responses increased by 1-2 logs for all groups, except for the lowest dose of soluble C97 Env + adjuvant. Animals immunized with empty SE or DE microspheres, or PBS, did not elicit any C97 Env-specific IgG response. It appears that antibody titers elicited by SE microspheres co-encapsulating Adju-Phos, MPLA or PBS elicited higher Env-specific IgG titers than the DE microspheres co-encapsulating the same adjuvant. DE microspheres co-encapsulating CpG continued to elicit higher Env-specific IgG titers than single emulsion microspheres. Overall, both SE and DE microspheres elicited

significantly higher antibody responses than their comparator soluble C97 Env + adjuvant bolus group.

Overall, DE (C97 Env + CpG) microspheres are the most immunogenic, generating peak endpoint antibody titers of around 5.5 logs post prime, and 7 logs post boost. This could be due to the higher encapsulation efficiency and cumulative release that was observed *in vitro* for this formulation (Table 4.1).

Mucosal binding antibody responses from immunized mice 12 weeks post prime were also assessed. No C97 Env-specific IgG responses were observed in the vaginal secretion (data not shown). In general, colorectal IgG responses at 12 weeks post prime were 1-2 logs lower than serum IgG responses 6 weeks post prime. Soluble C97 Env + adjuvant did not elicit any detectable IgG responses. DE (C97 Env + CpG) also elicited the highest Env-specific colorectal IgG responses post prime, reflecting the high IgG responses observed in serum responses (Figure 4.4C). Serum and mucosal IgG responses were correlated ($r=0.7011$, $p<0.0001$, Spearman rank correlation test) (Figure 4.4D).

Antigen-specific IgA and IgG subclasses (IgG1 and IgG2a) antibody responses were also evaluated (Figure 4.4E). Serum from weeks 4-6 and 16-18 (4-6 weeks post prime and boost) were used to evaluate binding IgG1, IgG2a and IgA responses against C97 Env. IgG1 is the predominant antigen-specific IgG subclass generated by immunization with either soluble or encapsulated C97 Env, regardless of the adjuvant that is co-encapsulated with it. No C97 Env-specific IgA and IgG2a responses were observed in serum (Figure 4.4E), and C97 Env-specific IgA responses were not observed in the colorectal secretions as well (data not shown). The differences in C97-specific IgG1 concentrations between the different groups were similar to those observed for C97-specific total IgG titers at both time points post prime and boost, with the

DE (C97 Env + CpG) formulations eliciting the highest concentrations of IgG1 (Figure 4.4B and E). The high IgG1 to IgG2a ratio suggests a Th2 biased response.

Figure 4.4 – Antibody responses elicited in mice following IM immunization with SE and DE microspheres encapsulating C97 Env and different adjuvants

(A) C57B/6 mice were intramuscularly (IM) immunized at weeks 0 and 12, with decreasing doses of single (SE) or double (DE) emulsion microspheres (formulations 1-8 from table 1), or with decreasing amounts of soluble protein and antigen. The values shown in parenthesis in each SE or DE group represent the amount of antigen and adjuvant that was loaded in the amount of microsphere injected into each mouse. Empty SE or DE microspheres, as well as PBS were used as negative controls. Comparator groups with similar amounts of loaded protein and adjuvant are shown in similar colors.

(B) Peak serum C97 Env-specific IgG responses elicited 4-6 weeks post-prime and post-boost were analyzed by endpoint ELISA. Horizontal broken lines represent assay threshold.

(C) Colorectal (CR) C97 Env-specific IgG responses elicited 12 weeks post-prime were analyzed by endpoint ELISA. Horizontal broken lines represent assay threshold.

(D) Correlations between C97 Env-specific IgG titers in serum and colorectal samples were evaluated for week 12. Correlations were analyzed using Spearman rank-correlation tests.

(E) Peak serum C97 Env-specific IgG1, IgG2a and IgA binding antibody responses were evaluated by endpoint ELISA 4-6 weeks post-prime and post-boost.

Means and standard errors of the mean (SEM) antibody concentrations are shown. Statistical significance was analyzed using the Mann Whitney test.

(figure on next page)

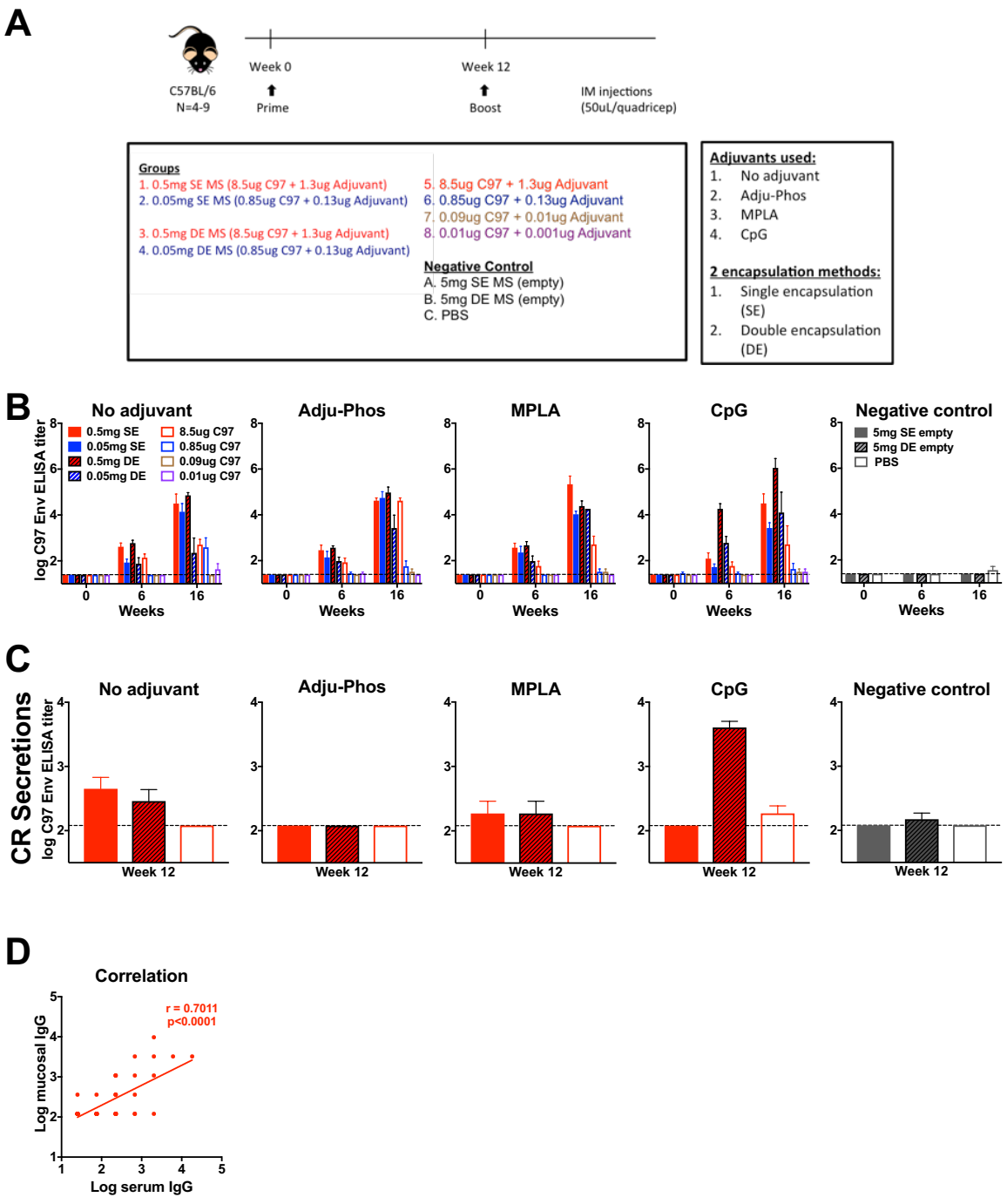

Figure 4.4 – Antibody responses elicited in mice following IM immunization with SE and DE microspheres encapsulating C97 Env and different adjuvants

(continued on next page)

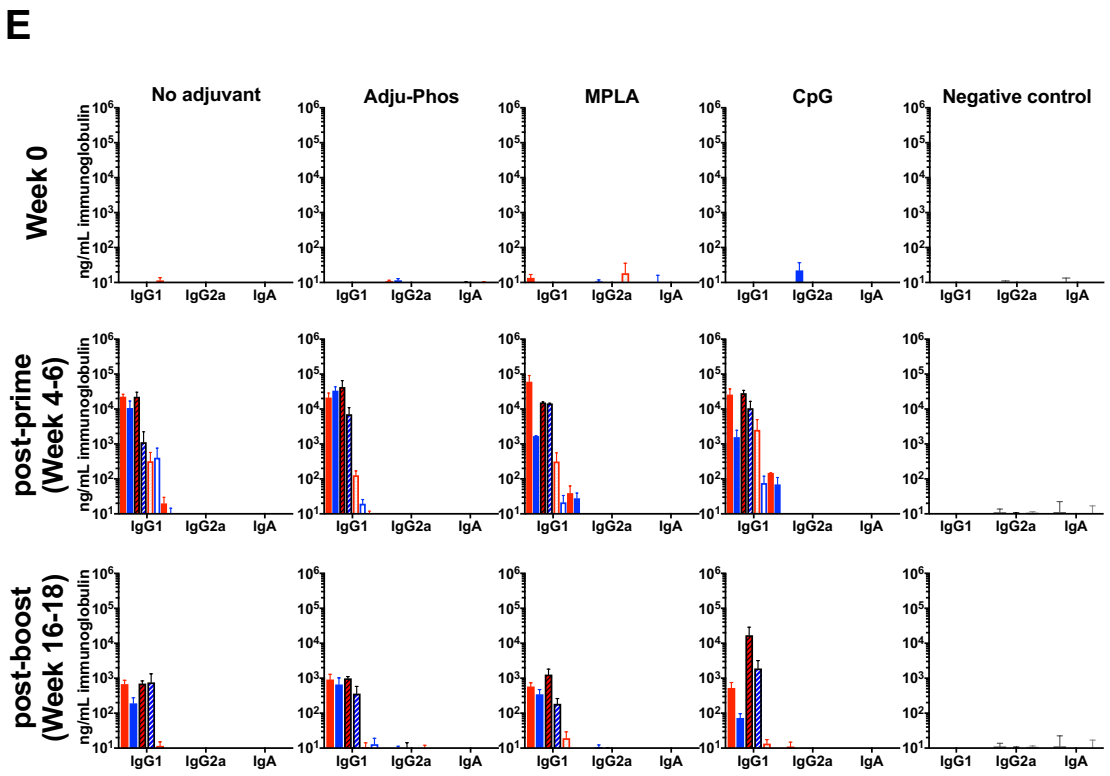

Figure 4.4 – Antibody responses elicited in mice following IM immunization with SE and DE microspheres encapsulating C97 Env and different adjuvants (continued)

Innate immune responses 8 hours post vaccination

We next assessed the systemic innate cytokine response 8 hours following immunizations with 0.5mg of SE or DE microspheres (Formulations 1-8, Table 4.1), or with comparable bolus (soluble) formulations (8.5ug C97 Env + 1.3ug of adjuvant), using a Luminex assay.

Of the 32 cytokines tested, 4 cytokines were not induced above the limits of detection of the assay (GM-CSF, IFN-γ, IL-3, IL-4). Five cytokines were induced by all groups (G-CSF, IL-6, KC, MIP-1α, and MIP-1β), above the levels induced by PBS (Figure 4.5A). Of these 5 groups, G-CSF, IL-6, KC and MIP-1α were significantly induced by SE or DE formulations, compared to their bolus groups using the same adjuvant, and DE formulations appear to induce higher responses than their respective SE formulations co-encapsulating the same adjuvant (Figure 4.5A and Supplemental Figure 4.S1). Eotaxin, IL-10, and TNF-α appear to generally be suppressed by all groups, as compared to the PBS group.

To assess whether any of the innate cytokines and chemokines induced 8 hours post vaccination had an impact on subsequent C97 Env-specific IgG titers at a peak time point (week 6), we evaluated the correlations between cytokine/chemokine concentrations and IgG endpoint titers. Induction of the chemokine KC ($r=0.5539$, $p\leq0.0001$) was shown to be strongly positively correlated with subsequent IgG titers, and G-CSF ($r=0.4402$, $p\leq0.0001$), IL-6 ($r=0.4157$, $p\leq0.0001$), and MIP-1β ($r=0.3565$, $p=0.0018$) were moderately positively correlated with subsequent IgG titers (Figure 4.5B). When these data were further analyzed based on the adjuvant that was contained within each group, correlations were strongest in groups containing MPLA (data not shown).

Figure 4.5 – Innate immune responses 8 hours post vaccination (continued)

Induction of cytokines and chemokines in mice following vaccination with SE and DE microspheres. Mice (n=4-5 per group) were I.M. immunized with 0.5mg of SE or DE microspheres (Formulations 1-8, Table 4.1), or with comparable amounts of soluble protein and adjuvant (8.5ug of C97 Env and 1.3ug of Adju-Phos, MPLA, CpG, or no adjuvant). Sera was collected at 8h post vaccination, and systemic levels of cytokines and chemokines were measured by luminex.

(A) Mean fold induction of cytokine responses relative to the PBS group 8h post vaccination. Data are log fold changes over the averaged cytokine levels in the PBS group (Empty, Bolus). Cytokines that were not bolded did not have any induction above the limit of detection of the assay.

(B) Correlation between log concentrations of selected cytokines with C97 Env-specific log endpoint IgG titers at week 6. Squares represent animals immunized with SE formulations, circles represent DE formulations, and triangles represent bolus (soluble) protein and adjuvant groups. Orange symbols represent groups with no adjuvant co-encapsulated, green symbols represent groups with Adju-Phos co-encapsulated, red symbols represent groups with MPLA co-encapsulated, blue symbols represent groups with CpG co-encapsulated. Correlations were analyzed using the Spearman rank-correlation test.

(figure on next page)

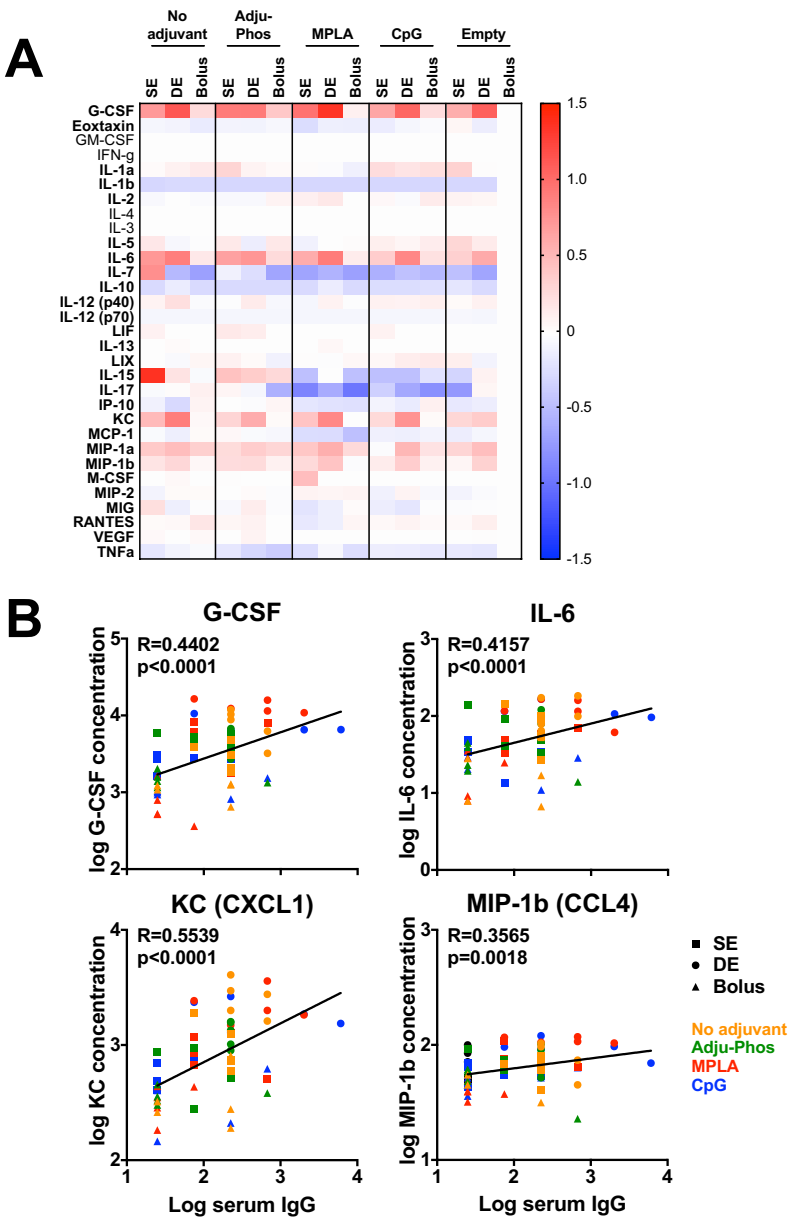

Figure 4.5 – Innate immune responses 8 hours post vaccination (continued)

DISCUSSION

PLGA microspheres have been widely studied as a vaccine delivery modality that could enhance the immune response (1, 15). Encapsulation prevents the antigen from degrading. Recent studies have also suggested that microspheres activate the NACHT, LRR and PYD domains-containing protein 3 (NALP3) inflammasome in dendritic cells (16). While there are many papers in the field studying the immunogenicity of microspheres, most use Bovine Serum Albumin (BSA), or the tetanus toxoid as a model antigen. Few studies have investigated the immunogenicity of encapsulating the HIV-1 Env protein (17). We aimed to investigate biodegradable PLGA microparticle-based delivery methods of vaccination, with the HIV-1 Env protein antigen, to improve the induction of systemic and mucosal antibodies.

We first investigated the immunogenicity of single emulsion (SE) particles co-encapsulating Adju-Phos, a suspension of aluminum salt. Alum is the only Food and Drug Administration (FDA) approved adjuvant in use. Encapsulation of C97 Env antigen, whether alone or with Adju-Phos, were immunogenic, and elicited higher antibody responses compared to bolus C97 Env (Figure 4.1). We also showed that PLGA itself did not have an adjuvant effect, as bolus C97 Env with empty microspheres did not elicit high antibody responses.

Immunization with SE encapsulated C97 Env also appeared to result in an expanded antibody response, resulting in a greater depth and breadth of linear Env epitopes targeted by vaccine-elicited IgG (Figure 4.2C, D). Most of the reactive linear Env epitopes targeted by both soluble and bolus groups were similar, suggesting that the additional breadth and depth we see elicited by the SE encapsulated C97 Env group was due to expansion of the antibody response (Figure 4.4E). This was an interesting observation as comparable binding antibody titers were elicited by either regimen. While it has been argued that persistent antigen exposure may result

in tolerance (18, 19), this is probably dependent on the antigen dose and local environment, as antigen persistency has also been suggested to periodically stimulate precursor B cells such that they differentiate into antibody-secreting plasma cells, thereby eliciting effective immune responses (20). It has also been suggested that continual antigen persistence, especially with increasing dosages over time, could mimic a pathogenic viral infection, resulting in induction of strong cellular and antibody responses (8, 21). It is possible that the sustained release of encapsulated Env could have expanded the diversity of the elicited antibody response, due to the continued stimulation of the immune system.

We next decided to encapsulate other adjuvants, MPLA and CpG, Toll-like receptor 4 (TLR4) and TLR9 agonists respectively, as well as use different formulation methods. Co-delivery of antigen with TLR agonists have been shown to synergistically increase the immunogenicity of the antigen, possibly by activating both the TLR and inflammasome signaling pathways (22, 23). The encapsulation efficiency, as well as the percentage of antigen released, varied between formulations and adjuvants (Table 4.1). Adju-Phos had the lowest encapsulation efficiency and percentage of antigen released, possibly due to the suspension nature of the adjuvant co-encapsulated, although it elicited comparable immune responses to the other formulations (Figure 4.4B). Double emulsion (DE) formulations co-encapsulating CpG elicited the highest antibody responses after prime and boost, possibly due to its high encapsulation release and amount of intact antigen released. CpG is also a small string of nucleotides that could possibly be more easily encapsulated.

The inflammatory environment induced after immunization attracts immune cell infiltrates and subsequently shapes the antigen-specific adaptive immune response. We observed that G-CSF, IL-6, KC (CXCL1), and MIP-1β (CCL4), were all strongly correlated with subsequent

peak antibody titers (Figure 4.5). IL-6 mediates neutrophilic inflammation, and also modulates the shift from innate to adaptive immune responses, while KC has a similar neutrophil chemoattractant ability. G-CSF mediates neutrophil survival, proliferation and differentiation, and MIP-1β is a chemoattractant for natural killer cells and monoctyes. These findings were similar to a previous study where G-CSF was shown to be strongly induced following a protein immunization, with KC and IL-6 induced to a lesser degree (24). There was no induction of the inflammatory cytokine IL-1β, which is induced by the NALP3 inflammasome (16, 25), although this could possibly be induced at an earlier or later time point.

Our findings demonstrate that encapsulating the HIV-1 Env antigen in either single or double emulsion formulations is more immunogenic than a comparable bolus immunization, and of these formulations, the double emulsion formulations co-encapsulating CpG was the most immunogenic. This increase in humoral immune response appears to be tied to the induction of certain cytokines that are chemoattractants for innate immune cells, including neutrophils, natural killer cells, and monocytes, and which mediate the survival and proliferation of these innate immune cells. Furthermore, encapsulation appears to expand the vaccine-elicited antibody repertoire. This suggests that co-encapsulating HIV-1 Env with CpG in biodegradable PLGA microspheres using the double emulsion formulation may warrant further investigation as a vaccine delivery method.

REFERENCES:

1. **O'Hagan DT**, **Jeffery H**, **Roberts MJ**, **McGee JP**, **Davis SS**. 1991. Controlled release microparticles for vaccine development. Vaccine **9**:768–771.

2. **Eldridge JH**, **Staas JK**, **Meulbroek JA**, **Tice TR**, **Gilley RM**. 1991. Biodegradable and biocompatible poly(DL-lactide-co-glycolide) microspheres as an adjuvant for staphylococcal enterotoxin B toxoid which enhances the level of toxin-neutralizing antibodies. Infect Immun **59**:2978–2986.

3. **Fu K**, **Harrell R**, **Zinski K**, **Um C**, **Jaklenec A**, **Frazier J**, **Lotan N**, **Burke P**, **Klibanov AM**, **Langer R**. 2003. A potential approach for decreasing the burst effect of protein from PLGA microspheres. J Pharm Sci **92**:1582–1591.

4. **Zhang Y-M**, **Yang F**, **Yang Y-Q**, **Song F-L**, **Xu A-L**. 2008. Recombinant interferon-alpha2b poly(lactic-co-glycolic acid) microspheres: pharmacokinetics-pharmacodynamics study in rhesus monkeys following intramuscular administration. Acta Pharmacol Sin **29**:1370–1375.

5. **Tabata Y**, **Gutta S**, **Langer R**. 1993. Controlled Delivery Systems for Proteins Using Polyanhydride Microspheres. Pharm Res **10**:487–496.

6. **Iqbal M**, **Zafar N**, **Fessi H**, **Elaissari A**. 2015. Double emulsion solvent evaporation techniques used for drug encapsulation. Int J Pharm **496**:173–190.

7. **Preis I**, **Langer RS**. 1979. A single-step immunization by sustained antigen release. J Immunol Methods **28**:193–197.

8. **Kemp JM**, **Kajihara M**, **Nagahara S**, **Sano A**, **Brandon M**, **Lofthouse S**. 2002. Continuous antigen delivery from controlled release implants induces significant and anamnestic immune responses. Vaccine **20**:1089–1098.

9. **Zinkernagel RM**, **Ehl S**, **Aichele P**, **Oehen S**, **Kundig T**, **Hengartner H**. 1997. Antigen localisation regulates immune responses in a dose- and time-dependent fashion: a geographical view of immune reactivity. Immunol Rev **156**:199–209.

10. **Kovacs JM**, **Nkolola JP**, **Peng H**, **Cheung A**, **Perry J**, **Miller CA**, **Seaman MS**, **Barouch DH**, **Chen B**. 2012. HIV-1 envelope trimer elicits more potent neutralizing antibody responses than monomeric gp120. Proc Natl Acad Sci USA **109**:12111–12116.

11. **Tzeng SY**, **McHugh KJ**, **Behrens AM**, **Rose S**, **Sugarman JL**, **Ferber S**, **Langer R**, **Jaklenec A**. 2018. Stabilized single-injection inactivated polio vaccine elicits a strong neutralizing immune response. Proc Natl Acad Sci USA **115**:E5269–E5278.

12. **Nkolola JP**, **Peng H**, **Settembre EC**, **Freeman M**, **Grandpre LE**, **Devoy C**, **Lynch DM**, **La Porte A**, **Simmons NL**, **Bradley R**, **Montefiori DC**, **Seaman MS**, **Chen B**, **Barouch DH**. 2010. Breadth of neutralizing antibodies elicited by stable, homogeneous clade A and clade C HIV-1 gp140 envelope trimers in guinea pigs. J Virol **84**:3270–3279.

13. **Stephenson KE**, **Neubauer GH**, **Reimer U**, **Pawlowski N**, **Knaute T**, **Zerweck J**, **Korber BT**, **Barouch DH**. 2014. Quantification of the epitope diversity of HIV-1-specific binding antibodies by peptide microarrays for global HIV-1 vaccine development. J Immunol Methods.

14. **Imholte GC**, **Sauteraud R**, **Korber B**, **Bailer RT**, **Turk ET**, **Shen X**, **Tomaras GD**, **Mascola JR**, **Koup RA**, **Montefiori DC**, **Gottardo R**. 2013. A computational framework for the analysis of peptide microarray antibody binding data with application to HIV vaccine profiling. J Immunol Methods **395**:1–13.

15. **Pavot V**, **Berthet M**, **Rességuier J**, **Legaz S**, **Handké N**, **Gilbert SC**, **Paul S**, **Verrier B**. 2014. Poly(lactic acid) and poly(lactic-co-glycolic acid) particles as versatile carrier platforms for vaccine delivery. Nanomedicine (Lond) **9**:2703–2718.

16. **Sharp FA**, **Ruane D**, **Claass B**, **Creagh E**, **Harris J**, **Malyala P**, **Singh M**, **O'Hagan DT**, **Pétrilli V**, **Tschopp J**, **O'Neill LAJ**, **Lavelle EC**. 2009. Uptake of particulate vaccine adjuvants by dendritic cells activates the NALP3 inflammasome. Proc Natl Acad Sci USA **106**:870–875.

17. **Cleland JL**, **Lim A**, **Daugherty A**, **Barron L**, **Desjardin N**, **Duenas ET**, **Eastman DJ**, **Vennari JC**, **Wrin T**, **Berman P**, **Murthy KK**, **Powell MF**. 1998. Development of a single-shot subunit vaccine for HIV-1. 5. Programmable in vivo autoboost and long lasting neutralizing response. J Pharm Sci **87**:1489–1495.

18. **DRESSER DW**, **GOWLAND G**. 1964. IMMUNOLOGICAL PARALYSIS INDUCED IN ADULT RABBITS BY SMALL AMOUNTS OF A PROTEIN ANTIGEN. Nature **203**:733–736.

19. **DIXON FJ**, **MAUER PH**. 1955. Immunologic unresponsiveness induced by protein antigens. Journal of Experimental Medicine **101**:245–257.

20. **Gray D**. 2002. A role for antigen in the maintenance of immunological memory. Nat Rev Immunol **2**:60–65.

21. **Tam HH**, **Melo MB**, **Kang M**, **Pelet JM**, **Ruda VM**, **Foley MH**, **Hu JK**, **Kumari S**, **Crampton J**, **Baldeon AD**, **Sanders RW**, **Moore JP**, **Crotty S**, **Langer R**, **Anderson DG**, **Chakraborty AK**, **Irvine DJ**. 2016. Sustained antigen availability during germinal center initiation enhances antibody responses to vaccination. Proc Natl Acad Sci USA **113**:E6639–E6648.

22. **Coffman RL**, **Sher A**, **Seder RA**. 2010. Vaccine adjuvants: putting innate immunity to work. Immunity **33**:492–503.

23. **Guy B**. 2007. The perfect mix: recent progress in adjuvant research. Nat Rev Micro **5**:505–517.

24. **Buglione-Corbett R**, **Pouliot K**, **Marty-Roix R**, **West K**, **Wang S**, **Lien E**, **Lu S**. 2013. Serum Cytokine Profiles Associated with Specific Adjuvants Used in a DNA Prime-

Protein Boost Vaccination Strategy. PLoS ONE **8**:e74820–16.

25. **Demento SL**, **Eisenbarth SC**, **Foellmer HG**, **Platt C**, **Caplan MJ**, **Mark Saltzman W**, **Mellman I**, **Ledizet M**, **Fikrig E**, **Flavell RA**, **Fahmy TM**. 2009. Inflammasome-activating nanoparticles as modular systems for optimizing vaccine efficacy. Vaccine **27**:3013–3021.

CHAPTER 5:

Conclusions

Parenteral immunization results in vaccine-elicited antibody responses that appear to be transudated from serum

We saw in Chapters 2 and 3 that I.M. immunizations with Adenovirus vectors (Ad) and/or HIV-1 envelope (Env) elicited both IgG and IgA responses in the colorectal compartment, and that these mucosal antibody responses appear to be immunologically coordinated with serum antibody responses. Vaccine-elicited mucosal IgG and IgA responses largely correlated with serum responses in monkeys that were immunized with Ad35/Ad26, Env/Env, or Ad26/Env regimens. The isotype, distribution, functionality, and the linear epitope specificities of vaccine-elicited mucosal IgG mirror those found in serum IgG, suggesting that these Env-specific mucosal IgG responses appear to reflect transudation of serum antibodies into mucosal compartments. IgG and IgA binding responses in both mucosal and systemic compartments were also shown to be correlated with sera neutralizing responses. SC-region containing Env-specific IgA was not detected in the mucosal compartment, suggesting that Env-specific IgA was also transudated from serum, rather than transported across the epithelial layer via interaction with pIgR. We also observed correlation between systemic and mucosal responses in systemically immunized mice in Chapter 4, further corroborating our earlier observations in non-human primates.

Transudation of systemic antibodies into the mucosal compartment has been widely suggested as the route by which vaccine-elicited antibodies in serum reach the mucosal compartment, especially after parenteral immunization (1-3). However, it has been difficult to show mechanistically how it happens. It has been suggested that high amounts of serum IgG induced by systemic immunization may subsequently find their way to the mucosal compartment, either by constitutive transcellular/paracellular transport of IgG from the systemic compartment and other specific transport mechanisms, or by transudation from the systemic compartment to the mucosal compartment, which could be promoted by

inflammatory processes triggered early during immunization (4). The transudation of antibodies into the mucosal compartment can be tangentially calculated through the transudation rate of serum proteins (e.g. albumin) into the mucosal compartment (5). However the most definite proof of transudation of serum antibodies into mucosal compartments is via passive transfer studies with monoclonal antibodies, and subsequent detection of the transferred antibodies in mucosal compartments. Passively transferred pIgA against influenza hemagluttanin (HA) via the intravenous route was detected in the nasal compartment of immunized mice, and was protective against a subsequent infection of influenza with a homologous HA (6). In monkeys that were systemically injected with monomeric or dimeric IgA forms of the broadly neutralizing antibody b12, both forms of IgA were found in mucosal compartments (7). This supports our hypothesis that the vaccine-elicited immunoglobulins we observed in the mucosal compartment of immunized mice and rhesus monkeys were passively transferred via transudation from the systemic compartment.

While we did not detect any SC-region containing Env-specific IgA in the mucosal compartment, it is possible that it may be present at low levels, below the limits of detection of the assay To further determine if vaccine-elicited antibodies in the mucosal secretion could perhaps be contributed by local production and subsequent transport across the epithelial lumen of antibody, a B cell ELISPOT could be used to determine the presence of antigen-specific antibody-secreting cells from mucosal biopsies, along with the detection of Env-specific plasma cells using flow cytometry.

A possible way of increasing vaccine-elicited immunity in mucosal compartments would be to include Vitamin A or its metabolite, retinoic acid, as an adjuvant. Vitamin A has been shown to be important for vaccine-elicited immune responses in the gastrointestinal tract (8), and studies have shown that retinoic acid increases the expression of the gut-homing markers α4β7 and CCR9 on T cells in mice (9). Furthermore, using retinoic acid as an

adjuvant in a mouse model has been shown to induce T and B cell homing to the gut following vaccination (10), and to increase the T cell response and mucosal protection from viral challenge by recombinant vaccinia virus expressing the vaccine antigen (11). Finally, human patients who were given retinoic acid as an adjuvant to the oral typhoid vaccine had enhanced specific IgA responses compared to those who were not given retinoic acid (12). It would be worth exploring the use of Vitamin A or retinoic acid as an adjuvant to increase the mucosal antibody response.

One of the main limitations of studying mucosal immune responses is the difficulty in obtaining mucosal samples – while obtaining samples from the male genital tract is straightforward (13), obtaining samples from the female genital tract and rectal secretions usually involve lavage (13) or the use of an absorbent material of some kind, such as Sno-strips (14), cellulose acetate wicks (15), or Weck Cels (16), as was used in this dissertation. Collection of samples by lavage or Sno-strip typically involve anoscopy, limiting the number of willing human participants. Additionally, lavage introduces unknown dilution factors into the collection of secretions. While it has been argued that the use of small absorbent wicks or spears such as Weck Cels are less invasive and traumatic, and more accurate (16), there is still inherent variability in sample collection, for example due to the positioning of the material, and the amount of mucosal sample collected is limited. The limited amount of mucosal sample prevented us from studying the mucosal responses in more detail. An interesting experiment to perform would be to evaluate the breadth and depth of mucosal IgG and IgA responses to linear Env, Gag and Pol peptides using peptide microarray. This would allow us to compare these responses to those in serum and to help confirm if these mucosal IgG and IgA are transudated from sera, or produced locally at mucosal sites. However due to the limited amounts of mucosal samples available, we were unable to purify sufficient amounts of mucosal IgG and IgA required for these experiments. Similarly, it would have

been interesting to be able to determine whether vaccine elicited mucosal antibodies were able to elucidate neutralizing antibody responses in Chapter 3, and if that correlated with mucosal and systemic binding antibody responses.

Relationship between IgG and IgA

In chapter 3, we showed that vaccine-elicited IgG and IgA targeted similar Env, Gag, and Pol linear peptide sequences (mean: Env: 67.1%, Gag: 67.33%, Pol: 69.5%), although both IgG and IgA had their own unique reactive linear peptide sequences. This suggests that a population of IgG and IgA could share common B cell precursors. It is thus possible that the majority of vaccine-elicited IgA could have been switched via an IgG intermediary, while the remaining were directly switched from IgM.

Class switch recombination diversifies antibody isotypes from the IgM and/or IgD that naïve B cells express on their surface. Studies have suggested that class switching is sequential and occurs in a stepwise manner. The downstream IgG subclasses IgG2 and IgG4 often contain parts of upstream switch regions, and their variable regions have more extensive mutations and higher antigen affinity than IgG1 and IgG3 that are upstream (17). Furthermore, *in vitro*, it has been shown that IgA is preferentially formed by sequential switching from IgM through IgG intermediaries (18-20). Antigen selection analysis between IgG and IgA subclasses in a Papua New Guinean population also suggested that IgA1 may arise from IgG1 class-switching, while IgA2 may arise from IgG2 class switching (17). In a study measuring antibody class switching using antibody repertoire sequencing, the authors determined a hierarchy of class switching pathways, which suggested that IgM frequently switched to IgG1, IgG2, and IgA1, while IgG1 had a 92% probability of switching to IgA1 and IgA2 (21).

While one could try to elucidate how and when class switching occurs following immunization with respect to our studies (via antibody repertoire sequencing), a more pertinent question would be whether these antibody isotypes would contribute to protection from HIV-1 transmission and infection. To that end, the neutralizing potency of purified serum IgG and IgA could be tested in TZM.bl neutralization assays. For example, purified serum IgG and IgA from our study in Chapter 3 could be tested against the easily neutralized Tier 1A viruses MW965.26 and SF162.LS. It is possible that serum IgA might have a limited contribution to the serum neutralizing antibody response in Chapter 3, as was suggested in an earlier study (22). However in the aforementioned study, the purified IgG and IgA antibodies were obtained from SIV-infected rhesus monkeys, and it is possible that vaccine-elicited IgA may have a greater contribution to neutralizing antibody responses. The functionality of vaccine-elicited IgA could also have been further investigated, and compared to that of vaccine-elicited IgG, via assays to measure antibody-mediated phagocytosis.

Another experiment that could be performed would be to compare the binding of IgG and IgA to linear Env, Gag and Pol peptides in vaccinated rhesus macaques challenged with a simian/human immunodeficiency virus (SHIV) that were subsequently protected or infected (23). While protection is likely connected to a complex immune profile, such as antibody dependent cellular phagocytosis (ADCP), antibody dependent cellular cytotoxicity (ADCC), and antibody dependent complement deposition (ADCD) activity (24), it would still be interesting to dissect and compare the IgG and IgA profiles in protected and infected rhesus monkeys that were challenged with SHIV, especially since an effective vaccine-induced IgA response may be required to prevent HIV-1 infection.

It has been suggested that while the immune-correlate analysis of the RV144 trial showed that anti-Env IgA from plasma was correlated to increased risk of HIV-1 acquisition (25), and that this was potentially mediated by IgA interfering with ADCC activity mediated

by C1-binding IgG, IgA responses may just be a marker for a less functional immune response, rather than having a direct causal effect to impaired humoral protection (24). Furthermore, HIV-1 specific IgA antibodies have been isolated from a RV144 trial participant that have demonstrated *in vitro* antiviral activity, by mediating phagocytosis by monocytes (26). In our experiments in Chapter 3, we did not observe any IgA competition with A32 binding to its C1 conformational epitope, and it is unlikely that IgA correlations from a canarypox ALVAC /gp120 monomeric Env immunization regimen would be expected to be relevant to an Ad26/Env immunization regimen.

Encapsulation of antigen enhances the humoral response

Poly (D, L-lactic-co-glycolic acid) (PLGA) microparticles have been widely studied as a potential vaccine delivery modality that enhances the immune response (reviewed in (27-29)). Encapsulation of the antigen in microparticles protects the antigen from degradation, while the adjuvant properties of microparticles have been attributed to enhanced phagocytosis of encapsulated antigen. Smaller microparticles (less than 10um) are directly phagocytosed by antigen presenting cells (APCs) including macrophages (30, 31), monocyte-derived dendritic cells (DCs) (32, 33), and plasmacytoid DCs (34). Larger microparticles are not phagocytosed, but still enhanced antibody responses (35, 36); it has been observed that microparticles that were not phagocytosed were found attached to the surface of macrophages (37). More recently, studies have suggested that nano- and micro-particles (ranging from 430nm to 32um in size) activate dendritic cells via the NACHT, LRR and PYD domains-containing protein 3 (NALP3) inflammasome, enhancing T cell responses, but not antibody responses, in immunized mice (38). The impact of how size might affect the cellular and humoral immune responses are varied and contradictory (37, 38), but this could be attributed to the difference in polymer composition, encapsulated antigen, and formulation method.

However what is certain is that they have been found to enhance both the T cell and antibody responses (39, 40), as well as subsequent memory antibody responses (41), when compared to bolus immunizations. We have indeed observed that antibody responses were enhanced, or at least comparable, in mice immunized with encapsulated Env, when compared to similar amounts of bolus immunization in Chapter 4. Additionally, at least in the single emulsion formulations, it appears that while encapsulated antigen in microparticles has increased immunogenicity compared to soluble antigen, this was due to the encapsulation of the antigen itself, and not the presence of PLGA microparticles. This increase in peak vaccine-elicited antibody responses was shown to be correlated to the induction of the cytokines G-CSF, IL-6, KC, and MIP-1β, at 8 hours post vaccination. These cytokines are chemoattractants for neutrophils, natural killer cells, and monocytes, as well as mediate their survival and proliferation. We did not observe any induction of the IL-1β cytokine, which is induced by the NALP3 inflammasome (30, 31), although this could be induced at an earlier or later time point. We could investigate the cytokine response by luminex at other earlier or later time points, such as at 4 hours, and 24 hours post vaccination, as well as at 2 weeks post vaccination. We hypothesize that certain inflammatory cytokines may still be elicited at higher levels in mice that were immunized with encapsulated Env 2 weeks post vaccination, compared to sham or bolus vaccinated mice, due to the continual release of antigen and degradation of the PLGA shell.

Incorporation of adjuvant, together with the antigen, into microparticles could increase immunogenicity

Incorporating adjuvants into vaccine regimens help to enhance immune responses and improve vaccine efficacy, potentially reducing the amount of antigen and doses that may be required (42, 43). Many experimental adjuvants are toll-like receptor (TLR) agonist that bind

to TLRs and stimulate corresponding signaling pathways (43), although the only licensed adjuvants are aluminum-based (alum and AS04) or emulsions (MF59 and AS03), that are thought to trigger inflammasomes or local tissue inflammation respectively (42, 44, 45).

Multiple groups have shown that encapsulating different adjuvants, especially TLR agonists, together with antigen, in micro- or nano- particles, would be advantageous by eliciting quantitatively and qualitatively better immune responses (46, 47). Co-delivery of antigen together with TLR agonists has been observed to synergistically increase immunogenicity versus a comparable amount of separate components (42). This is the case regardless of whether the antigen is coupled together with the TLR agonists (48-50), or associated together in micro- or nano- particle formulations (51). Most studies involving co-encapsulation of a TLR agonist together with antigen, use CpG (TLR9 agonist) (27, 52, 53), amongst many others), although Monophosphoryl Lipid A (MPLA; TLR4 agonist) has also used as well (54-56).

It is postulated that co-encapsulating TLR agonists and adjuvant in biodegradable microparticles synergistically enhances immune responses by activating both the TLR and inflammasome signaling pathways (27, 57, 58). Co-encapsulating a TLR agonist with the antigen could also selectively target it to APCs, enhancing its interaction with cellular TLRs (59). This also ensures that both adjuvant and antigen are taken up by the same APC, enhancing immune responses (60-62). Additionally, encapsulated delivery of TLR agonists increases its safety profile, as it results in a transient induction of innate immune responses that is localized, preventing off-target toxic effects (63). This results in increased vaccine-antibody responses (64), as well as cytotoxic T lymphocyte (CTL) responses (53). Increased activation of dendritic cells (DCs) with the upregulation of MHC class II molecules and CD86 markers was also observed (56).

In chapter 4, we chose to test the immunogenicity of 3 different adjuvants – Adju-Phos (an alum-based salt suspension), CpG, and MPLA – when co-encapsulated with a HIV-1 Env antigen. While we did not observe enhancement of antibody response in mice immunized with some formulations containing co-encapsulated adjuvant and antigen, compared with encapsulated antigen alone, as described by other groups (42, 51), this could be due to different adjuvant, dosage, or formulation method used. The exception was the double emulsion formulation co-encapsulating CpG which elicited much higher antibody responses of 1-2 logs in both systemic and mucosal compartments. As we had compared immunogenicity of the different formulations based on the input (amount of antigen loaded), it is possible that if we compared the immunogenicity of the different formulations based on the amount of antigen actually encapsulated, we would observe that the single emulsion formulation co-encapsulating Adju-Phos would elicit a significantly higher antibody response, compared to formulations encapsulating antigen alone. Furthermore, most adjuvants used in co-delivery studies in the literature involve CpG, MPLA, or some other TLR agonist, and not an alum-based adjuvant. This could be because of the mechanism of action of alum-based adjuvants. We have shown that co-delivery of Adju-Phos results in similar antibody titers as other TLR-based adjuvants, despite its much lower encapsulation efficiency.

To further expand the scope of our evaluation and comparison into the immunogenicity of microparticles as novel delivery methods of vaccination, we could characterize the B cell and germinal center T follicular helper cell (Tfh) responses following prime and boost. Flow cytometry can be ran on cells isolated from the spleen, inguinal (draining) and iliac lymph nodes to identify and compare B cell subsets (activated B cells, plasma cells, memory B cells) as well as germinal center B and Tfh cells.

Mice could be immunized with both SE and DE formulations, and at a timepoint with peak antibody responses following immunization, as well as at a later time point, at the 2 week mark, animals could be euthanized, and the tissues harvested and characterized with flow cytometry as described above. Histology could be performed to compare the size and number of germinal centers in mice immunized with either microparticle formulation with those from animals immunized with bolus protein. We expect that animals immunized with SE, DE microparticles would have peak GC responses at a later time point, but not those immunized with bolus protein, and they could also have expanded GC responses as well.

Antigen persistence and its effect on the immune system

A major concern of continuous release vaccination regimens is the induction of tolerance. Indeed some studies have suggested that continuous antigen delivery would result in tolerance induction (65, 66). However, it is possible that this is dose dependent. Indeed, there have been multiple studies with continuous antigen delivery involving either microparticles and osmotic pump devices where a high humoral response of long duration was induced (39-41). Antigen persistency has been suggested to elicit effective immune responses by periodically stimulating precursor B cells such that they differentiate to form antibody-secreting plasma cells (67).

Two separate studies explored the influence of antigen kinetics on humoral and cellular immune responses in mice. Mice were immunized with a fixed cumulative dose of either peptide or protein antigen by repeated injections following different kinetics, and in both cases, repeated injections with increasing doses resulted in greater CD8 T cell responses and antibody responses respectively (39, 68). It was hypothesized that increasing doses of vaccination mimicked a pathogenic viral infection, resulting in the induction of a strong immune response. While the *in vitro* release kinetics for our microparticle formulations in

Chapter 4 was not one that followed an increasing dosage profile, we still observed a significant increase in antibody titers compared to soluble immunizations. It is possible that this is due to the prolonged presence of antigen along with the presence of adjuvant used, possibly leading to better antigen capture in the germinal center, as postulated in one of the aforementioned papers (39). It is possible that the increased antibody diversity, in terms of the breadth and depth of reactive linear Env peptides, observed in mice immunized with single emulsion formulations containing Env and Adju-Phos, represented an increase in affinity maturation. This is interesting and bears further investigation, especially in light of a study in non-human primates, where adjuvants together with Env protein vaccines increased binding antibody titers, but that did not necessarily translate to an increase in somatic hypermutation and affinity maturation (69). We would determine if this increase in antibody diversity (via peptide microarray) really translates into an increase in affinity maturation, by analysis of the degree of somatic hypermutation. This could be done by sequencing and analysis of antibodies pre and post vaccination with encapsulated Env.

The prolonged presence of antigen has also been suggested to be necessary for a sustained B cell memory response (67, 70), and a study investigating the memory responses following microparticle vaccination suggest that persistent antigen release result in a long-lasting and enhanced memory response (41). To be able to better investigate how sustained release from our microparticle formulations might affect humoral immune responses, memory B cell responses in immunized mice can be assessed. B cell ELISPOTs analyzing antibody secreting B cell frequencies can be performed in immunized mice following challenge, and also by flow cytometry using panels containing memory B cell markers.

We could expand the analysis of the diversity of the antibody elicited against linear Env peptides using peptide microarrays from just a SE (Adju-Phos) regimen to all regimens. It is possible that we will see the expansion of antibody diversity for all formulations. It will be

interesting to compare the breadth and depth of antibody diversity between the different formulations and adjuvants.

Summary

The unifying theme of this dissertation is the evaluation of mucosal and systemic antibody responses induced against Adenovirus and Env HIV-1 vaccine candidates that were administered via a parenteral route. I hypothesized that HIV-1 vaccine candidates administered via the parenteral route can induce coordinated mucosal and systemic immune responses, and that we can improve the induction of these antibody responses via novel delivery methods.

Chapter 2 of this dissertation described the common features between mucosal and peripheral antibody responses following parenteral immunization of rhesus monkeys with Adenovirus and Env HIV-1 candidate vaccines. We showed that IgG isotypes, functionality, and pattern of IgG binding to linear Env peptides were similar between serum and mucosal samples. Chapter 3 of this dissertation further investigated the relationship between mucosal and peripheral responses, as well as the relationship between vaccine elicited systemic IgG and IgA in immunized rhesus monkeys. We showed that IgA responses are tightly coordinated with IgG following Ad26/Env vaccination and mucosal IgG and IgA responses largely reflect transudation from serum.

In Chapter 4, I evaluated the immunogenicity of a controlled antigen release vaccination regimen in a mouse model, using biodegradable PLGA microparticles encapsulating HIV-1 Env as a vaccine delivery modality, where antigen was continuously released over a period of weeks. Encapsulation of antigen elicited higher serum and mucosal antibody responses, compared to bolus immunizations, with or without co-encapsulated adjuvant. Encapsulated Env immunizations generated greater antibody diversity in terms of

breadth and depth. Double emulsion formulations have greater encapsulation efficiency, and a double emulsion formulation with CpG appear to be the most immunogenic

Humoral responses are likely to be important for the development of a prophylactic vaccine. These data show that vaccine-elicited antibodies are present in mucosal sites following parenteral immunization, and are immunologically coordinated with the systemic response, which is important as mucosal surfaces are a major portal of entry for HIV-1. Furthermore, PLGA microspheres appear to be a promising candidate for vaccine antigen delivery, as they are more immunogenic than traditional bolus immunizations.

REFERENCES:

1. **Russell MW**, **Moldoveanu Z**, **White PL**, **Sibert GJ**, **Mestecky J**, **Michalek S M**. 1996. Salivary, nasal, genital, and systemic antibody responses in monkeys immunized intranasally with a bacterial protein antigen and the Cholera toxin B subunit. Infect Immun **64**:1272–1283.

2. **Brandtzaeg P**. 1995. Molecular and cellular aspects of the secretory immunoglobulin system*. APMIS **103**:1–19.

3. **Brandtzaeg P**. 2007. Induction of secretory immunity and memory at mucosal surfaces. Vaccine **25**:5467–5484.

4. **Underdown BJ**, **Strober W**. 2015. Chapter 70 - Parenteral Immunization and Protection from Mucosal Infection, pp. 1391–1402. *In* Mestecky, J, Strober, W, Russell, MW, Kelsall, BL, Cheroutre, H, Lambrecht, BN (eds.), Mucosal Immunology (Fourth Edition)Fourth Edition. Academic Press, Boston.

5. **Meckelein B**, **Externest D**, **Schmidt MA**, **Frey A**. 2003. Contribution of Serum Immunoglobulin Transudate to the Antibody Immune Status of Murine Intestinal Secretions: Influence of Different Sampling Procedures. Clinical and Vaccine Immunology **10**:831–834.

6. **Renegar KB**, **Small PA**. 1991. Passive transfer of local immunity to influenza virus infection by IgA antibody. J Immunol **146**:1972–1978.

7. **Fouda GG**, **Eudailey J**, **Kunz EL**, **Amos JD**, **Liebl BE**, **Himes J**, **Boakye-Agyeman F**, **Beck K**, **Michaels AJ**, **Cohen-Wolkowiez M**, **Haynes BF**, **Reimann KA**, **Permar SR**. 2017. Systemic administration of an HIV-1 broadly neutralizing dimeric IgA yields mucosal secretory IgA and virus neutralization. Mucosal Immunol **10**:228–237.

8. **Kaufman DR**, **De Calisto J**, **Simmons NL**, **Cruz AN**, **Villablanca EJ**, **Mora JR**, **Barouch DH**. 2011. Vitamin A deficiency impairs vaccine-elicited gastrointestinal immunity. J Immunol **187**:1877–1883.

9. **Iwata M**, **Hirakiyama A**, **Eshima Y**, **Kagechika H**, **Kato C**, **Song S-Y**. 2004. Retinoic acid imprints gut-homing specificity on T cells. Immunity **21**:527–538.

10. **Hammerschmidt SI**, **Friedrichsen M**, **Boelter J**, **Lyszkiewicz M**, **Kremmer E**, **Pabst O**, **Förster R**. 2011. Retinoic acid induces homing of protective T and B cells to the gut after subcutaneous immunization in mice. J Clin Invest **121**:3051–3061.

11. **Tan X**, **Sande JL**, **Pufnock JS**, **Blattman JN**, **Greenberg PD**. 2011. Retinoic acid as a vaccine adjuvant enhances CD8+ T cell response and mucosal protection from viral challenge. J Virol **85**:8316–8327.

12. **Lisulo MM**, **Kapulu MC**, **Banda R**, **Sinkala E**, **Kayamba V**, **Sianongo S**, **Kelly P**. 2014. Adjuvant potential of low dose all-trans retinoic acid during oral typhoid vaccination in Zambian men. Clinical & Experimental Immunology **175**:468–475.

13. **Raux M**, **Finkielsztejn L**, **Salmon-Céron D**, **Bouchez H**, **Excler JL**, **Dulioust E**,

Grouin JM, **Sicard D**, **Blondeau C**. 1999. Comparison of the distribution of IgG and IgA antibodies in serum and various mucosal fluids of HIV type 1-infected subjects. AIDS Res Hum Retroviruses **15**:1365–1376.

14. **Mohamed OA**, **Ashley R**, **Goldstein A**, **McElrath J**, **Dalessio J**, **Corey L**. 1994. Detection of rectal antibodies to HIV-1 by a sensitive chemiluminescent western blot immunodetection method. J Acquir Immune Defic Syndr **7**:375–380.

15. **Quesnel A**, **Cu-Uvin S**, **Murphy D**, **Ashley RL**, **Flanigan T**, **Neutra MR**. 1997. Comparative analysis of methods for collection and measurement of immunoglobulins in cervical and vaginal secretions of women. J Immunol Methods **202**:153–161.

16. **Kozlowski PA**, **Lynch RM**, **Patterson RR**, **Cu-Uvin S**, **Flanigan TP**, **Neutra MR**. 2000. Modified wick method using Weck-Cel sponges for collection of human rectal secretions and analysis of mucosal HIV antibody. **24**:297–309.

17. **Jackson KJL**, **Wang Y**, **Collins AM**. 2014. Human immunoglobulin classes and subclasses show variability in VDJ gene mutation levels. Immunol Cell Biol **92**:729–733.

18. **Iwasato T**, **Arakawa H**, **Shimizu A**, **Honjo T**, **Yamagishi H**. 1992. Biased distribution of recombination sites within S regions upon immunoglobulin class switch recombination induced by transforming growth factor beta and lipopolysaccharide. Journal of Experimental Medicine **175**:1539–1546.

19. **Brinkmann V**, **Heusser CH**. 1993. T cell-dependent differentiation of human B cells into IgM, IgG, IgA, or IgE plasma cells: high rate of antibody production by IgE plasma cells, but limited clonal expansion of IgE precursors. Mol Immunol **152**:323–332.

20. **Deenick EK**, **Hasbold J**, **Hodgkin PD**. 1999. Switching to IgG3, IgG2b, and IgA is division linked and independent, revealing a stochastic framework for describing differentiation. J Immunol **163**:4707–4714.

21. **Horns F**, **Vollmers C**, **Croote D**, **Mackey SF**, **Swan GE**, **Dekker CL**, **Davis MM**, **Quake SR**. 2016. Lineage tracing of human B cells reveals the in vivo landscape of human antibody class switching. Elife **5**:5.

22. **Permar SR**, **Wilks AB**, **Ehlinger EP**, **Kang HH**, **Mahlokozera T**, **Coffey RT**, **Carville A**, **Letvin NL**, **Seaman MS**. 2010. Limited contribution of mucosal IgA to Simian immunodeficiency virus (SIV)-specific neutralizing antibody response and virus envelope evolution in breast milk of SIV-infected, lactating rhesus monkeys. J Virol **84**:8209–8218.

23. **Barouch DH**, **Stephenson KE**, **Borducchi EN**, **Smith K**, **Stanley K**, **McNally AG**, **Liu J**, **Abbink P**, **Maxfield LF**, **Seaman MS**, **Dugast A-S**, **Alter G**, **Ferguson M**, **Li W**, **Earl PL**, **Moss B**, **Giorgi EE**, **Szinger JJ**, **Eller LA**, **Billings EA**, **Rao M**, **Tovanabutra S**, **Sanders-Buell E**, **Weijtens M**, **Pau MG**, **Schuitemaker H**, **Robb ML**, **Kim JH**, **Korber BT**, **Michael NL**. 2013. Protective Efficacy of a Global HIV-1 Mosaic Vaccine against Heterologous SHIV Challenges in Rhesus Monkeys. Cell **155**:531–539.

24. **Chung AW**, **Kumar MP**, **Arnold KB**, **Yu WH**, **Schoen MK**, **Dunphy LJ**, **Suscovich TJ**, **Frahm N**, **Linde C**, **Mahan AE**, **Hoffner M**, **Streeck H**, **Ackerman ME**, **McElrath MJ**, **Schuitemaker H**, **Pau MG**, **Baden LR**, **Kim JH**, **Michael NL**, **Barouch DH**, **Lauffenburger DA**, **Alter G**. 2015. Dissecting Polyclonal Vaccine-Induced Humoral Immunity against HIV Using Systems Serology. Cell **163**:988–998.

25. **Haynes BF**, **Gilbert PB**, **McElrath MJ**, **Zolla-Pazner S**, **Tomaras GD**, **Alam SM**, **Evans DT**, **Montefiori DC**, **Karnasuta C**, **Sutthent R**, **Liao HX**, **DeVico AL**, **Lewis GK**, **Williams C**, **Pinter A**, **Fong Y**, **Janes H**, **DeCamp A**, **Huang Y**, **Rao M**, **Billings E**, **Karasavvas N**, **Robb ML**, **Ngauy V**, **de Souza MS**, **Paris R**, **Ferrari G**, **Bailer RT**, **Soderberg KA**, **Andrews C**, **Berman PW**, **Frahm N**, **De Rosa SC**, **Alpert MD**, **Yates NL**, **Shen X**, **Koup RA**, **Pitisuttithum P**, **Kaewkungwal J**, **Nitayaphan S**, **Rerks-Ngarm S**, **Michael NL**, **Kim JH**. 2012. Immune-correlates analysis of an HIV-1 vaccine efficacy trial. N Engl J Med **366**:1275–1286.

26. **Wills S**, **Hwang K-K**, **Liu P**, **Dennison SM**, **Tay MZ**, **Shen X**, **Pollara J**, **Lucas JT**, **Parks R**, **Rerks-Ngarm S**, **Pitisuttithum P**, **Nitayapan S**, **Kaewkungwal J**, **Thomas R**, **Kim JH**, **Michael NL**, **Robb ML**, **McRaven M**, **Montefiori DC**, **Hope TJ**, **Liao HX**, **Moody MA**, **Ferrari G**, **Haynes BF**, **Alam SM**, **Bonsignori M**, **Tomaras GD**. 2018. HIV-1-Specific IgA Monoclonal Antibodies from an HIV-1 Vaccinee Mediate Galactosylceramide Blocking and Phagocytosis. J Virol **92**.

27. **San Román B**, **Gómez S**, **Irache JM**, **Espuelas S**. 2014. Co-encapsulated CpG oligodeoxynucleotides and ovalbumin in PLGA microparticles; an in vitro and in vivo study. J Pharm Pharm Sci **17**:541–553.

28. **O'Hagan DT**, **Jeffery H**, **Roberts MJ**, **McGee JP**, **Davis SS**. 1991. Controlled release microparticles for vaccine development. Vaccine **9**:768–771.

29. **Pavot V**, **Berthet M**, **Rességuier J**, **Legaz S**, **Handké N**, **Gilbert SC**, **Paul S**, **Verrier B**. 2014. Poly(lactic acid) and poly(lactic-co-glycolic acid) particles as versatile carrier platforms for vaccine delivery. Nanomedicine (Lond) **9**:2703–2718.

30. **Tabata Y**, **Ikada Y**. 1988. Macrophage phagocytosis of biodegradable microspheres composed of L-lactic acid/glycolic acid homo- and copolymers. J Biomed Mater Res **22**:837–858.

31. **Newman KD**, **Elamanchili P**, **Kwon GS**, **Samuel J**. 2002. Uptake of poly (D, L-lactic-co-glycolic acid) microspheres by antigen-presenting cells in vivo. J Biomed Mater Res **60**:480–486.

32. **Walter E**, **Dreher D**, **Kok M**, **Thiele L**, **Kiama SG**, **Gehr P**, **Merkle HP**. 2001. Hydrophilic poly(DL-lactide-co-glycolide) microspheres for the delivery of DNA to human-derived macrophages and dendritic cells. Journal of Controlled Release **76**:149–168.

33. **Mohanan D**, **Gander B**, **Kündig TM**, **Johansen P**. 2012. Encapsulation of antigen in poly(D,L-lactide-co-glycolide) microspheres protects from harmful effects of γ-irradiation as assessed in mice. Eur J Pharm Biopharm **80**:274–281.

34. **Salvador A**, **Sandgren KJ**, **Liang F**, **Thompson EA**, **Koup RA**, **Pedraz JL**,

Hernandez RM, **Loré K**, **Igartua M**. 2015. Design and evaluation of surface and adjuvant modified PLGA microspheres for uptake by dendritic cells to improve vaccine responses. Int J Pharm **496**:371–381.

35. **Shi L**, **Caulfield MJ**, **Chern RT**, **Wilson RA**, **Sanyal G**, **Volkin DB**. 2002. Pharmaceutical and Immunological Evaluation of a Single-Shot Hepatitis B Vaccine Formulated With PLGA Microspheres. J Pharm Sci **91**:1019–1035.

36. **Hilbert AK**, **Fritzsche U**, **Kissel T**. 1999. Biodegradable microspheres containing influenza A vaccine: immune response in mice. Vaccine **17**:1065–1073.

37. **Kanchan V**, **Panda AK**. 2007. Interactions of antigen-loaded polylactide particles with macrophages and their correlation with the immune response. Biomaterials **28**:5344–5357.

38. **Sharp FA**, **Ruane D**, **Claass B**, **Creagh E**, **Harris J**, **Malyala P**, **Singh M**, **O'Hagan DT**, **Pétrilli V**, **Tschopp J**, **O'Neill LAJ**, **Lavelle EC**. 2009. Uptake of particulate vaccine adjuvants by dendritic cells activates the NALP3 inflammasome. Proc Natl Acad Sci USA **106**:870–875.

39. **Tam HH**, **Melo MB**, **Kang M**, **Pelet JM**, **Ruda VM**, **Foley MH**, **Hu JK**, **Kumari S**, **Crampton J**, **Baldeon AD**, **Sanders RW**, **Moore JP**, **Crotty S**, **Langer R**, **Anderson DG**, **Chakraborty AK**, **Irvine DJ**. 2016. Sustained antigen availability during germinal center initiation enhances antibody responses to vaccination. Proc Natl Acad Sci USA **113**:E6639–E6648.

40. **Kemp JM**, **Kajihara M**, **Nagahara S**, **Sano A**, **Brandon M**, **Lofthouse S**. 2002. Continuous antigen delivery from controlled release implants induces significant and anamnestic immune responses. Vaccine **20**:1089–1098.

41. **Kanchan V**, **Katare YK**, **Panda AK**. 2009. Memory antibody response from antigen loaded polymer particles and the effect of antigen release kinetics. Biomaterials **30**:4763–4776.

42. **Coffman RL**, **Sher A**, **Seder RA**. 2010. Vaccine adjuvants: putting innate immunity to work. Immunity **33**:492–503.

43. **Duthie MS**, **Windish HP**, **Fox CB**, **Reed SG**. 2011. Use of defined TLR ligands as adjuvants within human vaccines. Immunol Rev **239**:178–196.

44. **Marrack P**, **McKee AS**, **Munks MW**. 2009. Towards an understanding of the adjuvant action of aluminium. Nat Rev Immunol **9**:287–293.

45. **McKee AS**, **Munks MW**, **Marrack P**. 2007. How Do Adjuvants Work? Important Considerations for New Generation Adjuvants. Immunity **27**:687–690.

46. **Salvador A**, **Igartua M**, **Hernandez RM**, **Pedraz JL**. 2014. Designing improved poly lactic-co-glycolic acid microspheres for a malarial vaccine: incorporation of alginate and polyinosinic-polycytidilic acid. J Microencapsul **31**:560–566.

47. **Salvador A**, **Igartua M**, **Hernández RM**, **Pedraz JL**. 2012. Combination of immune stimulating adjuvants with poly(lactide-co-glycolide) microspheres enhances the

immune response of vaccines. Vaccine **30**:589–596.

48. **Wu CCN**, **Hayashi T**, **Takabayashi K**, **Sabet M**, **Smee DF**, **Guiney DD**, **Cottam HB**, **Carson DA**. 2007. Immunotherapeutic activity of a conjugate of a Toll-like receptor 7 ligand. PNAS **104**:3990–3995.

49. **Tighe H**, **Takabayashi K**, **Schwartz D**, **Van Nest G**, **Tuck S**, **Eiden JJ**, **Kagey-Sobotka A**, **Creticos PS**, **Lichtenstein LM**, **Spiegelberg HL**, **Raz E**. 2000. Conjugation of immunostimulatory DNA to the short ragweed allergen amb a 1 enhances its immunogenicity and reduces its allergenicity. J Allergy Clin Immunol **106**:124–134.

50. **Wille-Reece U**, **Flynn BJ**, **Loré K**, **Koup RA**, **Kedl RM**, **Mattapallil JJ**, **Weiss WR**, **Roederer M**, **Seder RA**. 2005. HIV Gag protein conjugated to a Toll-like receptor 7/8 agonist improves the magnitude and quality of Th1 and CD8+ T cell responses in nonhuman primates. PNAS **102**:15190–15194.

51. **O'Hagan DT**, **De Gregorio E**. 2009. The path to a successful vaccine adjuvant--'the long and winding road'. Drug Discov Today **14**:541–551.

52. **Malyala P**, **Chesko J**, **Ugozzoli M**, **Goodsell A**, **Zhou F**, **Vajdy M**, **O'Hagan DT**, **Singh M**. 2008. The potency of the adjuvant, CpG oligos, is enhanced by encapsulation in PLG microparticles. J Pharm Sci **97**:1155–1164.

53. **Lee Y-R**, **Lee Y-H**, **Kim K-H**, **Im S-A**, **Lee C-K**. 2013. Induction of Potent Antigen-specific Cytotoxic T Cell Response by PLGA-nanoparticles Containing Antigen and TLR Agonist. Immune Netw **13**:30–33.

54. **Kasturi SP**, **Skountzou I**, **Albrecht RA**, **Koutsonanos D**, **Hua T**, **Nakaya HI**, **Ravindran R**, **Stewart S**, **Alam M**, **Kwissa M**, **Villinger F**, **Murthy N**, **Steel J**, **Jacob J**, **Hogan RJ**, **García-Sastre A**, **Compans R**, **Pulendran B**. 2011. Programming the magnitude and persistence of antibody responses with innate immunity. Nature **470**:543–547.

55. **Kazzaz J**, **Singh M**, **Ugozzoli M**, **Chesko J**, **Soenawan E**, **O'Hagan DT**. 2006. Encapsulation of the immune potentiators MPL and RC529 in PLG microparticles enhances their potency. J Control Release **110**:566–573.

56. **Elamanchili P**, **Diwan M**, **Cao M**, **Samuel J**. 2004. Characterization of poly (D, L-lactic-co-glycolic acid) based nanoparticulate system for enhanced delivery of antigens to dendritic cells. Vaccine **22**:2406–2412.

57. **Guy B**. 2007. The perfect mix: recent progress in adjuvant research. Nat Rev Micro **5**:505–517.

58. **Demento SL**, **Eisenbarth SC**, **Foellmer HG**, **Platt C**, **Caplan MJ**, **Mark Saltzman W**, **Mellman I**, **Ledizet M**, **Fikrig E**, **Flavell RA**, **Fahmy TM**. 2009. Inflammasome-activating nanoparticles as modular systems for optimizing vaccine efficacy. Vaccine **27**:3013–3021.

59. **Krishnamachari Y**, **Salem AK**. 2009. Innovative strategies for co-delivering antigens and CpG oligonucleotides. Adv Drug Deliv Rev **61**:205–217.

60. **Diwan M**, **Tafaghodi M**, **Samuel J**. 2002. Enhancement of immune responses by co-delivery of a CpG oligodeoxynucleotide and tetanus toxoid in biodegradable nanospheres. Journal of Controlled Release **85**:247–262.

61. **Xie H**, **Gursel I**, **Ivins BE**, **Singh M**, **O'Hagan DT**, **Ulmer JB**, **Klinman DM**. 2005. CpG oligodeoxynucleotides adsorbed onto polylactide-co-glycolide microparticles improve the immunogenicity and protective activity of the licensed anthrax vaccine. Infect Immun **73**:828–833.

62. **Zhang XQ**, **Dahle CE**, **Weiner GJ**, **Salem AK**. 2007. A comparative study of the antigen-specific immune response induced by co-delivery of CpG ODN and antigen using fusion molecules or biodegradable microparticles. J Pharm Sci **96**:3283–3292.

63. **Didierlaurent AM**, **Morel S**, **Lockman L**, **Giannini SL**, **Bisteau M**, **Carlsen H**, **Kielland A**, **Vosters O**, **Vanderheyde N**, **Schiavetti F**, **Larocque D**, **Van Mechelen M**, **Garçon N**. 2009. AS04, an aluminum salt- and TLR4 agonist-based adjuvant system, induces a transient localized innate immune response leading to enhanced adaptive immunity. J Immunol **183**:6186–6197.

64. **Kasturi SP**, **Skountzou I**, **Albrecht RA**, **Koutsonanos D**, **Hua T**, **Nakaya HI**, **Ravindran R**, **Stewart S**, **Alam M**, **Kwissa M**, **Villinger F**, **Murthy N**, **Steel J**, **Jacob J**, **Hogan RJ**, **García-Sastre A**, **Compans R**, **Pulendran B**. 2011. Programming the magnitude and persistence of antibody responses with innate immunity. Nature **470**:543–547.

65. **DIXON FJ**, **MAUER PH**. 1955. Immunologic unresponsiveness induced by protein antigens. Journal of Experimental Medicine **101**:245–257.

66. **DRESSER DW**, **GOWLAND G**. 1964. IMMUNOLOGICAL PARALYSIS INDUCED IN ADULT RABBITS BY SMALL AMOUNTS OF A PROTEIN ANTIGEN. Nature **203**:733–736.

67. **Gray D**. 2002. A role for antigen in the maintenance of immunological memory. Nat Rev Immunol **2**:60–65.

68. **Johansen P**, **Storni T**, **Rettig L**, **Qiu Z**, **Der-Sarkissian A**, **Smith KA**, **Manolova V**, **Lang KS**, **Senti G**, **Müllhaupt B**, **Gerlach T**, **Speck RF**, **Bot A**, **Kündig TM**. 2008. Antigen kinetics determines immune reactivity. Proc Natl Acad Sci USA **105**:5189–5194.

69. **Francica JR**, **Sheng Z**, **Zhang Z**, **Nishimura Y**, **Shingai M**, **Ramesh A**, **Keele BF**, **Schmidt SD**, **Flynn BJ**, **Darko S**, **Lynch RM**, **Yamamoto T**, **Matus-Nicodemos R**, **Wolinsky D**, **NISC Comparative Sequencing Program**, **Nason M**, **Valiante NM**, **Malyala P**, **De Gregorio E**, **Barnett SW**, **Singh M**, **O'Hagan DT**, **Koup RA**, **Mascola JR**, **Martin MA**, **Kepler TB**, **Douek DC**, **Shapiro L**, **Seder RA**. 2015. Analysis of immunoglobulin transcripts and hypermutation following SHIV(AD8) infection and protein-plus-adjuvant immunization. Nat Commun **6**:6565.

70. **Gray D**, **Skarvall H**. 1988. B-cell memory is short-lived in the absence of antigen. Nature **336**:70–73.

APPENDIX:

Supplemental Figures

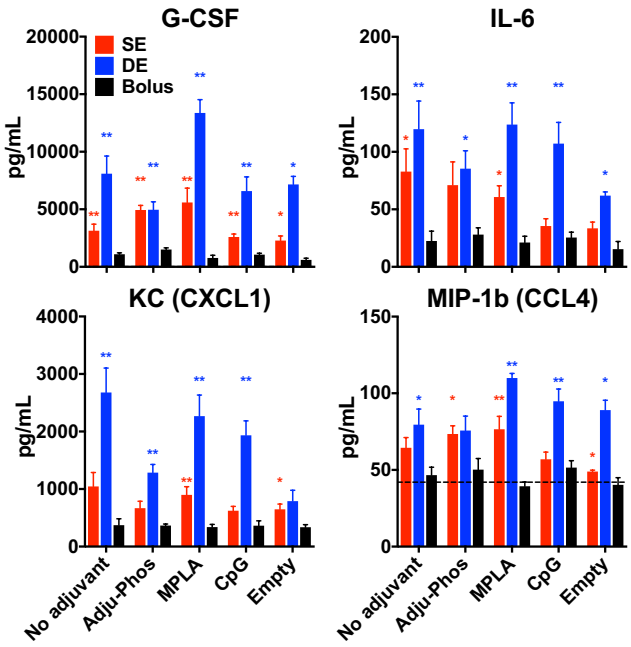

Supplemental Figure 4.S1 – Concentration of selected cytokines 8 hours post vaccination.

Mice (n=4-5 per group) were I.M. immunized with 0.5mg of SE or DE microspheres (Formulations 1-8, Table 4.1), or with comparable amounts of soluble protein and adjuvant (8.5ug of C97 Env and 1.3ug of Adju-Phos, MPLA, CpG, or no adjuvant). Sera was collected at 8h post vaccination, and systemic levels of cytokines and chemokines were measured by luminex

Cytokine concentrations of SE (red) and DE (blue) microsphere groups were compared to the soluble protein group, for each adjuvant. Statistical significance was analyzed using the Mann-Whitney test (*: $p \leq 0.05$, **: $p \leq 0.01$). Mean and SEM values are shown.